รายงานวิจัยฉบับสมบูรณ์

โครงการ การใช้พอลิเมอร์บรัชที่มีหมู่คาร์บอกซิลเป็นฟิล์มบางฟังก์ชันแนลสำหรับการประยุกต์ทางเทคโนโลยีชีวภาพและนาโนเทคโนโลยี

โดย วรวีร์ โฮเว่น และคณะ

ธันวาคม 2553

สัญญาเลขที่ **RMU 5080072**

รายงานวิจัยฉบับสมบูรณ์

โครงการ การใช้พอลิเมอร์บรัชที่มีหมู่คาร์บอกซิลเป็นฟิล์มบางฟังก์ชันแนลสำหรับการประยุกต์ทางเทคโนโลยีชีวภาพและนาโนเทคโนโลยี

คณะผู้วิจัย	สังกัด
1. รองศาสตราจารย์ ดร.วรวีร์ โฮเว่น	ภาควิชาเคมี คณะวิทยาศาสตร์ จุฬาลงกรณ์มหาวิทยาลัย
2. นางสาวปิยะพร อรรคฮาต	สาขาปิโตรเคมีและวิทยาศาสตร์พอลิเมอร์ คณะวิทยาศาสตร์ จุฬาลงกรณ์มหาวิทยาลัย
3. นางสาวสุดารัตน์ พุกบุญมี	สาขาปิโตรเคมีและวิทยาศาสตร์พอลิเมอร์ คณะวิทยาศาสตร์ จุฬาลงกรณ์มหาวิทยาลัย

สนับสนุนโดยสำนักงานคณะกรรมการการอุดมศึกษา และสำนักงานกองทุนสนับสนุนการวิจัย

ACKNOWLEDGEMENT

This research was financially supported by the Commission on Higher Education and the Thailand Research Fund (RMU5080072), the Rachadapisek Sompoj Endowment Fund for graduate students from Chulalongkorn University for Miss Sudarat Pookboonmee and Miss Piyaporn Akkahat, and a Ph.D. scholarship to Miss Piyaporn Akkahat from Strategic Scholarships Fellowships Frontier Research Networks, the Commission on Higher Education. The authors are grateful to the Capability Building Unit for Nanoscience and Nanotechnology, Mahidol University, for providing the Ellipsometry facility. Appreciation is also extended to Assistant Professor Thanapat Palaka of Department of Microbiology, Faculty of Science, Chulalongkorn University, for providing access to a fluorescence microscope.

บทคัดย่อ

พอลิอะคริลิกแอซิด (พีเอเอ) บรัชที่ยึดติดบนพื้นผิวมีศักยภาพในการนำไปใช้เป็นฟิล์มบางฟังก์ชันแนลสำหรับการประยุกต์ทางเทคโนโลยีชีวภาพและนาโนเทคโนโลยี หมู่คาร์บอกซิลสามารถจับยึดกับสารชีวโมเลกุลได้ผ่านทั้งพันธะโควาเลนต์และไอออนิก ในงานวิจัยนี้เตรียมพีเอเอบรัชโดยปฏิกิริยาพอลิเมอไรเซชันริเริ่มจากพื้นผิวด้วยกลไกแบบอะตอมทรานส์เฟอร์แรดิคัลพอลิเมอไรเซชันของเทอร์เทียรีบิวทิลอะคริเลต ตามด้วยการกำจัดหมู่เทอร์เทียรีบิวทิลด้วยปฏิกิริยาไฮโดรไลซิสในสภาวะกรด ความหนาแน่นของหมู่คาร์บอกซิลบนพื้นผิวจะแปรเปลี่ยนตามความยาวและความหนาแน่นการกราฟต์ของโซ่พอลิเมอร์ จากการวิเคราะห์การจับยึดอย่างจำเพาะเจาะจงระหว่างไบโอตินที่ยึดติดกับพีเอเอบรัชและสเตรปทาวิดินโดยใช้เทคนิคเซอร์เฟสพลาสมอนเรโซแนนต์แสดงให้เห็นว่าพีเอเอบรัชสามารถทำหน้าที่เป็นฟิล์มบางสำหรับประยุกต์ทางด้านไบโอเซนเซอร์ได้ ทั้งนี้ได้ทำการศึกษาผลของความหนาแน่นในการกราฟต์ของไบโอตินและความสามารถในการบวมตัวของพีเอเอบรัชที่มีต่อความสามารถในการตรวจวัดสเตรปทาวิดิน พีเอเอบรัชแสดงสมบัติที่เหนือกว่าฟิล์มบางชั้นเดียวประกอบด้วยตัวเองที่มีหมู่ปลายเป็นคาร์บอกซิลซึ่งเป็นฟิล์มบางที่นิยมใช้ทางด้านไบโอเซนเซอร์ ทั้งในแง่ของความสามารถในการจับยึดกับสารตัวอย่างอย่างจำเพาะเจาะจงและความสามารถในการต้านการดูดซับอย่างไมจำเพาะเจาะจงของโปรตีน นอกจากนี้พีเอเอบรัชยังสามารถทำหน้าที่เป็นสับสเตรทสำหรับการประกอบฟิล์มแบบชั้นต่อชั้น เพื่อเตรียมฟิล์มมัลทิเลเยอร์ของพอลิอิเล็กโทรไลท์ ได้แก่ ไคโทซาน พอลิอะคริลิกแอซิด และ พอลิ(10,12-เพนทาโคซาดิโนอิกแอซิด)เวสิคัล พีเอเอบรัชมีความหนาแน่นการกราฟท์สูงพอที่จะเหนี่ยวนำให้เกิดการยืดออกของโซ่พอลิเมอร์ส่งผลให้ชั้นเดี่ยวที่ดูดซับมีความหนาตามไปด้วย ผลจากการทดลองแสดงให้เห็นว่าความหนาแต่ละชั้นและมัลทิเลเยอร์แปรผันเป็นสัดส่วนกับความหนาของพีเอเอบรัช ซึ่งสามารถเตรียมให้แต่ละชั้นมีความหนาได้มากถึง 10 นาโนเมตร เมื่อใช้ภาวะในการดูดซับที่เหมาะสม จากผลการศึกษาการดูดซับของโปรตีนพบว่าสามารถเปลี่ยนไบโอแอคติวิตีของฟิล์มมัลทิเลเยอร์ได้โดยการเปลี่ยนฟิล์มชั้นสุดท้ายที่ดูดซับ แนวทางในการวิจัยนี้เป็นประโยชน์อย่างยิ่งต่อการประยุกต์ใช้งานที่ต้องการฟิล์มที่เสถียรซึ่งมีความหนาในระดับนาโนเมตรโดยไม่ต้องใช้จำนวนรอบในการดูดซับหลายรอบ

คำหลัก : พอลิอะคริลิกแอซิด, พอลิเมอร์บรัช, เอทีอาร์พี, ไบโอเซนเซอร์, ฟิล์มมัลทิเลเยอร์

ABSTRACT

Surface-tethered poly(acrylic acid) (PAA) brushes can potentially be used as functional thin film for applications in biotechnology and nanotechnology. Their carboxyl groups serve as versatile moieties for both covalent and ionic immobilization of bioactive molecules. In this research, poly(*tert*-butyl acrylate) (P*t*-BA) brushes were prepared by surface-initiated atom transfer radical polymerization of *t*-BA. PAA brushes were subsequently obtained after the *tert*-butyl groups of the P*t*-BA brushes were removed by acid hydrolysis. Carboxyl group density on the surface was varied as a function of polymer chain length (MW) and graft density. Using surface plasmon resonance (SPR) technique, the potential of the PAA brushes as precursor layer for the biosensing applications based on specific molecular recognition between biotin attached PAA brushes and streptavidin (SA) can be demonstrated. The SA detectability as a function of immobilized biotin density, swellability of the PAA brushes was evaluated. In comparison with carboxyl-terminated self-assembled monolayer, a conventional precursor layer for biosensor, the PAA brushes showed superior characteristics in terms of the specific binding with the analyte as well as the ability to maintain high resistance to nonspecific protein adsorption. In addition, the PAA brushes can be used as a substrate for layer-by-layer assembly of selected polyelectrolytes, chitosan, poly(acrylic acid) and poly(10,12-pentacosadiynoic acid) vesicles to generate multilayer films. The graft density of the PAA brushes was high enough to induce chain stretching allowing a thicker individual adsorbed layer to be formed. It was demonstrated that the thickness of each individual layer and multilayer varied in proportion to the thickness of the PAA brushes. An increment of up to 10 nm in thickness of the individual layer can be achieved under an appropriate adsorption condition. According to protein adsorption studies, the bioactivity of the multilayer film can be tailored by changing the last polyelectrolyte deposited. This approach offers a great benefit for applications which require fabrication of stable nanometer-thick film without having to use many cycles of deposition.

Keywords : poly(acrylic acid), polymer brush, ATRP, biosensor, multilayer film

CONTENTS

		Page
ACKNOWLEDGEMENT		i
ABSTRACT IN THAI		ii
ABSTRACT IN ENGLISH		iii
LIST OF FIGURES		vi
LIST OF TABLES		x
CHAPTER I : INTRODUCTION		1
1.1	Significance of Research Problem	1
1.2	Objectives	5
CHAPTER II : THEORY AND LITERATURE REVIEW		6
2.1	Polymer brushes	6
2.2	Atom transfer radical polymerization	11
2.3	Poly(acrylic acid)	15
2.4	Polymeric thin films for biosensing applications	16
2.5	Layer-by-layer adsorption	17
2.6	Formation of polyelectrolyte multilayer assemblies on polyelectrolyte brushes	19
CHAPTER III : EXPERIMENTAL		23
3.1	Materials	23
3.2	Equipments	24
3.3	Procedures	25
CHAPTER IV : RESULTS AND DISCUSSION		30
4.1	Formation of surface-tethered PAA brushes	30
4.2	Determination of SA binding to the biotin-attached PAA brushes	38
4.3	Swelling behavior of the PAA brushes	44
4.4	Effect of the PAA brushes graft density on the SA binding of the biotin attached PAA brushes	47

4.5 Multilayer assembly on the surface-tethered PAA brushes …… 53

4.6 Stability of CHI/PAA multilayer films on the surface-tethered PAA brushes...…….....……... 61

4.7 Protein adsorption of the multilayer film deposited on the surface-tethered PAA

brushes…….....…….. 62

65

67

CHAPTER V : EXECUTIVE SUMMARY ……..…… 73

REFERENCES……... 75

OUTPUT…….…….

APPENDIX …….

LIST OF FIGURES

Figure Page

1.1	Schematic representation of (a) SAM of carboxyl-terminated alkanethiol (b) poly(acrylic acid) brushes attached on substrate ……..	3
1.2	Schematic representation of polymeric film assembled on (a) conventional charged substrate and (b) surface-attached poly(acrylic acid) brushes……	4
2.1	Examples of polymer systems comprising polymer brushes ……..	7
2.2	Classification of linear polymer brushes, (a_1–a_4) homopolymer brushes; (b) mixed homopolymer brush; (c) random copolymer brush; (d) block copolymer brush ……..	8
2.3	Preparation of polymer brushes by “physisorption”, “grafting to” and “grafting from” ……...	9
2.4	Architectural forms of polymers available by living polymerization techniques ……..……..	12
2.5	Mechanism of ATRP ……..……	13
2.6	Equilibrium reaction in ATRP ……..……	13
2.7	Copper complexes used as ATRP catalysts ……...…..……	14
2.8	Example of ligands used in copper-mediated ATRP ……..….	15
2.9	Representative examples of protected (meth)acrylic acid monomers with masked acid group ……..……..….	16
2.10	Alternate layer-by-layer adsorption of polyanion and polycation onto a positively charged substrate……..……..….	18
2.11	Film thickness as a function of the layer numbers for (a) MePVP/PSSNa multilayers using 7.6 nm(■) and 22.9 nm (★) MePVP covalently attached monolayer as the first layer and (b) PMAA/MePVP multilayers using 6 nm (□) and 30 nm (•) MePVP covalently attached monolayer as the first layer. The solid lines show a linear fit of the dependence of the film thickness on the number of deposited layers……..	21
2.12	Schematic depiction of the formation of PEL multilayers through PEL brushes. (A) strong/weak system; (B) strong/strong system ……	21
3.1	Schematic diagram showing the formation of P*t*-BA and PAA brushes followed by carboxyl group activation and biotin immobilization ……	27

LIST OF FIGURES (Continued)

Figure		Page
4.1	The molecular weight ($\overline{M}_n$) (●, ■) of the P*t*-BA in solution and thickness (○, □) of the P*t*-BA brushes as a function of the polymerization time and formed from a targeted DP of 100 (●,○) or 200 (■, □). Data are shown as the mean ± SD and are derived from 3 repeats……..	31
4.2	Schematic representation of activation/deactivation cycles of ATRP process……	31
4.3	^{1}H-NMR spectra of (A) *t*-BA and (B) P*t*-BA in solution ……	32
4.4	Relationship between the ellipsometric thickness of P*t*-BA brushes with the molecular weight ($\overline{M}_n$) of free P*t*-BA for the targeted DP = 100…	33
4.5	Relationship between the ellipsometric thickness of P*t*-BA brushes with the molecular weight ($\overline{M}_n$) of free P*t*-BA for targeted DP = 200…..…	33
4.6	AFM micrographs of the gold-coated SPR substrate (a) before and (b) after being grafted with P*t*-BA brushes obtained from the targeted DP of 200 and reaction time 24 h……	34
4.7	Section analysis of the side-viewed cross-section of the gold-coated SPR substrate grafted with P*t*-BA brushes after being scraped by AFM tip showing the thickness of P*t*-BA brushes ……..……	35
4.8	FT-IR spectra of (a) bare silica particles and the silica particles surface-functionalized with (b) P*t*-BA brushes, (c) PAA brushes, (d) activated PAA brushes, and (e) PAA brushes-biotin, obtained from a targeted DP of 200..... ……..……	37
4.9	The density of carboxyl groups of the PAA brushes on the silicon oxide surface as a function of $\overline{M}_n$ when derived from a targeted DP of 100 (○) or 200 (●) at different polymerization time. Data are shown as the mean ± SD and are derived from 3 repeats……	38

LIST OF FIGURES (Continued)

Figure		Page
4.10	Optical (top) and fluorescence (bottom) images of silica particles grafted with biotin-attached PAA brushes after binding with FITC-SA, showing the (a) control and (b) PAA brushes-biotin obtained from a targeted DP of 200 using a polymerization time of 24 h. Images shown are representative of at least 3 such fields of view per sample and 3 independent samples……	39
4.11	Representative SPR sensorgrams of the gold-coated SPR substrate bearing PAA brushes (3D-matrix) and MUA (2D-matrix) before and after (a) biotin immobilization and (b) SA binding. Sensorgrams shown are representative of 3 independent samples……	41
4.12	SPR angle shifts after the step of biotin immobilization and SA binding on the PAA brushes as a function of their $\overline{M}_n$, as determined by SPR analysis. Numbers above each pair of bar graphs are the binding ratio between biotin and SA. Data are shown as the mean ± SD and are derived from 3 repeats ……	42
4.13	Adsorption of proteins in PBS (10 mM, pH 7.4) on the MUA-biotin and PAA brushes-biotin based sensing platforms. Data are shown as the mean ± SD and are derived from 3 repeats ……	43
4.14	SPR angle shift of PAA brushes: (a) target DP = 100 and (b) target DP = 200 before (solid line) and after (dashed line) biotin immobilization …	46
4.15	SPR angle shift of PAA brushes having target DP = 200 after biotin immobilization and SA binding as a function of degree of carboxyl group activation which is expressed in term of the amount of introduced *N*-succimidyl groups……	47
4.16	The synthetic pathway for preparation of grafted PAA brushes having varied graft density onto SPR chip ……	48
4.17	AFM images of (a) bare gold surface before and after being grafted with PAA brushes having (b) 10%, (c) 50%, and (d) 100% graft density ……	49
4.18	Carboxyl group density as a function of graft density of PAA polymer brushes……	50

LIST OF FIGURES (Continued)

Figure		Page
4.19	SPR angle shift of PAA brushes having target DP = 200 after biotin immobilization and SA binding as a function of graft density ……	51
4.20	Adsorption of proteins at pH 7.4 on PAA brushes having target DP of 200 as a function of graft density in comparison with MUA ……	52
4.21	Adsorption of proteins at pH 7.4 on biotinylated PAA brushes having target DP of 200 as a function on graft density in comparison with biotinylated MUA……..	53
4.22	UV-Vis absorbance at 640 nm of CHI/ PPCDA vesicles multilayer ($\overline{M}_n$ of CHI =100,000 g/mole) on glass-tethered PAA brushes having $\overline{M}_n$ = 9,125 (■) and 12,661(□) as a function of number of layer……	54
4.23	Ellipsometric thickness of CHI/PAA multilayer on silicon-tethered PAA brushes having $\overline{M}_n$ = 24,797 (○) and 13,835 (●) as a function of number of layer ……	56
4.24	FT-IR spectra of silica particles having (a) PAA brushes, (b) 1 layer of CHI on PAA brushes, and (c) CHI/PAA bilayer on PAA brushes ……	57
4.25	Water contact angle of CHI/PAA multilayer on surface-tethered PAA brushes …….……	58
4.26	AFM images of surface-tethered P*t*-BA brushes in comparison with the virgin silicon surface ……..……	58
4.27	AFM images of surface-tethered PAA brushes with CHI/PAA multilayer	60
4.28	FT-IR spectra of silica particles having $(CHI/PAA)_2CHI$ on PAA brushes (a) before and after soaking in buffer solution at (b) pH 3.5, (c) pH 7.4, and (d) pH 10.0…..……	62
4.29	Amount of adsorbed albumin on CHI/PAA multilayer on PAA brushes. The number written above the bar graph is the number of layer……	63
4.30	Chemical structures of HTACC and heparin……	64

LIST OF TABLES

Table		Page
4.1	Advancing (θ_A) and receding (θ_R) water contact angles of functionalized silicon substrates obtained with a targeted DP of 200 Data are shown as the mean ± SD and are derived from 5 repeats	36
4.2	Advancing (θ_A) water contact angle of the functionalized gold-coated SPR substrates obtained with a targeted DP of 200. Data are shown as the mean ± SD and are derived from 5 repeats……..	48
4.3	Advancing water contact angle of $(CHI/PAA)_2CHI$ on PAA brushes before and after soaking in buffer solutions ……..	62
4.4	Adsorbed albumin on CHI/PAA multilayer on PAA brushes ……	64

CHAPTER I

INTRODUCTION

1.1 Significance of Research Problem

Surface-initiated polymerization (SIP) has been introduced as a potential tool to generate a thin film of surface-tethered polymer brushes that can act as a modifying layer for the material's surface and so should be useful for biotechnology- and nanotechnology-related applications. The SIP, or so-called "grafting from", method holds advantages over the "grafting to" method of which the process suffers from the entropic barrier due to the crowding of the initial grafting polymer chains that prevent further insertion of the polymer onto the surface and so leads to a relatively low graft density. The "grafting from" method, on the other hand, involves a stepwise growth of the polymer chain from the surface by insertion of monomer, which allows a better control over the polymer chain length, graft density and thickness. SIP coupled with "living radical polymerization" has proven to be the most popular method for creating surface-tethered polymer brushes.

The development of biosensors largely relies on the immobilization of bioactive species to a sensor or measurement platform. The density of the immobilized bioactive species, as well as the distance between the surface of sensor and the bioactive species, should, in principle, affect the sensitivity, detection limit and signal-to-noise ratio of the biosensor. The precursor layer onto which the bioactive molecules (probes) are immobilized is conventionally based on a self-assembled monolayer (SAM) of end-functionalized alkanethiol, especially for gold-coated substrates, but the density of this cannot be greatly enhanced. Variation of the alkyl chain length, which is generally used for controlling the distance between the measurement platform and the sensing probes, is also limited due to the fact that long alkyl chains tend to induce non-specific adsorption of the bioactive molecules during the immobilization. This often causes an adverse effect on the biosensor efficiency.

Polymeric thin film has recently been recognized as an alternative precursor layer for the covalent attachment of biomolecules, such as proteins, antibodies, enzymes and DNA. In principle, its three-dimensional (3D) characteristic should allow for a higher functional group

density or binding capacity (mole of bioactive species per unit area), a less confined reactivity, and provides a greater design flexibility than the two dimensional (2D) SAM-based system. Carboxymethylated dextran (CM-dextran) is currently the most popular 3D matrix system. It is commercially available as 3D chips with different thicknesses and modifiers that can readily be used for biosensing applications. By using surface plasmon resonance (SPR), it has been reported that when a streptavidin (SA) layer was immobilized on the 3D matrix of the CM-dextran, it provided twice the amount of immobilized biotinylated DNA in comparison with the SA layer that was built on the 2D carboxyl-terminated SAM. The greater DNA probe density of the 3D matrix, however, yielded an inferior DNA hybridization efficiency than that of the 2D matrix. This unsatisfactory performance was explained as the result of limited accessibility of the DNA analyte to the immobilized DNA probes embedded inside the 3D matrix of the 50 nm thick polymeric film. If so, it should become even more problematic for larger sized biomolecules with a much more diversified structural variation in comparison to DNA.

The ability to fine tune the thickness of polymer brushes, even as thin as a few nanometers, by controlling the polymerization conditions has led to the suggestion that SIP can be employed as an alternative method to overcome the above-mentioned obstacles imposed by the diffusion barrier of analytes into the relatively thick polymeric coating, especially in the case of the CM-dextran. Therefore, the first part of this research aims to determine the feasibility of using surface-tethered poly(acrylic acid) (PAA) brushes generated by surface-initiated polymerization for biosensing applications. It is anticipated that carboxyl groups along poly(acrylic acid) brushes can function as precursor moieties for immobilization of bioactive species that act as sensing probes of biosensor. Using “living” atom transfer radical polymerization (ATRP), the carboxyl group density which depends on molecular weight of polymer brushes should be conveniently controlled as a function polymerization condition. Reactivity of the carboxyl group was tested against the immobilization of biotin, a frequently used bioactive molecule in biosensor. Subsequent binding with fluorescent-labeled streptavidin was thereby determined. Biospecific recognition between the biotin-attached PAA brushes and SA was also investigated using SPR in comparison with the 2D matrix of the SAM carboxyl-terminated alkanethiol (Figure 1.1). In addition, the ability to resist non-specific interactions with two non-target proteins of a similar pI but different sizes and structures was also evaluated to determine the applicability of the developed 3D platform for biosensing applications.

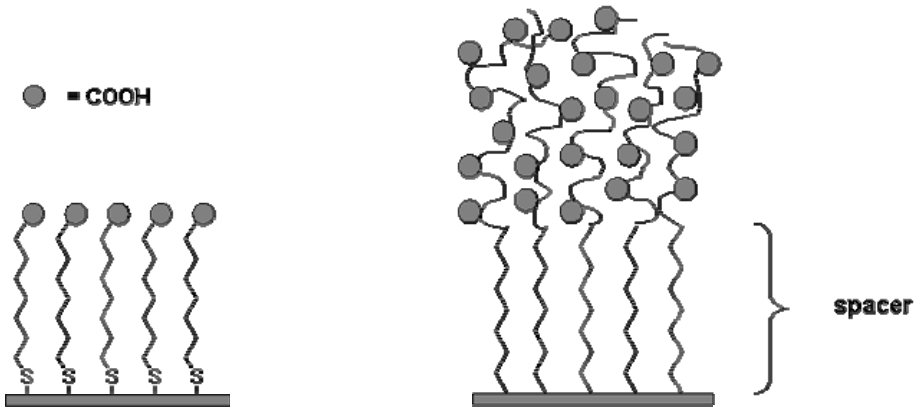

Figure 1.1 Schematic representation of (a) SAM of carboxyl-terminated alkanethiol (b) poly(acrylic acid) brushes attached on substrate.

Layer-by-layer (LBL) assembly of oppositely charged polyelectrolytes (PEL) has been recognized as a powerful, yet simple strategy to engineer surfaces with specific properties. This versatile technique offers the benefit of solvent-free processing as well as the ability to coat all available surfaces of virtually any material, irrespective of shape or size, with uniform ultrathin films of precisely controlled thickness. Surface properties of the assembled multilayer film depend on the type of polyelectrolytes, thickness and roughness. However, the stability of the multilayer system is often of concern, especially in the environment that causes the displacement of the first adsorbed layer of polyelectrolyte and the subsequent desorption of the whole multilayer assembly i.e. changing the sign of the surface charge of the substrate or by addition of competing low molecular weight electrolytes.

The second part of this research thus concentrates on the use of a surface-tethered polyelectrolyte brushes as a substrate for multilayer assembly. It is believed that the problem of stability can be overcome since the polyelectrolyte chains, generated by SIP approach, are attached to the substrate by covalent bonds. PAA brushes are weak anionic polyelectrolyte when pH of the solution is appropriately adjusted and thus can be used as charged substrate for fabrication of multilayer films by LBL method. Generated by SIP, it is anticipated that the graft density of the PAA brushes is high enough to induce chain stretching allowing a thicker individual layer to be formed. In general, the greater carboxyl group density and graft density of the PAA brushes should yield the thicker individual layer (Figure 1.2). The concept of using surface-tethered polyelectrolyte brushes as a substrate for multilayer assembly not only can

help improving the stability of the multilayer film, but also reduce the number of deposition step. This approach offers a great benefit for applications which require fabrication of nanometer-thick film without having to use many cycles of deposition.

In this particular study, two multilayer systems were fabricated. The first system is carboxyl-terminated polydiacetylene vesicles/poly(acrylic acid) (PPCDA/PAA). The effect of PAA molecular weight and adsorption time on the growth of PPCDA/PAA multilayer on glass-tethered PAA brushes can be conveniently monitored using UV-Vis spectroscopy. The second system is chitosan/poly(acrylic acid) (CHI/PAA). CHI is of particular interest because of its natural origin and favorable physicochemical and biological properties. CHI is a partially deacetylated form of chitin, a natural substance found abundantly in the exoskeletons of insects, shells of crustaceans, and fungal cell walls. It is also biocompatible, non-toxic, and antibacterial. CHI is thus considered as an attractive material that can be potentially used in many biomedical-related applications. The deposition of bioactive polyelectrolytes such as heparin sodium salt, *N*-[(2-hydroxyl-3-trimethylammonium)propyl] chitosan chloride as the outermost layer on the CHI/PAA multilayer was also studied to generate the biofunctional thin film. Biological responses in terms of protein adsorption and antibacterial activity of some multilayer films were tested. We hypothesize that alternate response can be achieved as long as each layer is thick enough and overall biological response depends on the outermost layer. The consequence of this study should provide fundamental information that can lead to the development of thin-film fabrication for applications in nanotechnology and biotechnology.

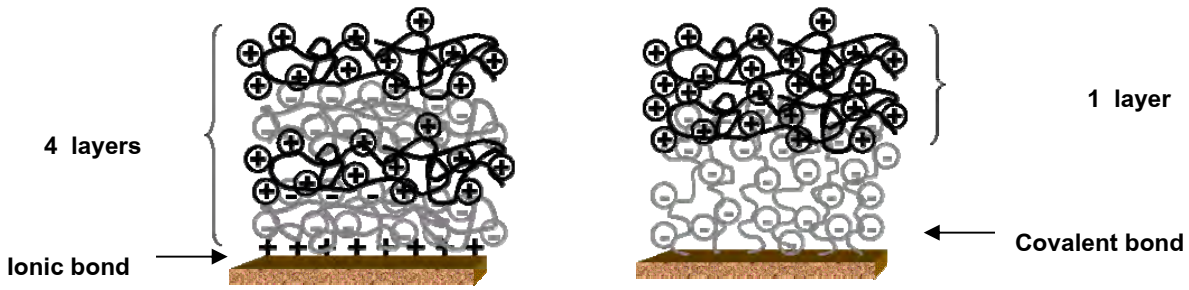

Figure 1.2 Schematic representation of polymeric film assembled on (a) conventional charged substrate and (b) surface-attached poly(acrylic acid) brushes.

1.2 Objectives

1. To synthesize poly(acrylic acid) brushes by surface-initiated atom transfer radical polymerization
2. To determine the ability of the surface-grafted poly(acrylic acid) brushes as the precursor layer for biosensing appplications in comparison with the SAM-based system
3. To determine the ability of the surface-grafted poly(acrylic acid) brushes as the substrate for depositing multilayer film of polyelectrolytes by layer-by-layer assembly

CHAPTER II

THEORY AND LITERATURE REVIEW

2.1 Polymer brushes

Polymer brushes refer to an assembly of polymer chains which are tethered by one end to a surface or an interface. Tethering is sufficiently dense that the polymer chains are crowded and forced to stretch away from the surface or interface to avoid overlapping, sometimes much further than the typical unstretched size of a chain. These stretched configurations are found under equilibrium conditions; neither a confining geometry nor an external field is required. This situation, in which polymer chains stretch along the direction normal to the grafting surface, is quite different from the typical behavior of flexible polymer chains in solution where chains adopt a random-walk configuration. A series of discoveries show that the deformation of densely tethered chains affects many aspects of their behavior and results in many novel properties of polymer brushes [1].

Polymer brushes are a central model for many practical polymer systems such as polymer micelles, block copolymers at fluid–fluid interfaces (e.g. microemulsions and vesicles), grafted polymers on a solid surface, adsorbed diblock copolymers and graft copolymers at fluid–fluid interfaces. All of these systems, illustrated in Figure 2.1, have a common feature: the polymer chains exhibit deformed configurations. Solvent can be either present or absent in polymer brushes. In the presence of a good solvent, the polymer chains try to avoid contact with each other to maximize contact with solvent molecules. With solvent absent (melt conditions), polymer chains must stretch away from the interface to avoid overfilling incompressible space.

The interface to which polymer chains are tethered in the polymer brushes may be a solid substrate surface or an interface between two liquids, between a liquid and air, or between melts or solutions of homopolymers. Tethering of polymer chains on the surface or interface can be reversible or irreversible. For solid surfaces, the polymer chains can be chemically bonded to the substrate or may be just adsorbed onto the surface. Physisorption on a solid surface is usually achieved by block copolymers with one block interacting strongly with the substrate and another block interacting weakly. For interfaces between

fluids, the attachment may be achieved by similar adsorption mechanisms in which one part of the chain prefers one medium and the rest of the chain prefers the other.

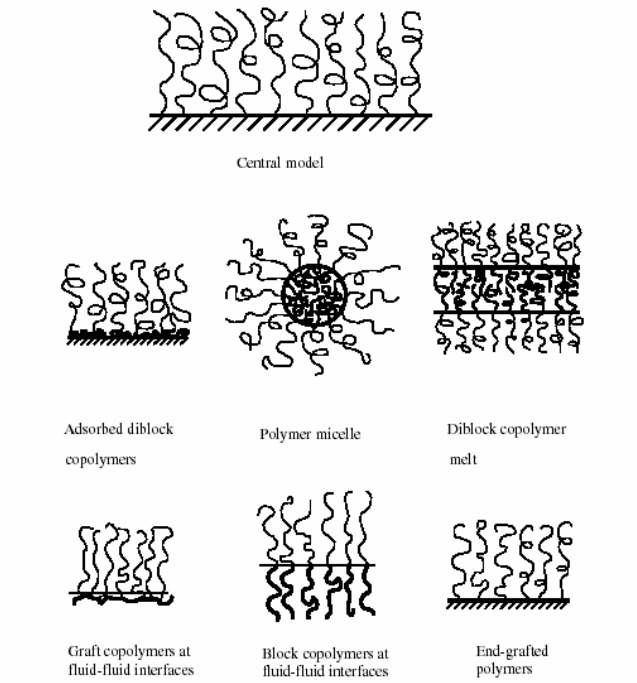

Figure 2.1 Examples of polymer systems comprising polymer brushes.

In terms of polymer chemical compositions, polymer brushes tethered on a solid substrate surface can be divided into homopolymer brushes, mixed homopolymer brushes, random copolymer brushes and block copolymer brushes. Homopolymer brushes refer to an assembly of tethered polymer chains consisting of one type of repeat unit. Mixed homopolymer brushes are composed of two or more types of homopolymer chains [2]. Random copolymer brushes refer to an assembly of tethered polymer chains consisting of two different repeat units which are randomly distributed along the polymer chain [3]. Block copolymer brushes refer to an assembly of tethered polymer chains consisting of two or more homopolymer chains covalently connected to each other at one end [4]. Homopolymer brushes can be further divided into neutral polymer brushes and charged polymer brushes. They may also be classified in terms of rigidity of the polymer chain and would include flexible polymer brushes, semiflexible polymer brushes and liquid crystalline polymer brushes. These different polymer brushes are illustrated in Figure 2.2.

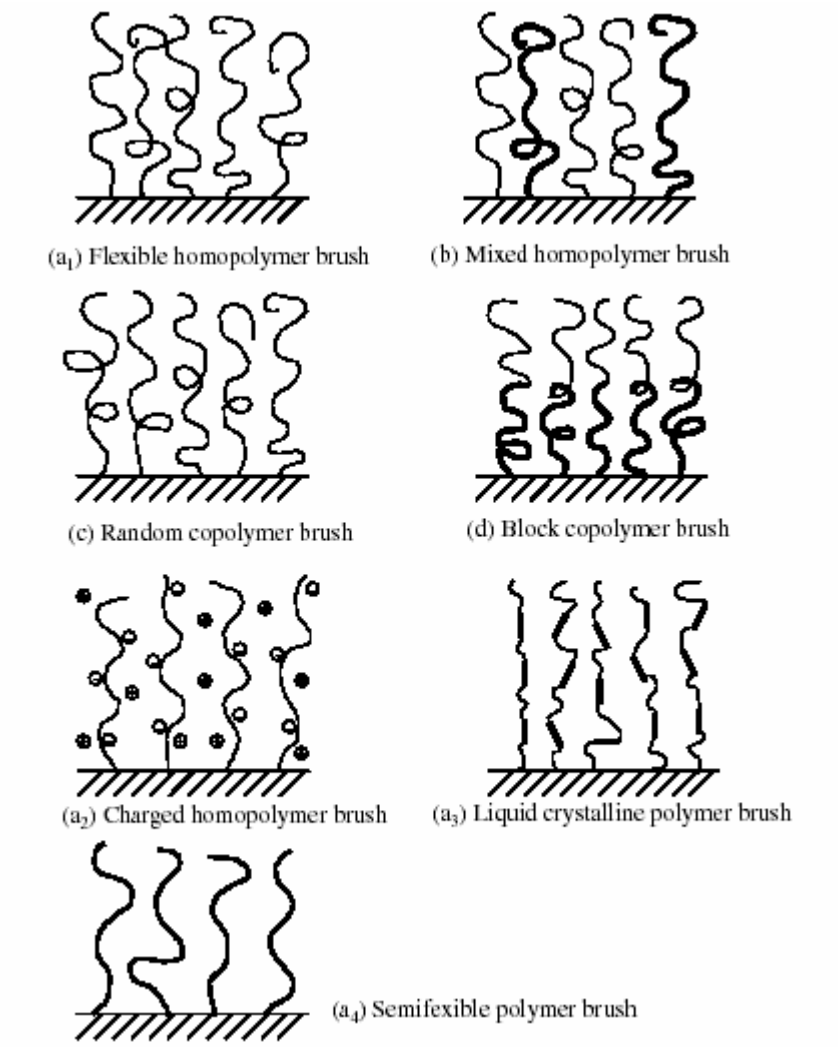

Figure 2.2 Classification of linear polymer brushes, (a_1–a_4) homopolymer brushes; (b) mixed homopolymer brush; (c) random copolymer brush; (d) block copolymer brush.

Generally, there are two ways to fabricate polymer brushes: physisorption and covalent attachment (Figure 2.3). For polymer physisorption, block copolymers adsorb onto a suitable substrate with one block interacting strongly with the surface and the other block interacting weakly with the substrate. The disadvantages of physisorption include thermal and solvolytic instabilities due to the non-covalent nature of the grafting, poor control over polymer chain density and complications in synthesis of suitable block copolymers. Tethering of the polymer chains to the surface is one way to surmount some of these disadvantages. Covalent attachment of polymer brushes can be accomplished by either “grafting to” or “grafting from” approaches. In a “grafting to” approach, preformed end-functionalized polymer molecules react with an appropriate substrate to form polymer brushes. This technique often leads to low grafting density and low film thickness, as the

polymer molecules must diffuse through the existing polymer film to reach the reactive sites on the surface. The steric hindrance for surface attachment increases as the tethered polymer film thickness increases. The “grafting from” approach is a more promising method in the synthesis of polymer brushes with a high grafting density. “Grafting from” can be accomplished by treating a substrate with plasma or glow-discharge to generate immobilized initiators onto the substrate followed by in situ surface-initiated polymerization. However “grafting from” well-defined self-assembled monolayers (SAMs) is more attractive due to a high density of initiators on the surface and a well-defined initiation mechanism. Also progress in polymer synthesis techniques makes it possible to produce polymer chains with controllable lengths. Polymerization methods that have been used to synthesize polymer brushes include cationic, anionic, TEMPO-mediated radical, atom transfer radical polymerization (ATRP) and ring opening polymerization.

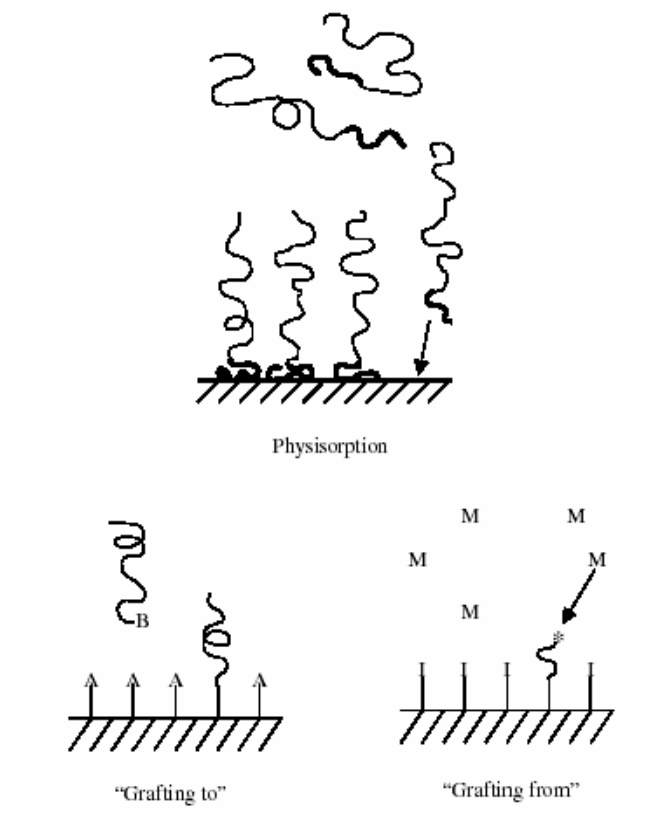

Figure 2.3 Preparation of polymer brushes by “physisorption”, “grafting to” and “grafting from”.

In order to achieve a better control of molecular weight and molecular weight distribution and to obtain novel polymer brushes like block copolymer brushes, controlled radical polymerizations including ATRP, reverse ATRP, TEMPO-mediated and iniferter

radical polymerizations have been used to synthesize tethered polymer brushes on solid substrate surfaces [5-10].

In recent years, ATRP has been the most widely employed technique for the formation of polymer brushes *via* surface initiated polymerization. ATRP is compatible with a variety of functionalized monomers. The living/controlled character of the ATRP process yields polymers with a low polydispersity ($\overline{M}_w/\overline{M}_n$) that are end-functionalized and so can be used as macroinitiators for the formation of di- and triblock copolymers. Equally important, surface-initiated ATRP is experimentally more accessible than for example, the living anionic and cationic polymerizations, which require rigorously dry conditions. The synthesis of thiol and silane derivatized surface-bound initiators is easier than AIBN-silane derivative or the nitroxide silane derivative for free radical and NMP polymerizations.

In 1998, Ejaz and coworkers prepared poly(methyl methacrylate) brushes on silicon surface *via* surface-initiated atom transfer radical polymerization. The addition of free initiator to the polymerization solution yields free polymer which can be characterized by conventional methods. The relatively narrow polydispersities of these polymers in conjunction with the molecular weights were proportional to monomer conversion points towards the surface polymerization being controlled. The thickness of the polymer brushes was related to the concentration of the free initiator added, the lower concentration of free initiator the thicker the films being achieved [6].

Husseman and coworkers [7] applied ATRP in the synthesis of tethered polymer brushes on silicon wafers and achieved great success. They prepared SAMs of 5-trichlorosilylpentyl-2-bromo-2-methylpropionate on silicate substrates. The α-bromoester is a good initiator for ATRP. They have successfully synthesized PMMA brushes by the polymerization of MMA initiated from the SAMs. It has also been reported that tethered polyacrylamide has been obtained from surface initiated ATRP of acrylamide on a porous silica gel surface [8].

Matyjaszewski and coworkers [11] reported a detailed study of polymer brush synthesis using ATRP in controlled growth of homopolymer and block copolymers from silicon surfaces. They described that the persistent radical effect must be considered in controlled radical polymerizations. In other words, a sufficient concentration of deactivation must be available to provide control over chain lengths and distributions. The Cu (II) can be supplied by termination of initiator molecules in the early stages of the polymerization or by addition of the transition metal complex prior to commencement of the reaction. Moreover, the only factor affected is the kinetics of the reaction; in the former case, first-order

consumption of monomer is dictated by the chains generated from the free initiator while in the latter, due to the extremely low concentration of alkyl halide bound to the surface and low monomer conversion, growth of polymer chains scales linearly with reaction time. Their conclusion suggested that the design of such complex structures whether in solution or at an interface, understanding of the relative rates of chain propagation, equilibrium constants, and the influences of the end group, metal, and ligand in crossover reaction are important. Factors such as initiator functionality and blocking efficiency can have a profound influence on the physical properties of the resulting material.

In 2001, Werne and Patten [12] reported the preparation of structurally well-defined polymer-nanoparticle hybrids by modifying the surface of silica nanoparticles with initiators for ATRP and by using these initiator-modified nanoparticles as macroinitiators. They found that polymerizations of styrene and methyl methacrylate (MMA) using the nanoparticle initiators displayed the diagnostic criteria for a controlled/“living” radical polymerization: an increase in the molecular weight of the pendant polymer chains with monomer conversion and a narrow molecular weight distribution for the grafted chains. Polymerization of styrene from smaller silica nanoparticles (75-nm-diameter) exhibited good molecular weight control, while polymerization of MMA from the same nanoparticles exhibited good molecular weight control only when a small amount of free initiator was added to the polymerization solution. For the polymerizaiton of both styrene and MMA from larger silica nanoparticles (300-nm-diameter) did not exhibit molecular weight control. Molecular weight control was induced by the addition of a small amount of free initiator to the polymerization but was not induced when 5-15 mol% of deactivator (Cu(II) complex) was added. These findings provide guidance for efforts in using ATRP for the controlled grafting of polymers from high and low surface area substrates.

2.2 Atom transfer radical polymerization

Living polymerization techniques give the synthetic chemist two particularly powerful tools for polymer chain design: the synthesis of block copolymers by sequential addition of monomers and the synthesis of functional-ended polymers by selective termination of living ends with appropriate reagents. The main architectural features available starting with these two basic themes are listed in Figure 2.4 along with applications for the various polymer types.

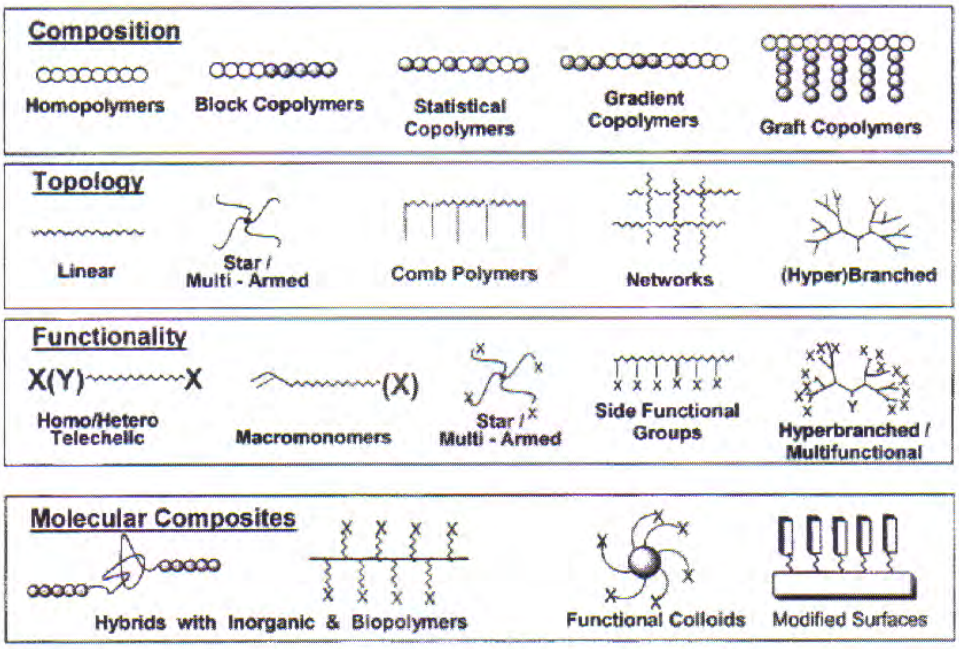

Figure 2.4 Architectural forms of polymers available by living polymerization techniques.

In this research, free radical process for living polymerization is selected and described. The concept of using stable free radicals, such as nitroxides, to reversibly react with the growing polymer radical chain end can be traced back to the pioneering work of Rizzardo and Mozd [13]. After further refinement by Georges [14], the basic blueprint for all subsequent work in the area of "living" free radical polymerization was developed. Subsequently, the groups of Sawamoto [15], Matyjaszewski [16], Percec [17] and others [18-19] have replaced the stable nitroxide free radical with transition metal species to obtain a variety of copper-, nickel-, or ruthenium-mediated "living" free radical systems. These systems were called atom transfer radical polymerization (ATRP).

This mechanism is an efficient method for carbon-carbon bond formation in organic synthesis. In some of these reactions, a transition-metal catalyst acts as a carrier of the halogen atom in a reversible redox process (Figure 2.5). Initially, the transition-metal species, M_t^n, abstracts halogen atom X from the organic halide, RX, to form the oxidized species, $M_t^{n+1}X$, and the carbon-centered radical $R^\bullet$. In the subsequent step, the radical $R^\bullet$ participates in an inter- or intramolecular radical addition to alkene, Y, with the formation of the intermediate radical species, $RY^\bullet$. The reaction between $M_t^{n+1}X$ and $RY^\bullet$ results in a target product, RYX, and regenerates the reduced transition-metal species, M_t^n, which further promotes a new redox process. The fast reaction between $RY^\bullet$ and $M_t^{n+1}X$

apparently suppresses biomolecular termination between alkyl radicals and efficiently introduces a halogen functional group X into the final product in good to excellent yields.

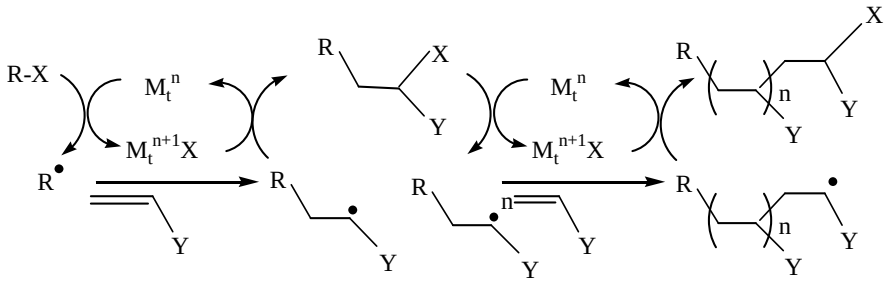

Figure 2.5 Mechanism of ATRP.

The ATRP system relies on one equilibrium reaction in addition to the classical free-radical polymerization scheme (Figure 2.6). In this equilibrium, a dormant species, RX, reacts with the activator, M_t^n, to form a radical $R^\bullet$ and deactivating species, $M_t^{n+1}X$. The activation and deactivation rate parameters are k_{act} and k_{deact}, respectively. Since deactivation of growing radicals is reversible, control over the molecular weight distribution and, in the case of copolymers, over chemical composition can be obtained if the equilibrium meets several requirements [20-21].

1. The equilibrium constant, k_{act}/k_{deact}, must be low in order to maintain a low stationary concentration of radicals. A high value would result in a high stationary radical concentration, and as a result, termination would prevail over reversible deactivation.

2. The dynamics of the equilibrium must be fast; i.e. deactivation must be fast compared to propagation in order to ensure fast interchange of radicals in order to maintain a narrow molecular weight distribution.

$$R\text{-}X + M_t^n \underset{k_{deact}}{\overset{k_{act}}{\rightleftharpoons}} R^\bullet + M_t^{n+1}X$$

Figure 2.6 Equilibrium reaction in ATRP [22].

Transition metal complexes (catalyst) are perhaps the most important components of ATRP. It is the key to ATRP since it determines the position of the atom transfer equilibrium and the dynamics of exchange between the dormant and active species. There are several prerequisites for an efficient transition metal catalyst. First, the metal center must have at least two readily accessible oxidation states separated by one electron. Second, the metal center should have reasonable affinity toward a halogen. Third, the coordination sphere around the metal should be expandable upon oxidation to selectively

accommodate a (pseudo)-halogen. Fourth, the ligand should complex the metal relatively strongly. Eventually, the position and dynamics of the ATRP equilibrium should be appropriate for the particular system. A variety of transition-metal complexes have been studied as ATRP catalysts.

Copper catalysts are superior in ATRP in terms of versatility and cost. Styrenes, (meth)acrylate esters and amides, and acrylonitrile have been successfully polymerized using copper-mediated ATRP. Examples of copper complexes used in ATRP are shown in Figure 2.7.

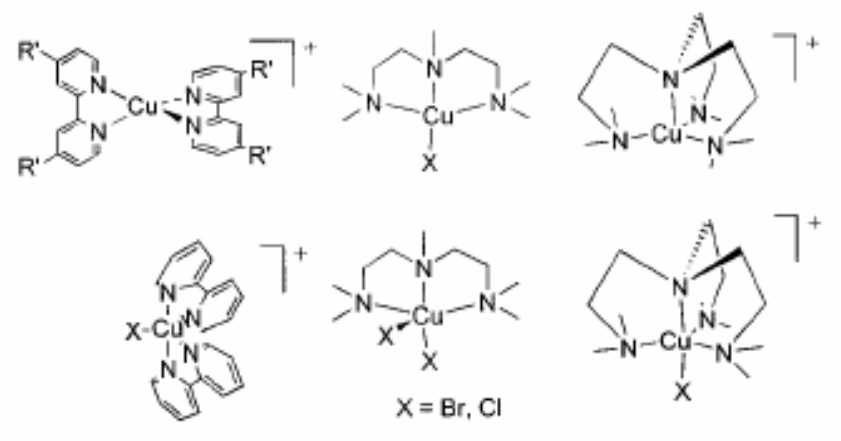

Figure 2.7 Copper complexes used as ATRP catalysts [23].

Nitrogen ligands have been used in copper-mediated ATRP. The monodentate (e.g., N(*n*Bu)$_3$), bidentate (e.g., dNbpy), and multidentate nitrogen ligands have been applied to copper-based ATRP. The electronic and steric effects of the ligands are important. Reduced catalytic activity or efficiency is observed when there is excessive steric hindrance around the metal center or the ligand has strongly electron-withdrawing substituents. A recent survey summarized different ligands employed in copper-mediated ATRP. The effect of the ligands and guidelines for ligand design were reviewed. Activity of N-based ligands in ATRP decreases with the number of coordinating sites N4 > N3 >N2, N1 and with the number of linking C-atoms C2 > C3, C4. It also decreases in the order R_2N- ≈ PyrEnDash-> R-N= > Ph-N=> Ph-NR-. Activity is usually higher for bridged and cyclic systems than for linear analogues. Examples of some N-based ligands used successfully in Cu-based ATRP are shown in Figure 2.8.

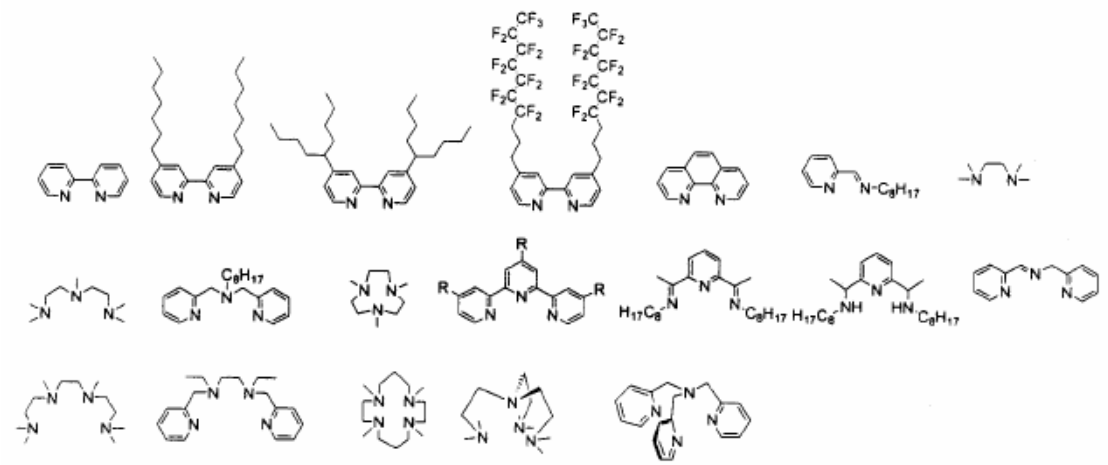

Figure 2.8 Example of ligands used in copper-mediated ATRP [23].

2.3 Poly(acrylic acid)

Poly(acrylic acid) (PAA) is a weak polyelectrolyte, in which the degree of ionization is governed by the pH and ionic strength of aqueous solution. PAA has been extensively investigated, owing to many scientific and industrial applications. PAA can be covalently modified with a broad range of functional groups, such as fluorophores, electroactive groups, dyes and other biomolecules. Recent advances of the controlled/living polymerization techniques made it possible to produce well-defined polymer structures, such as graft copolymers, star polymers, polymer brushes, etc. The interest in synthesis and characterization of such complex polymer systems containing acrylic acid segments has increased enormously.

For the synthesis of well-defined polymers, controlled/living polymerization techniques have been traditionally employed where the polymerizations proceed in the absence of irreversible chain transfer and chain termination. Controlled/living polymerization of acrylic acid by ATRP presents a challenging problem because the acid monomer can poison the catalysts in system of ATRP by coordinating to the transition metal. In addition, nitrogen containing ligands can be protonated, which interferes with the metal complexation ability. Thus, typically, protected monomers have been employed, followed by a polymer-analogous deprotection, e.g. hydrolysis of protecting ester groups. Protected monomers with masked acid groups involve *tert*-butyl acrylate (*t*BuA), *tert*-butyl methacrylate (*t*BuMA), trimethylsilyl methacrylate (TMSMA), benzyl methacrylate (BzMA), 2-tetrahydropyranyl methacrylate (THPMA) and *p*-nitrophenyl methacrylate (PNPMA) (Figure 2.9). After acid hydrolysis, thermolysis, or catalytic hydrogenolysis, these protective groups liberate their original acid functionality. Essential prerequisites for the protected monomer are good

'livingness' under each polymerization condition and selective deprotection under mild conditions.

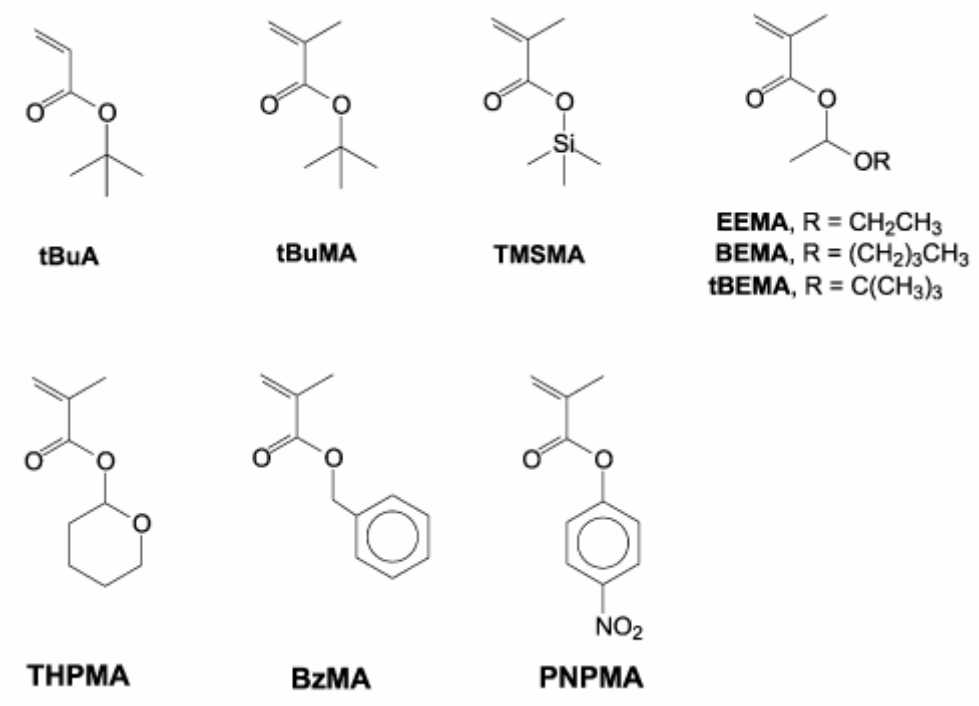

Figure 2.9 Representative examples of protected (meth)acrylic acid monomers with masked acid group.

For the ATRP system, Matyjaszewski et al [24-25] reported controlled polymerization of *t*BuA using methyl 2-bromopropionate, as the initiator and the CuBr/N,N,N',N'',N''-pentamethyldiethylenetriamine (PMDETA) catalyst system. In most ATRP based syntheses for block and further complex polymer systems, *t*BuA has been employed as a protected monomer, which may be due to the feasibility to control the polymerization and easy hydrolysis.

2.4 Polymeric thin film for biosensing applications

The success of utilizing polymer brushes in the fields of biotechnology has been continuously demonstrated. As monitored by SPR, the enhanced binding specificity/capacity of biotin-SA can be achieved through the use of poly(oligo(ethylene glycol) methacrylate) brushes as linkers with a 10-fold higher signal-to-noise ratio compared to that obtained with the SAM-based system [26]. Poly(acrylic acid) (PAA) brushes, on the other hand, were employed as matrices for binding a number of proteins, namely bovine serum albumin

(BSA), myoglobin, anti-IgG antibodies [27] and ribonuclease A [28]. Their high-protein binding capacity has made the surface-tethered PAA brushes a potential candidate for the development of affinity-based chromatography media for protein purification and protein microarrays. A new strategy to indirectly immobilize small biological molecules has been recently reported on the patterned surface-grafted PAA brushes using specific interactions between avidin that was attached to the PAA brushes and biotin-tagged proteins or between the biotin-tagged BSA that was bound to the PAA brushes and streptavidin which can later be used to bind with other biotinylated molecules [29]. The immunoreaction between anti-C-reactive protein (CRP) antibodies attached to PAA brushes and CRP in solution has also been described but with the detection being based upon quartz crystal microbalance analysis [30].

2.5 Layer-by-layer adsorption

The fabrication of ultrathin polymer films on modified surfaces of material is important for various scientific and biological fields in order to modify the intact characteristics of these surfaces exposed to biological system. In most cases, the material characteristics seem to be governed by the chemical composition of the surface. Coating a substrate surface with polymeric ultrathin films can maintain the original mechanical properties and/or fine structure of the substrate. The sequential adsorption of oppositely charged polyelectrolytes (PEL) by layer-by-layer (LBL) deposition technique is an efficient method for obtaining multilayer thin films with well-defined thickness, composition and functionalities. Due to the simplicity and the versatility of the buildup process, this technique opens enormously new opportunities to achieve the ideal model surface for use in applications such as biosensing [31], separation membrane [32] and optical devices [33]. LBL process was first introduced by Decher *et al.* in 1991. They have demonstrated the basic principle of buildup of multilayer materials using alternating adsorption of PEL [34]. The crucial feature of the sequential adsorption is the excessive adsorption at every stage of the polycation/polyanion assembly, which led to the recharging of the outermost surface at every step of film formation (Figure 2.10). Hence, the electrostatic interaction between the surface and polyions in solution is usually considered as the driving force for multilayer formation. The adsorption behavior of polyelectrolytes is influenced by a number of factors such as the charge density [35], the ionic strength or the pH of the solutions and the solvent quality [36].

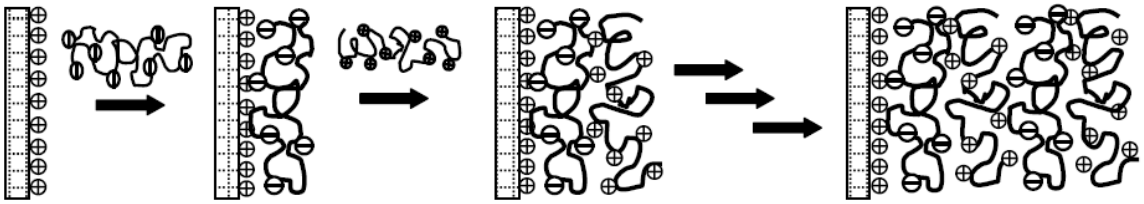

Figure 2.10 Alternate layer-by-layer adsorption of polyanion and polycation onto a positively charged substrate

In view of alternate layer-by-layer assembly of cationic chitosan and anionic PAA with oppositely charged polyelectrolytes, the following related publications have been reported.

In 1998, Lvov, *et al.* [37] prepared biocompatible molecular surfaces by an alternate assembly of cationic chitosan and anionic PSS at pH 4. Film growth and its dependence on ionic strength were analyzed by the QCM method. In addition, surface structure of the ultrathin films was examined by non-contact atomic force microscopy.

In 2002, Serizawa, *et al.* [38] generated multilayer systems based on chitosan. They varied concentration of NaCl as 0.2, 0.5 and 1 M. They found that the apparent film thickness increased upon increasing NaCl concentration. There was a critical concentration for the alternating activity; above a concentration of 0.5 M NaCl, both anti-and procoagulation could be observed on the dextran sulfate and chitosan surfaces, respectively. They also studied the formation of assembled film from a combination of chitosan and heparin, but the activity was different from that of the former system. They suggested that the polymer species and/or the assembly conditions are key factors for realizing the alternating bioactivities of films prepared by the layer-by-layer assembly.

Although LBL assembly normally includes noncovalent interactions between polymers, the technique can be used for the formation of covalent bonds between polymers using sequential chemical reactions. For the assembly with covalent bonds, the formation of covalent bonds by heat treatment after polymer assembly [39], the assembly of polymers with activated functional groups [40] and assembly based on metal coordination [41] have been demonstrated. These assemblies should become more stable under certain atmospheres as compared to conventional assembly, and their applications will expand even more.

In 2002, Serizawa, *et al.* [42] prepared thermoresponsive ultrathin hydrogels by the sequential chemical reaction of poly(vinylamine-*co*-*N*-vinylisobutyramide) [poly(VAm-*co*-

NVIBA)] and poly(acrylic acid) (polyAAc) on a gold surface. The carboxyl group of polyAAc was activated by 1-ethyl-3-(3-(dimethylamino)propyl)-carbodiimide hydrochloride (EDC) for the reaction with the amino group of poly(VAm-*co*-NVIBA) to yield the amide linkage. Layer-by-layer assembly using chemical reactions will open a new field of research on the suitable selection of functional polymers.

In 2004, Yang, *et al.* [43] prepared bioinert polyelectrolyte multilayers comprised of poly(acrylic acid) and polyacrylamide, deposited on colloidal particles at low pH conditions by layer-by-layer assembly using hydrogen bonding interactions. The multilayer films were coated uniformly on the colloidal particles without causing any flocculation of the colloids, and the deposited films were subsequently cross-linked by a single treatment of a carbodiimide aqueous solution. The lightly cross-linked multilayer films show excellent stability at physiological conditions (pH 7.4, phosphate-buffered saline), whereas untreated multilayer films dissolved. The multilayer-coated surfaces, both on flat substrates and on colloidal particles, exhibit excellent resistance toward mammalian cell adhesion. With this new solution-based cross-linking method, bioinert H-bonded multilayer coatings offer potential for biomedical applications.

2.6 Formation of polyelectrolyte multilayer assemblies on polyelectrolyte brushes

Polyelectrolyte built up by layer-be-layer adsorption represents a simple pathway to fabricate a film with well-controlled thickness. However, the stability of the multilayered system in different environment is generally of concern. Especially the adhesion of the first layer to the surface poses a problem which should not be neglected. Because the attachment of the first layer depends solely on the interaction of the polymers with surface charges, the whole multilayer assembly can be desorbed by either changing the sign of the surface charge of the substrate or by addition of competing low molecular weight electrolytes, which can displace the polymer molecules in the first monolayer [44-45]. Another general problem of the LBL method is the low thickness of each single deposited layer, which is on the order of 0.5 nm [46]. Such a small increase in film thickness per deposited layer is rather inconvenient if a thicker PEL multilayer assembly is desired, as in this case many layers must be deposited. Recently, the use of the surface-attached polyelectrolyte brushes for layer-by-layer build-up of polyelectrolyte multilayers has been introduced as a way to overcome the above-mentioned problems. Because the PEL monolayers generated are directly in contact with the surface and are attached to it through chemical bonds, the PEL complexes and the PEL multilayers could, potentially, be very

stable. In principle, the grafting density of the surface-attached polyelectrolyte brushes should be high enough to induce stretching of the polymer chains away from the surface. The thickness of the adsorbed polyelectrolyte should thus be as high as the polyelectrolyte brushes. For the formation of polyelectrolyte multilayers assemblies, the brushes are alternatively dipped into PEL solutions, one of which consists of a positively charged PEL, and the other of a negatively charged PEL.

In 2003, Zhang and Rühe [47] reported the deposition of poly(4-vinyl-Nmethylpyridinum) iodide/poly(styrene sulfonate) sodium (MePVP/PSSNa) multilayer on positively charged MePVP brushes which were covalently attached on the silicon surface. It was found that when PSSNa was added to the MePVP brushes, which was swollen in salt-free water, the MePVP brushes collapsed rapidly. Once the MePVP collapses, the diffusion of PSS into MePVP layer essentially stops and a strongly nonstoichiometric, insoluble polyelectrolyte-polyelectrolyte complex is formed. From Figure 2.11(a), it can be seen that the increase in thickness due to the absorption of the second layer (PSSNa) is larger than that of the following layers deposited onto it. However, from the third layer onwards the thickness increases by only about 0.5 nm per deposition cycle (i.e., deposition of two monolayers), and a linear relationship between layer thickness and the number of deposited layers is observed. In this system, after deposition of a total of three or four PEL-layers the brush no longer affects the properties of the outer layers.

Later in 2005, Zhang and Rühe [48] reported the formation of poly(methacrylic acid)/ poly(4-vinyl-*N*-methylpyridinum)iodide (PMAA/MePVP) on negatively charged PMAA brushes which were covalently attached on the silicon surface. It should be noted that PMAA brushes are weak polyelectrolyte. The film thickness of the PMAA/MePVP multilayer (Figure 2.11(b)) increases linearly with the number of dipping cycles. It is also clear that the thickness of each layer in the multilayer assembly depends heavily on the thickness of the initial brush layer. The increase in layer thickness per monolayer, and even when a very thick brush is used. The outermost layer resembles closely the intermost (the brush layer), and a very strong template effect is observed. Even though the overall architecture of the two systems is very similar (surface-attached PEL brush with electrostatically attached monolayers of alternating charge sign), the film formation behavior of the two systems is very different, as shown schematically in Figure 2.12. Although this difference is not yet fully understood, it is evident that the basic difference between the systems is the water solubility of the PEL-PEL complex formed. This difference is directly evident if solutions of the two PELs are mixed. While in the first (weak/weak) case the complex remains soluble if

solutions containing equimolar amounts of polyanion and polycation are mixed, in the latter (strong/strong) case immediate precipitation occurs due to the hydrophobicity of the neutral complex formed.

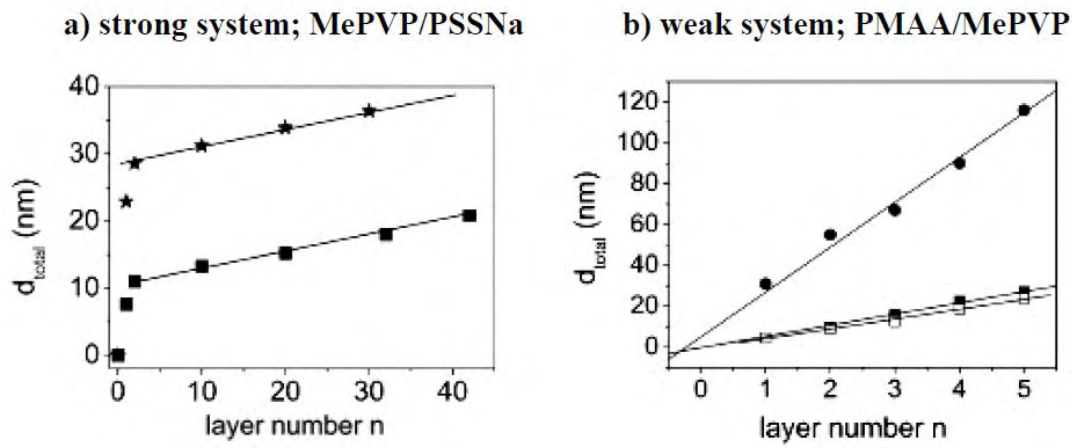

Figure 2.11 Film thickness as a function of the layer numbers for (a) MePVP/PSSNa multilayers using 7.6 nm(■) and 22.9 nm (★) MePVP covalently attached monolayer as the first layer and (b) PMAA/MePVP multilayers using 6 nm (□) and 30 nm (•) MePVP covalently attached monolayer as the first layer. The solid lines show a linear fit of the dependence of the film thickness on the number of deposited layers [48-49]

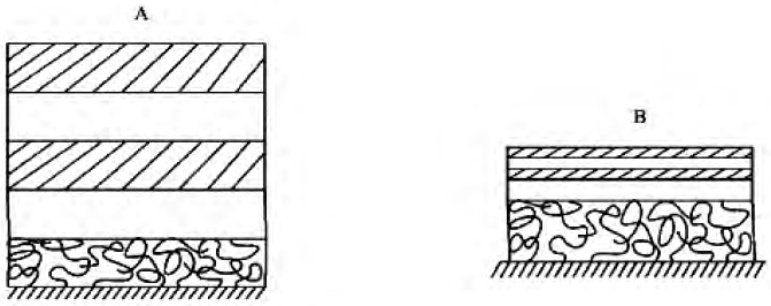

Figure 2.12 Schematic depiction of the formation of PEL multilayers through PEL brushes. (A) strong/weak system; (B) strong/strong system [49]

The formatiom of weak PEL-PEL complexes and multilayers at solid surfaces via polymer brushes is quite different from the case where two strong PEIs are used. Interestingly, in the strong/weak PEL system, each adsorbed layer has the same thickness, which closely resembles that of the innermost brush layer. By contrast, in the strong/strong

system the formation of PEL multilayers resembles more the traditional LBL technique in so far as the increase in layer thickness per deposition cycle is well below 1 nm. In the strong/weak case, however, more than 100 nm of polyelectrolyte can easily be deposited per dipping cycle, and this allows the simple generation of very thick PEL multilayers assemblies. However, the exact mechanism and the internal structures of the weak PEL complexes and multilayer assemblies are still not clear. Since many biopolymers (proteins, nucleic acids and DNA) are polyelectrolytes, the systems described here are interesting models for biomaterials.

CHAPTER III

EXPERIMENTAL

3.1 Materials

t-Butyl acrylate (*t*-BA, 98%, Aldrich) was extracted three times with 5% (w/v) aqueous NaOH and then washed with distilled water. After drying over anhydrous $MgSO_4$ and filtering off the drying agent, the *t*-BA was distilled under reduced pressure (60^{O}C/60 mmHg). Tris(2-(dimethylamino)ethyl)amine (Me_6TREN), 2-bromo-2-methylpropionic acid 3-(ethoxydimethylsilanyl)propyl ester ($BrC(CH_3)_2COO(CH_2)_3(CH_3)_2Si(OC_2H_5)$) and ω–mercaptoundecyl bromoisobutyrate ($BrC(CH_3)_2COO(CH_2)_{11}SH$) were prepared following the methods described in the literature [11,49-50]. CuBr (95%, Fluka), ethyl 2-bromoisobutyrate (EBiB, 98%, Fluka), Toluidine Blue O (TBO, 98%, Fluka), 1-(3-dimethylaminopropyl)-3-ethylcarbodiimide hydrochloride (EDCI, 98%, Fluka), *N*-hydroxysuccinimide (NHS, 98%, Fluka), *N,N,N′,N″,N‴*-pentamethyldiethylenetriamine (PMDETA, 99%, Aldrich), (+)-biotinyl-3,6,9-trioxaundecanediamine (NH_2-biotin, Bioactive), fluorescein-conjugated streptavidin (FITC-SA, Bioactive), bovine serum albumin (BSA, Aldrich), 11-mercaptoundecanoic acid (MUA, Aldrich), fibrinogen (FIB, Aldrich), streptavidin (SA, Bioactive), phosphate buffered saline (PBS, Aldrich) and trifluoroacetic acid (TFA, Fluka), Chitosan, Mw = 100,000 ; 96%DD (Seafresh Lab Co. Ltd.) , poly(acrylic acid), sodium salt (PAA), Mw = 60,000 (Fluka), and sodium dodecyl sulfate (SDS, Fluka) were used as received. Poly(10,12-pentacosadiynoic acid) (PPCDA) vesicles and *N*-[(2-hydroxyl-3-trimethylammonium)propyl]chitosan chloride (HTACC) were synthesized according to a method of Potisatityuenyong *et al* [51]. and Seong *et al*. [52], respectively. Ultrapure distilled deionized water was obtained after purification using a Millipore Milli-Q system (USA) that involves reverse osmosis, ion exchange and a filtration step. Anhydrous toluene was prepared by distillation over calcium hydride under a nitrogen atmosphere.

3.2 Equipments

3.2.1 Ellipsometry

The thickness of samples was analyzed by an L115C Wafer™ Ellipsometer operating with a 70° of incidence angle at 632.8 nm. The calculation was based on refractive indices of 1.443, 1.460 and 1.462 for $N_{initiator}$, $N_{t\text{-}BA}$ and $N_{hydroxyl}$, respectively, and a silicon substrate refractive index ($N_{substrate}$) of 3.858.

3.2.2 Nuclear magnetic resonance spectroscopy (NMR)

The ^1H NMR spectra was recorded in $CDCl_3$ or D_2O using a Varian, NMR spectrophotometer operating at 400 MHz (model Mercury-400; USA). Chemical shifts (δ) are reported in part per million (ppm) relative to tetramethylsilane (TMS) or using the residual protonated solvent signal as a reference.

3.2.3 Fourier transform -infrared (FT-IR) spectroscopy

The FT-IR spectra of surface-modified silica particles prepared as KBr pellets were recorded with a FT-IR spectrometer (Perkin Elmer), model system 2000, with 32 scans at a resolution of 4 cm^{-1} using a TGS detector.

3.2.4 Contact angle measurements

Contact angle goniometer model Ramé-Hart 100-00 was used for the determination of water contact angles. The measurements were carried out in air at the room temperature. A droplet of testing water is placed on the tested surface by bringing the surface into contact with a droplet suspended from a needle of the syringe. A silhouette image of droplet was projected on the screen and the angle was measured. Dynamic advancing and receding angles were recorded while water was added to and withdrawn from the drop, respectively. The reported angle is an average of 5 measurements on different area of each sample.

3.2.5 Atomic force microscopy (AFM)

AFM images were recorded with Scanning Probe Microscope model NanoScope®IV, Veeco, USA. Measurements were performed in air using tapping mode. Silicon nitride tip with a resonance frequency of 267-295 KHz and a spring constant 20-80 N/m were used.

3.2.6 Gel permeation chromatography (GPC)

The molecular weight and the molecular weight distribution of the P*t*-BA homopolymer were determined by a Water GPC system (USA) with a Water E600 column connected to a RI detector. The column was eluted with THF at a flow rate of 1 mL/min. Narrow PS standards were used for generating a calibration curve. In case of the PAA, aqueous gel permeation chromatogram obtained from Water 600 controller chromatograph equipped with ultrahydrogel linear and guard column at 30 $^{\circ}$C. Water was used as eluent with the flow rate of 0.6 mL/min. Poly(ethylene glycol)(PEG) was used standards for calibration. The molecular weight as determined by a refractive index detector, Waters 2410.

3.3 Procedures

3.3.1 Preparation of the surface grafted α-bromoester initiator

Silicon substrates (wafers or particles) were submerged in a freshly prepared piranha solution (7:3 (v/v) mixture of concentrated H_2SO_4 and 30% (v/v) H_2O_2) at ambient temperature for 2 h, rinsed with 5 - 7 aliquots of deionized water and dried in a clean oven at 120 $^{\circ}$C for 2 h. Anhydrous toluene (30 mL) containing 4 mmol (33 μL) of $BrC(CH_3)_2COO(CH_2)_3(CH_3)_2Si(OC_2H_5)$ was added via a syringe to a dried Schlenk flask containing freshly cleaned silicon substrates. Reactions were carried out under a nitrogen atmosphere at ambient temperature for 18 h. The substrates were sequentially rinsed with (all 10 mL) toluene, 2-propanol (twice), ethanol (twice), 1:1 (v/v) ethanol-water, water, ethanol and finally water before being dried *in vacuo*.

In the case of the gold-coated SPR disks, the disks were cleaned in a freshly prepared piranha solution at ambient temperature for 15 min, rinsed with 5 - 7 aliquots of deionized water and dried by a gentle stream of nitrogen gas. Freshly cleaned disks were then immersed in 1 mM ethanolic mixed solution of $BrC(CH_3)_2COO(CH_2)_{11}SH$ and 11-mercatoundecanol with a designated dilution percentage (100, 50, and 10%) for 24 h at ambient temperature. After this treatment, the disk was rinsed with ethanol and dried by light stream of nitrogen gas. For comparison, a gold-coated SPR disk bearing a monolayer of carboxyl-terminated thiol, 11-mercatoundecanoic acid (MUA) were prepared by immersing the cleaned disk in an ethanolic solution of MUA (1 μM) at ambient temperature for 24 h. The disk was then rinsed thoroughly with ethanol and then dried *in vacuo.*

3.3.2 Formation of PAA brushes

The synthetic route for the formation of PAA brushes is schematically shown in Figure 3.1. The substrates having surface grafted initiators, $BrC(CH_3)_2COO(CH_2)_3(CH_3)_2SiO\text{-}SiO_2$ **(1)** or $BrC(CH_3)_2COO(CH_2)_{11}S\text{-}Au$ **(2)** (obtained from section *3.3.1)*, were placed in a Schlenk flask and sealed with a rubber septum. The flask was evacuated and back-filled with nitrogen three times and then left under a nitrogen atmosphere. CuBr (49.3 mg, 0.34 mmol), *t*-BA (10 mL, 68 mmol) and acetone (15 mL) were added to a separate Schlenk flask with a magnetic bar, sealed with a rubber septum, and degassed by purging with nitrogen for 1 h. PMDETA (71.8 μL, 0.34 mmol) was added to the mixture via a syringe, and the solution was stirred at 60 °C until it became homogeneous. For the gold-coated substrates, the more active ligand, Me_6TREN (88 μL, 0.34 mmol) was used instead of PMDETA so that the polymerization could be performed at ambient temperature without thermal treatment. This was done in order to avoid the gold detachment from the substrate upon elevating the temperature. The solution was then transferred to the flask containing the substrates, **(1)** or **(2)**, via a cannula, followed by the addition of the sacrificial initiator, EBiB (54.6 μL, 0.34 mmol). The polymerization was allowed to proceed for a set reaction time (0 - 24 h) at 60 $^{\circ}$C for the silicon substrates and at ambient temperature for the gold-coated substrates. The substrates were removed from the solution, rinsed by acetone and THF, and soxhlet extracted with THF before being dried *in vacuo*. The substrates bearing P*t*-BA brushes were then analyzed by surface characterization techniques. Free polymer from the polymerization solution was isolated by first evaporating the residual monomer and solvent under reduced pressure, dissolving in THF, and then passing the polymer solution in THF through a short column of silica to remove any residual catalyst and analyzed by gel permeation chromatography (GPC).

The substrates containing the tethered P*t*-BA brushes were placed in a Schlenk flask. A solution of 2.5 M TFA in dichloromethane was added and stirred at ambient temperature for 6 h. The substrates were removed and rinsed thoroughly with dichloromethane, and then dried *in vacuo*. This step was carried out in order to remove the *t*-butyl groups from the P*t*-BA brushes. The resulting surface-tethered PAA brushes were then subjected to characterization and biotin binding.

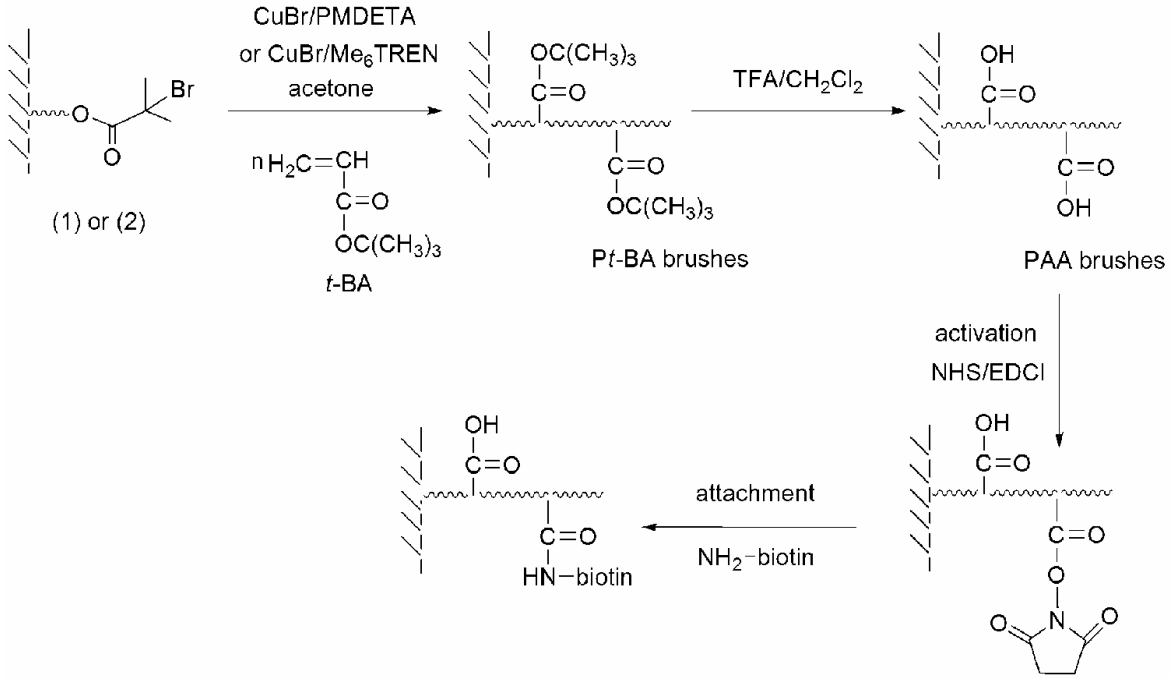

Figure 3.1 Schematic diagram showing the formation of P*t*-BA and PAA brushes followed by carboxyl group activation and biotin immobilization**.**

3.3.3 Determination of carboxyl group density of the surface-grafted PAA brushes

The TBO staining method was employed to determine the amount of carboxyl groups on the PAA brushes. A 0.5 mM TBO aqueous solution was prepared at pH 10 and the substrate bearing PAA brushes were immersed in the dye solution for 6 h at 30 °C. The substrates were then removed and thoroughly rinsed with a 0.4 mM NaOH (aq) (pH 9) for 2 h to remove any non-complexed dye adhering to the substrate. The dye complexed with the carboxyl groups was then desorbed from the surface by soaking the substrates in a 50% (v/v) acetic acid solution for 16 h, and the desorbed dye content was obtained by measuring the optical density of the solution at 633 nm with an UV-vis spectrophotometer (Model Techne Specgene, UK). The PAA content was determined from a predetermined calibration curve (0.001-0.05 mM) of the optical density versus dye concentration assuming one carboxyl group reacted with one dye molecule [53].

3.3.4 Determination of SA binding to biotin-attached PAA brushes by fluorescence microscopy

The carboxyl groups of the PAA brushes on the silica particles were activated by suspending the substrates bearing PAA brushes in an aqueous solution of 0.05 M EDCI / 0.1 M NHS for 30 min. The substrates were rinsed with deionized water before suspended in a solution of NH_2-biotin (1 mg/mL) in PBS (pH 7.4) for 2 h at ambient temperature and washed thoroughly with PBS solution. A schematic representation of the carboxyl group activation and biotin attachment step is outlined in Figure 3.1. The silica particles bearing biotin-attached PAA brushes were suspended in a solution of PBS containing 0.1% (w/v) BSA for 60 min and then rinsed thoroughly with PBS. The particles were then incubated in a solution of FITC-SA (0.1 mg/mL) in PBS at ambient temperature. After 14 h, the particles were rinsed thoroughly with PBS followed by distilled water and then spread on a glass slide and covered with a thin cover slip. A fluorescence microscope equipped with a digital camera was used to examine the SA bound on the particles.

3.3.5 Determination of SA binding to biotin-attached PAA brushes by SPR

SPR measurements were conducted using a double channel, AutoLab ESPR (Eco Chemie, The Netherlands) at 25 ^{o}C, with the plane face of the prism coupled to the gold-coated glass via index matching fluid. An auto-sampler was used to inject the test solutions and the measurement of the SPR angle shift was done under non-flow liquid conditions. The shift of the SPR angle at the end-point of each step and after baseline subtraction (“angle shift”) was used to calculate the amount of the molecules bound onto the surface or target density, using a sensitivity factor of 120 mDegrees equals 100 ng/cm^2 and its molecular weight, as previously reported [54].

For comparison, a gold-coated SPR disk bearing a monolayer of the carboxyl-terminated thiol, MUA, as a so-called 2D substrate, was prepared by immersing the cleaned disk in an ethanolic solution of MUA (1 mM) at ambient temperature for 24 h. The disk was then rinsed thoroughly with ethanol and dried *in vacuo.* The gold-coated SPR disk bearing PAA brushes (3D) or MUA (2D) was first seated in the SPR cell before being rinsed with a running solution of sodium acetate buffer (10 mM, pH 4.5). After a baseline SPR response was established, the activation by EDCI (0.05 M) and NHS (0.1 M), the attachment of NH_2-biotin (1 mg/mL), and the subsequent blocking by ethanolamine (1 M) were all carried out sequentially *in situ* in the

sodium acetate buffer for 15, 30, and 15 min, respectively. The disk was rinsed with a running solution of sodium acetate buffer for 3 - 5 min after each step. The binding of SA was performed in PBS. After a baseline SPR response was recorded, 50 μL of SA in PBS (0.1 mg/mL) was applied to the biotin-immobilized disk and left for 15 min. The unbound SA was removed by washing with PBS for 5 min. Non-specific interactions of the gold-coated SPR disks bearing PAA brushes-biotin (3D matrix) and MUA-biotin (2D matrix) were tested against BSA and FIB by passing the 0.2 mg/mL protein solution in PBS over the discs for 15 min.

3.3.6 Multilayer assembly on surface-tethered PAA brushes

Layer-by-layer deposition was carried out by alternatively dipping the surface-tethered PAA brushes into 1 mg/mL of chitosan (Mw = 100,000 ; 96%DD) and 1 mg/mL of PAA (Mw = 60,000) at pH 4 or 1 mM PPCDA at pH 5.6 for 40 min interval. The substrates were rinsed thoroughly with Milli-Q water three times after each deposition step. After the final deposition, the substrates were dried under stream of nitrogen and dried *in vacuo*.

3.3.7 Protein adsorption of the multilayer film deposited on surface-tethered PAA brushes

The deposited multilayer films on PAA brushes substrates were placed into 24-well plate containing Milli-Q water in each well overnight to reach an equilibrium hydration. Each sample was removed from Milli-Q water and suspended into the well containing 2.0 mL albumin solution before incubated at 37 °C for 3 h. Three pieces of samples were analyzed for each condition. The samples were removed from protein solution and rinsed thoroughly twice with PBS to remove any loosely attached protein. The adsorbed protein on the sample surface was detached by soaking each sample in 2.0 mL of 1 % aqueous solution of SDS for 30 min. A protein analysis kit based on the BCA method (Bicinchoninic assay kit, QuantiProTM BCA assay, Sigma) was used to determine the concentration of the protein dissolved in the SDS solution. 100 μL (0.1 mL) of SDS solution that soak each sample was added into designated 96 wells. 100 μL of BCA working solution was then added in each well before the well-plate was incubated at 37°C for 2 h. The absorbance of the solution was measured at 562 nm by microplate reader. The amount of protein adsorbed on the samples was calculated from the protein concentration in the SDS solution. The data are expressed as mean ± standard deviation (S.D).

CHAPTER IV

RESULTS AND DISCUSSION

In this chapter, the results are divided into 7 sections. The first section mainly focuses on the synthesis and characterization of surface-tethered PAA brushes on both silicon and gold-coated SPR substrates. The second section is devoted to the determination of SA binding to the biotin-attached PAA brushes mainly by SPR technique. The third section involves the determination of swelling behavior of the PAA brushes both before and after biotin attachment. The fourth section explains the effect of the PAA brushes graft density on the SA binding of the biotin-attached PAA brushes. The fifth section is devoted to the formation and characterization of multilayer films on the surface-tethered PAA brushes. And the last two sections address stability and the biological responses in term of protein adsorption of the multilayer films that were assembled on the surface-tethered PAA brushes.

4.1 Formation of surface-tethered PAA brushes

The molecular weight and thickness of the PAA brushes can be controlled by the reaction time as well as the monomer to initiator ratio (the targeted DP) in the solution, (Figure 4.1). The molecular weight of the P*t*-BA brushes on surface was determined by measuring the molecular weight of a free polymer simultaneously formed in the solution from the “sacrificial” or “added” initiator. It is rather difficult to obtain the molecular weight of the polymer brush directly since the amount of polymer on the silicon substrate is too small to be degrafted and analyzed. It has previously been demonstrated that the molecular weight of this free polymer closely resembled that of the grafted polymer brushes cleaved from the surface [55]. Thus, it can be used to monitor the SIP process. Figure 4.1 clearly shows that the change in the molecular weight ($\overline{M}_n$) of the free P*t*-BA and the thickness of the P*t*-BA brushes on the silicon substrate both increased as the polymerization time increased (over the tested range of 0 – 24 h) for the P*t*-BA brushes made from both targeted DPs of 100 and 200. The fact that the molecular weight distribution is close to 1 and that the thickness of P*t*-BA brushes increased linearly as a

function of the polymerization time suggests that the polymerization is living and can be well controlled.

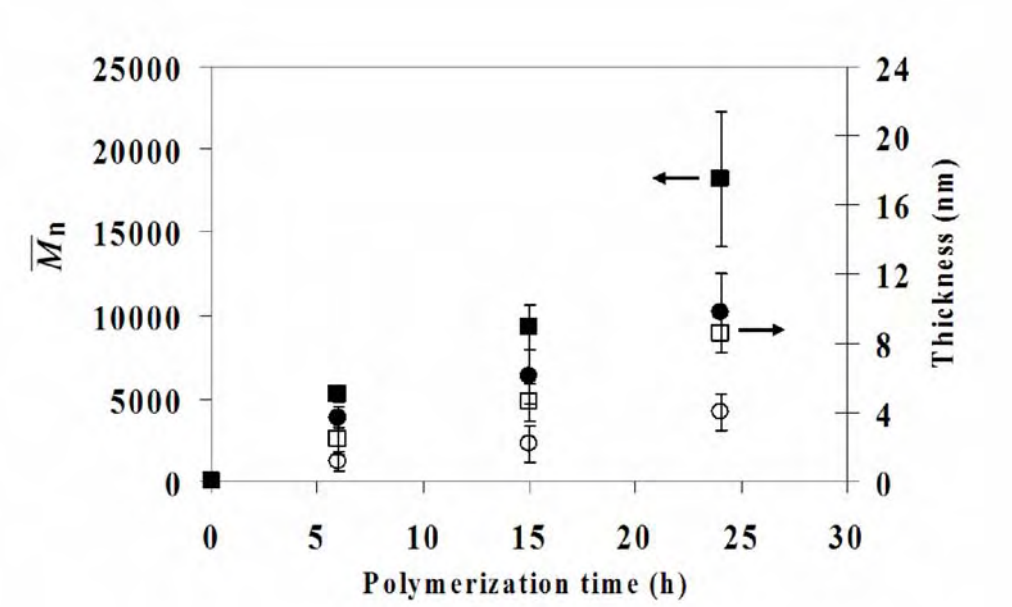

Figure 4.1 The molecular weight ($\overline{M}_n$) (●,■) of the P*t*-BA in solution and thickness (○, □) of the P*t*-BA brushes as a function of the polymerization time and formed from a targeted DP of 100 (●,○) or 200 (■, □). Data are shown as the mean ± SD and are derived from 3 repeats.

The free initiator plays a role not only as an indicator of the polymerization but also as a controller for the ATRP on the surface (Figure 4.2). The concentration of the Cu^{II} complex produced from the reaction at the substrate surface is too low to reversibly deactivate polymer radicals with a sufficiently high rate. The addition of the free initiator creates the necessary concentration of the Cu(II) complex, which in turn controls the polymerization on the substrate as well as in solution.

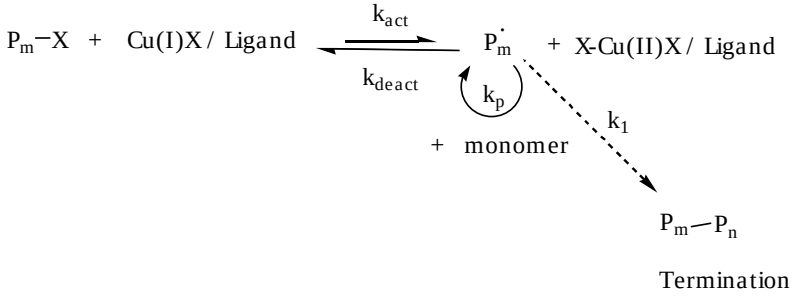

Figure 4.2 Schematic representation of activation/deactivation cycles of ATRP process.

The ^{1}H-NMR spectra shown in Figure 4.3 indicates that the signals of the double bond of monomer disappeared while the CH proton of the polymer appeared at 2.16 ppm and the CH_3 protons shift from 1.49 ppm to 1.37 ppm.

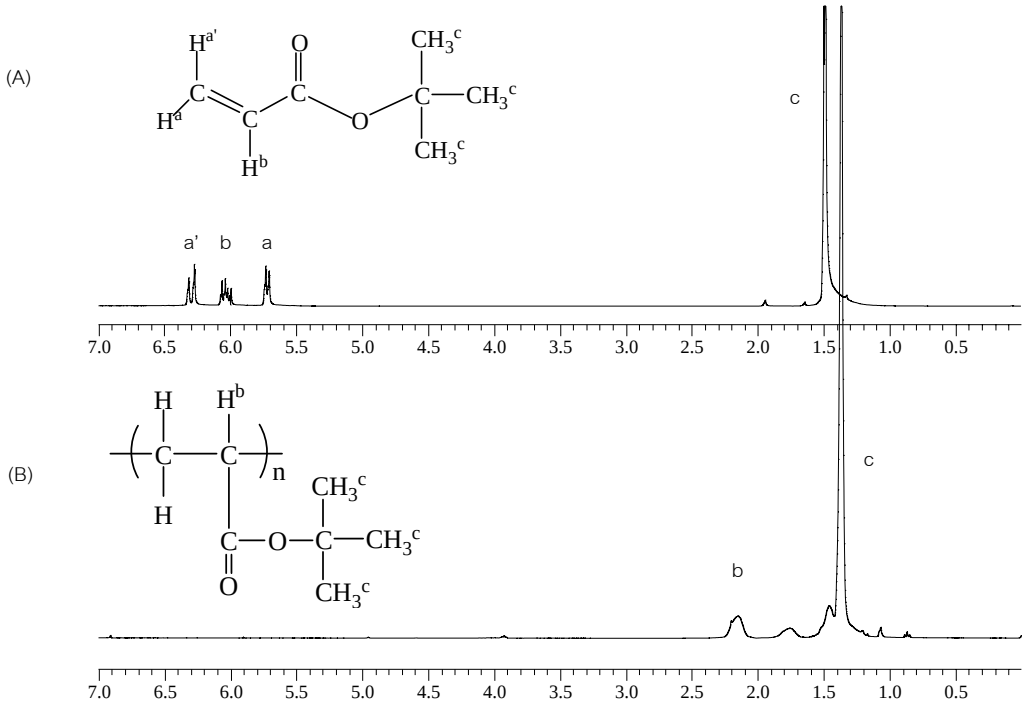

Figure 4.3 ^{1}H-NMR spectra of (A) *t*-BA and (B) P*t*-BA in solution.

The information related to the molecular weight and thickness obtained in Figure 4.1 can be used to calculate a grafting density of polymer brushes. The grafting density (σ) which is a reciprocal unit of cross-sectional area (A_x) per chain can be determined from the corresponding film thickness (t) and the molecular weight of the chain ($\overline{M}_n$) from the following equation

$$\sigma = \frac{t\rho N_A}{M_n} = \frac{1}{A_x} \qquad (4.1)$$

Where ρ is the mass density (1.1 g/cm^3 for P*t*-BA) and N_A is Avogadro's number. Using slopes obtained from the plots in Figures 4.4 and 4.5 which correspond to t/M_n, the calculated grafting density is 0.25 and 0.32 chains/nm^2 for the targeted DP = 100 and 200, respectively. These

results agree quite well with the data previously reported that the grafting densities for various polymers prepared by surface-initiated ATRP were also ranged from 0.1 to 0.6 chains/nm^2.

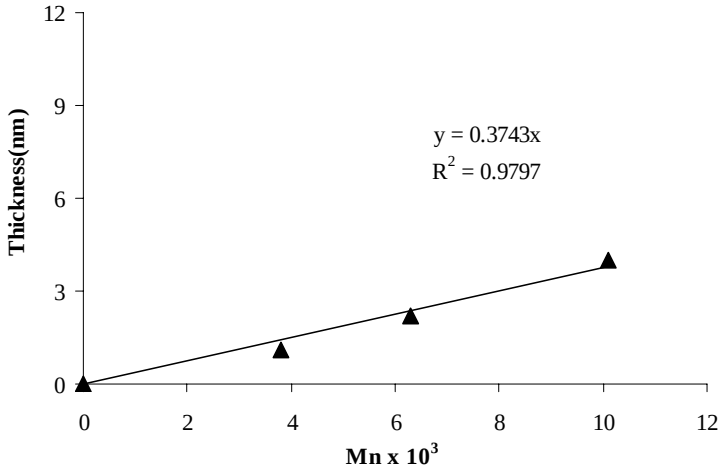

Figure 4.4 Relationship between the ellipsometric thickness of P*t*-BA brushes with the molecular weight ($\overline{M}_n$) of free P*t*-BA for the targeted DP = 100.

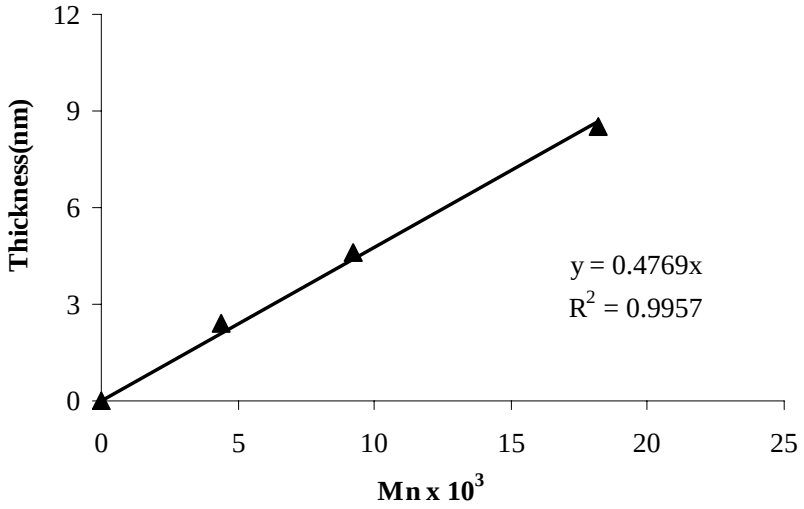

Figure 4.5 Relationship between the ellipsometric thickness of P*t*-BA brushes with the molecular weight ($\overline{M}_n$) of free P*t*-BA for targeted DP = 200.

Another evidence of the P*t*-BA brushes formation, especially on the gold-coated SPR substrate is based on AFM analysis. According to the AFM micrographs shown in Figure 4.6,

the topography of the gold-coated SPR substrate has been changed with larger groove dimension upon the coating of the P*t*-BA brushes. The root mean square roughness (rms) was also increased from 1.2 to 1.9 nm. The presence of the polymer layer can be clearly seen from the AFM micrograph in Figure 4.7 demonstrating the section analysis of the gold-coated SPR substrate of which the P*t*-BA layer was intentionally scraped off. Using the average thickness (9.5±0.6 nm) obtained from this particular image together with the free P*t*-BA formed in solution at the target DP of 200, the graft density of 0.31 chain/nm^2 can be calculated. The fact that the graft density calculated from the AFM data is essentially the same as that obtained from the ellipsometric analysis at the same targeted DP suggested that the method for the preparation is potentially reliable although the values were determined on different substrates by different techniques.

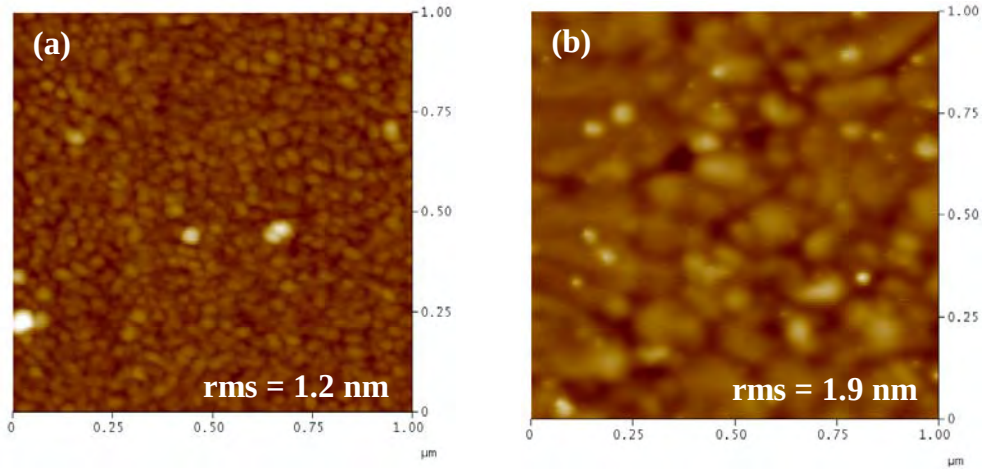

Figure 4.6 AFM micrographs of the gold-coated SPR substrate (a) before and (b) after being grafted with P*t*-BA brushes obtained from the targeted DP of 200 and reaction time 24 h.

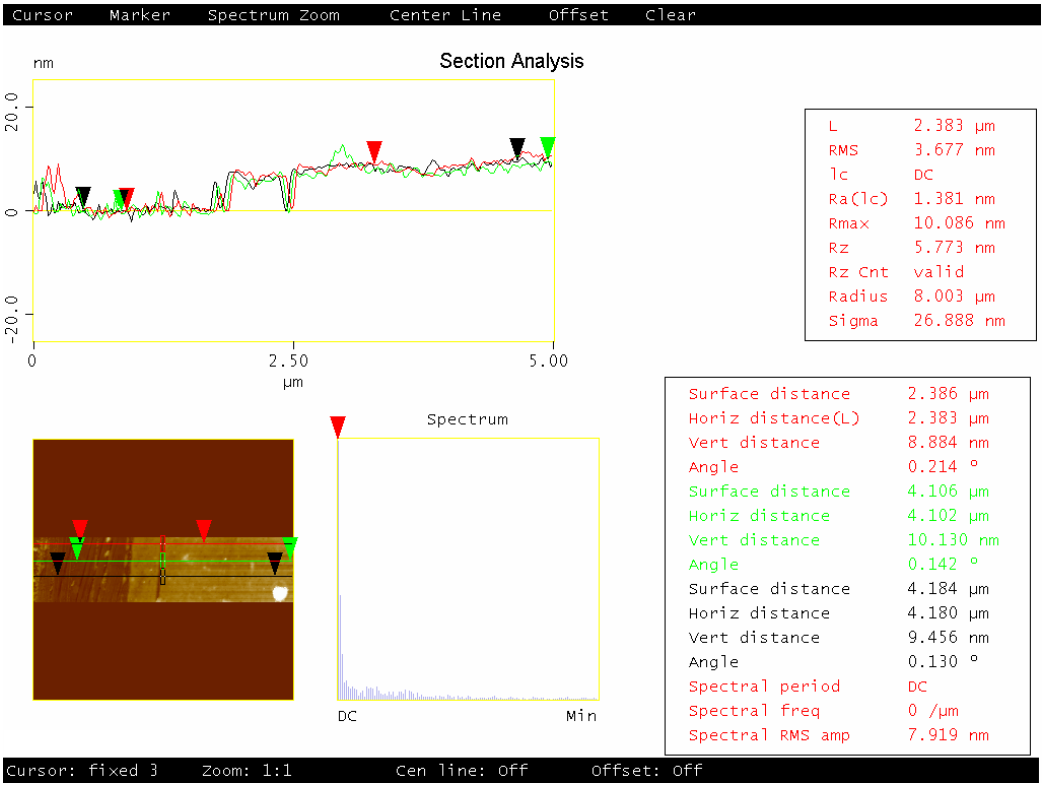

Figure 4.7 Section analysis of the side-viewed cross-section of the gold-coated SPR substrate grafted with P*t*-BA brushes after being scraped by AFM tip showing the thickness of P*t*-BA brushes.

The growth of the P*t*-BA brushes and their hydrolyzed counterparts, PAA brushes, on the silica or gold substrates was also confirmed by water contact angle measurements and FT-IR analysis. As a consequence of the formation of P*t*-BA brushes, the advancing (θ_A) and receding (θ_A) water contact angles of the substrate having surface-grafted initiator markedly increased (Table 4.1). After hydrolysis, the water contact angles decreased significantly as the hydrophobic P*t*-BA brushes were hydrolyzed to hydrophilic PAA brushes. To achieve the covalent attachment of biotin to the carboxyl group of the PAA brushes, a method to introduce the reactive intermediate NHS ester was used. The carboxyl group of the PAA brushes was first activated by the water-soluble carbodiimide EDCI and NHS to form the NHS group, and this was then coupled with NH_2-biotin, leading to amide bond formation. The increasing θ_A/θ_R observed after the activation (Table 4.1) suggests that the hydrophilic carboxyl groups of PAA

brushes were converted to the hydrophobic *N*-succinimidyl groups. The water contact angles did not significantly change after biotin attachment.

Table 4.1 Advancing (θ_A) and receding (θ_R) water contact angles of functionalized silicon substrates obtained with a targeted DP of 200. Data are shown as the mean ± SD and are derived from 5 repeats.

Sample	Water contact angle (degree)	
	Advancing (θ_A)	Receding (θ_R)
surface-grafted initiator	72 ± 1.8	68 ± 1.2
P*t*-BA brushes	95 ± 1.7	76 ± 4.0
PAA brushes	60 ± 1.7	43 ± 0.8
Activated PAA brushes	80 ± 0.8	47 ± 1.4
PAA brushes-biotin	79 ± 0.6	51 ± 1.7

The FT-IR spectra of the surface-functionalized silica particles revealed the presence of signals corresponding to the desired functionalities of the polymer brushes (Figure 4.8). Evidently, the carbonyl stretching peak at 1727 cm^{-1} shifted slightly to 1713 cm^{-1} after the P*t*-BA brushes were transformed to PAA brushes. Also, the intensity of the O-H stretching peak (2400 - 3800 cm^{-1}) was enhanced after hydrolysis of the P*t*-BA brushes to PAA brushes due to H-bonded carboxyl groups of the PAA brushes. The shoulder peaks that appear at 1734 and 1778 cm^{-1} were assigned to the carbonyl stretching of the succinimidyl ester after activation of the PAA brushes and so indicate that the carboxyl group was transformed to a NHS group after activation by the EDCI/NHS treatment. The binding of NH_2-biotin can be verified by the appearance of the amide II band at 1558 cm^{-1} (N-H bending) and the disappearance of the signals belonging to succinimidyl ester at 1734 and 1778 cm^{-1}. It should be emphasized that the data shown in Table 4.1 and Figure 4.8 were obtained from the polymer brushes having a targeted DP of 200. As determined by the TBO assay, the density of the carboxyl groups of the PAA brushes on the silicon oxide surface increased as a function of $\overline{M}_{n,}$ or chain length of the polymer brushes obtained with both a targeted DP of 100 and 200 (Figure 4.9). The carboxyl

group density increased some three-fold from 1.67 ± 0.19 to 5.04 ± 0.87 nmol/cm^2 as the $\overline{M}_n$ increased from 3.8 to 14 kDa.

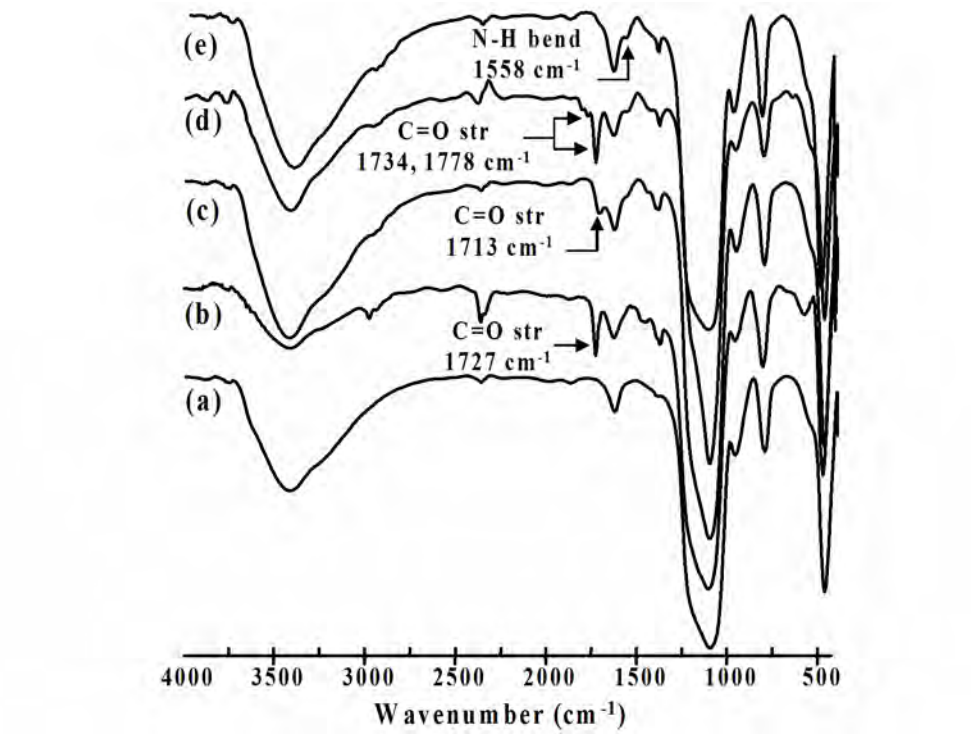

Figure 4.8 FT-IR spectra of (a) bare silica particles and the silica particles surface-functionalized with (b) P*t*-BA brushes, (c) PAA brushes, (d) activated PAA brushes, and (e) PAA brushes-biotin, obtained from a targeted DP of 200.

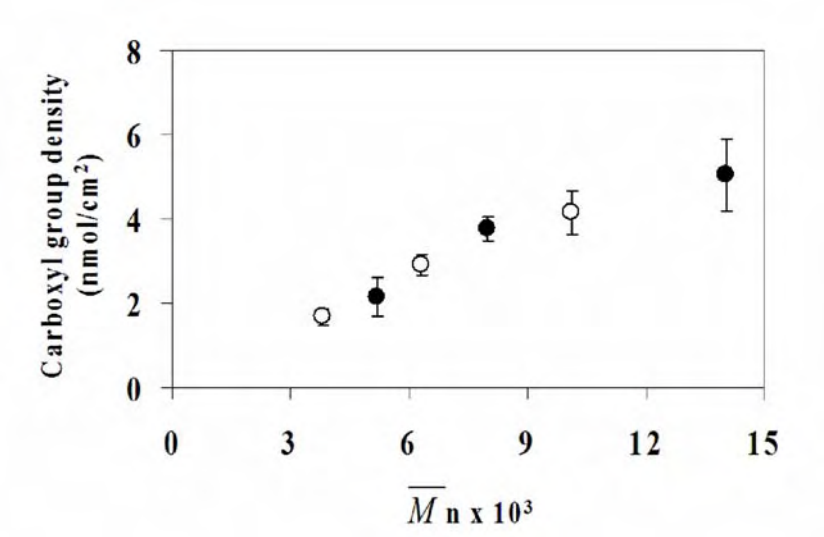

Figure 4.9 The density of carboxyl groups of the PAA brushes on the silicon oxide surface as a function of $\overline{M}_n$ when derived from a targeted DP of 100 (○) or 200 (●) at different polymerization time. Data are shown as the mean ± SD and are derived from 3 repeats.

4.2 Determination of SA binding to the biotin-attached PAA brushes

The attachment of the biotin was qualitatively confirmed by fluorescence microscopic analysis. The optical and fluorescence images of the PAA brushes-biotin grafted on silica particles after incubation in the solution of FITC-SA are shown in Figure 4.10. The dark area of the optical images in the top row is the area that was covered by the silica particles while the bright area is the empty space on the glass slide. Upon exposure to fluorescent irradiation (λ = 488 nm), the dark area appeared green while the bright area turned dark and the control sample (blank silica particles) appeared totally dark indicating there was no FITC-SA adsorbed. This result strongly suggests that NH_2-biotin can covalently attach to the carboxyl groups of the PAA brushes, and that the attached biotin can effectively act as an active binding site for FITC-SA.

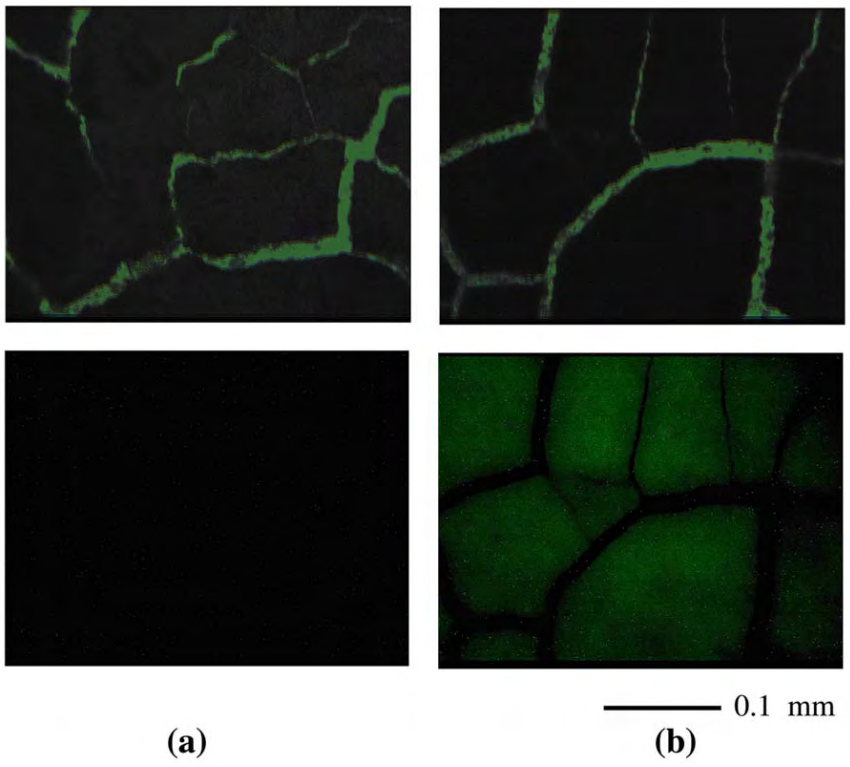

Figure 4.10 Optical (top) and fluorescence (bottom) images of silica particles grafted with biotin-attached PAA brushes after binding with FITC-SA, showing the (a) control and (b) PAA brushes-biotin obtained from a targeted DP of 200 using a polymerization time of 24 h. Images shown are representative of at least 3 such fields of view per sample and 3 independent samples.

SPR is a surface-sensitive technique based on the detection of change in the refractive index (RI) that is known to provide quantitative information and can be used for the detection of the desired analyte with a high specificity and sensitivity. The changes in the SPR angle (angle shift, expressed as $\Delta\theta$), can be determined from the difference in the SPR angle at the baseline and after the washing, and is proportional to the quantity of molecules on the gold-coated SPR disks. The $\Delta\theta$ values of the substrates bearing PAA brushes (derived from P*t*-BA having $\overline{M}_n$ of 30 kDa) after biotin attachment is 851 m° (Figure 4.11(a)), which is equivalent to a biotin density of 709.2 ng/cm^2 or 1,896 pmol/cm^2 (based on a sensitivity factor of 120 m°/100 ng/cm^2 [54] and a MW of 374 g/mol for biotin). The calculated immobilized biotin density was 171 pmol/cm^2 ($\Delta\theta$ = 77 m°) for the MUA. The results, therefore, suggest that the layer of PAA

brushes possessed an 11-fold higher biotin density compared to the MUA system. Moreover, the $\Delta\theta$ following SA binding is proportional to the quantity of the immobilized biotin (Figure 4.11(b)). Using a MW of 60,000 g/mol for SA, the 3D PAA brushes-biotin exhibited just over a two-fold higher SA binding density compared to the 2D MUA-biotin (12.2 and 5.9 pmol/cm^2), as calculated from a $\Delta\theta$ of 881 (734.2 ng/cm^2) and 428 m° (356.7 ng/cm^2), respectively. This is in good agreement with the work reported by Lee and coworkers [26], who found that the binding capacity of SA to the biotinylated layer prepared on poly(oligo(ethylene glycol) methacrylate) brushes was some 2.5-fold higher than that on the carboxylic acid terminated SAM (648.5 ng/cm^2 and 255.6 ng/cm^2, respectively).

Taking advantage of the ability to fine tune the carboxyl group density as a function of the molecular weight of the polymer brushes ($\overline{M}_n$), the effect of varying the carboxyl group density as a function of the $\overline{M}_n$ on the binding capacity of biotin and SA was evaluated (Figure 4.12). As anticipated, the amount of attached biotin increased with increasing $\overline{M}_n$. It should be noted that the $\overline{M}_n$ of 8, 19 and 30 kDa yielded carboxyl group densities of 3.8, 7.0 and 10.6 nmol/cm^2, respectively. Considering the carboxyl group density, it was found that approximately 6 - 17% of the carboxyl groups were immobilized with biotin implying that there were still a significant proportion of free carboxyl groups along the chains of the PAA brushes. The SA binding density was increased less than 1.1-fold, from 12.7 to 13.6 pmol/cm^3, when the immobilized biotin density was increased over 2.9-fold from 600 to 1,760 pmol/cm^2. In principle, the binding ratio between biotin and SA should be four if all of biotin molecules were bound to SA. However, it was found that the biotin/SA binding ratios (the number written above each set of bar graphs in Figure 4.12) were significantly greater than the theoretical value indicating that most of the immobilized biotin was not bound to the SA. The biotin/SA binding was found to increase with increasing $\overline{M}_n$. This may be explained as a result of the limited accessibility of the SA to the immobilized biotin that was embedded inside the inner layer of the polymer brushes.

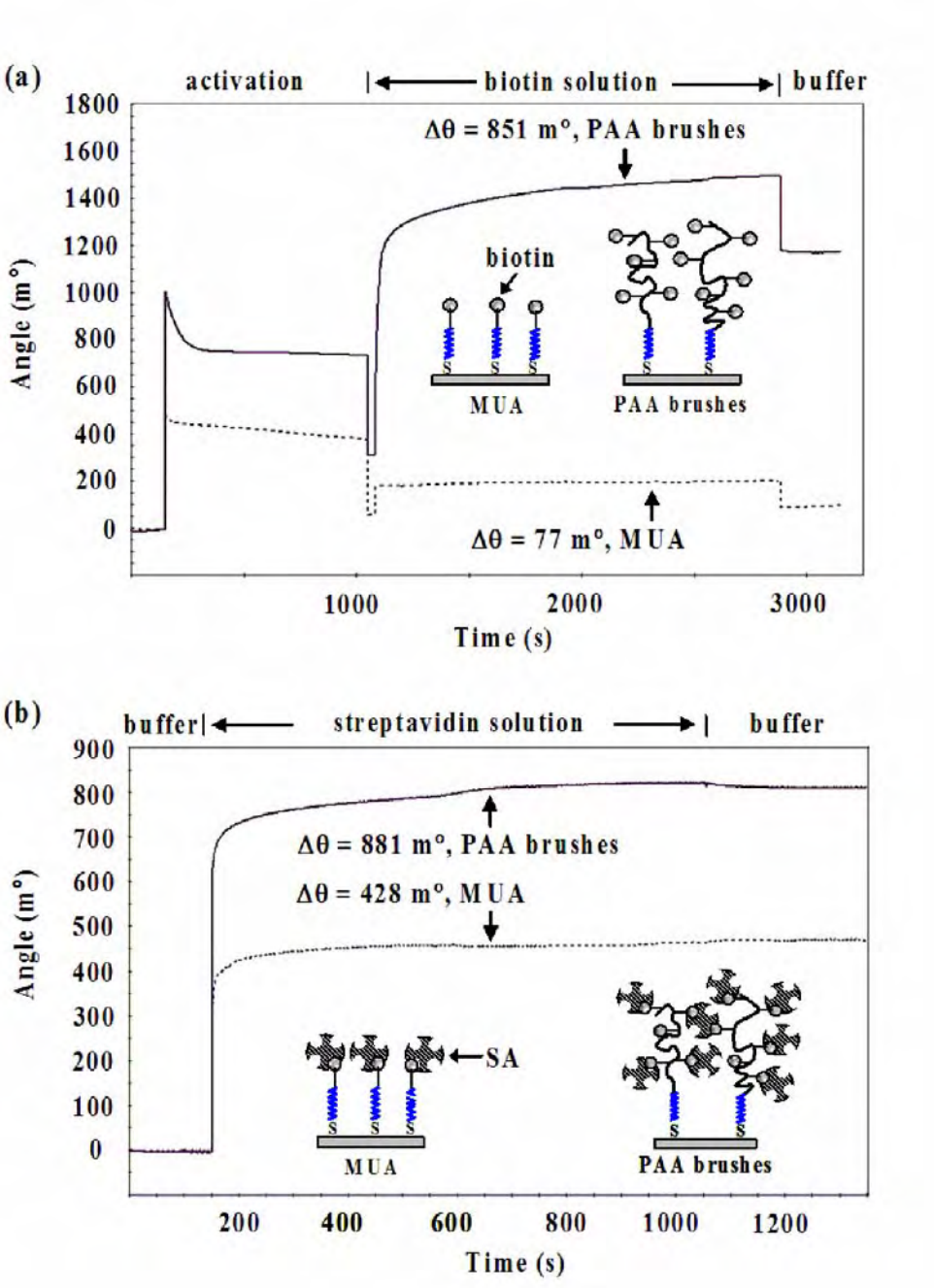

Figure 4.11 Representative SPR sensorgrams of the gold-coated SPR substrate bearing PAA brushes (3D-matrix) and MUA (2D-matrix) before and after (a) biotin immobilization and (b) SA binding. Sensorgrams shown are representative of 3 independent samples.

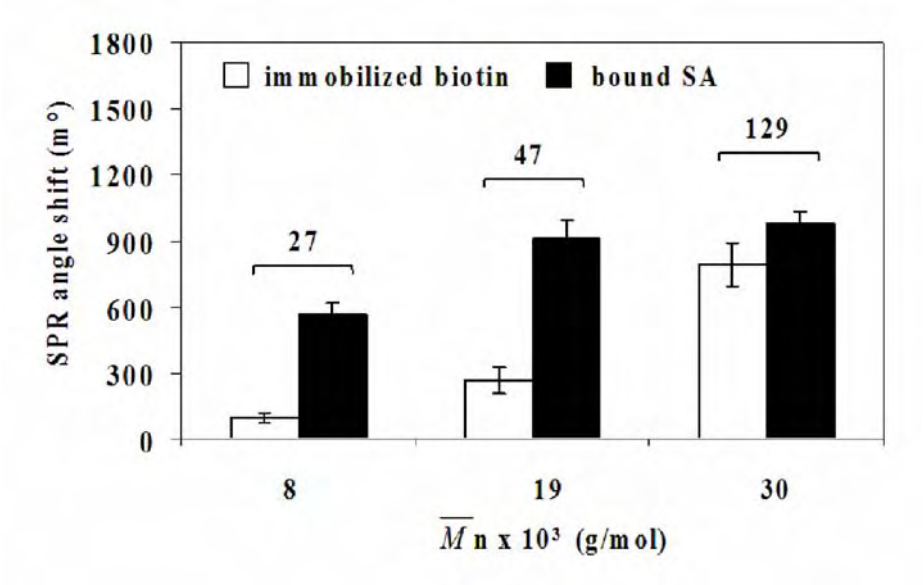

Figure 4.12 SPR angle shifts after the step of biotin immobilization and SA binding on the PAA brushes as a function of their $\overline{M}_n$, as determined by SPR analysis. Numbers above each pair of bar graphs are the binding ratio between biotin and SA. Data are shown as the mean ± SD and are derived from 3 repeats.

The success of a sensing platform cannot be judged only from the biospecific detection of the expected analyte, but it also depends upon the ability to resist adsorption of non-specific components. Here, the two model proteins, BSA and FIB, that have a similar isoelectric point (pI) to that of the target analyte, SA, were evaluated for non-specific binding. The pI of SA, BSA and FIB is 5.0, 4.8 and 5.5, respectively, and so these three proteins should be negatively charged in PBS at pH 7.4. The results (Figure 4.13) indicated that the biotinylated PAA brushes not only have good specific binding with SA but also prevent adsorption of other non-specific proteins. Apparently, the non-specific adsorption of BSA and FIB was much more suppressed on the PAA brushes-biotin (3D-matrix) than that on the MUA-biotin (2D-matrix). This may stem from the hydrophilic nature of the PAA brushes as opposed to the hydrophobic hydrocarbon linker of the MUA. This is a desirable characteristic of the sensing platform. The ability to prevent non-specific adsorption is comparable with the PAA brushes prepared by ATRP of different monomer, sodium acrylate, as recently reported by Rastogi and co-workers [56].

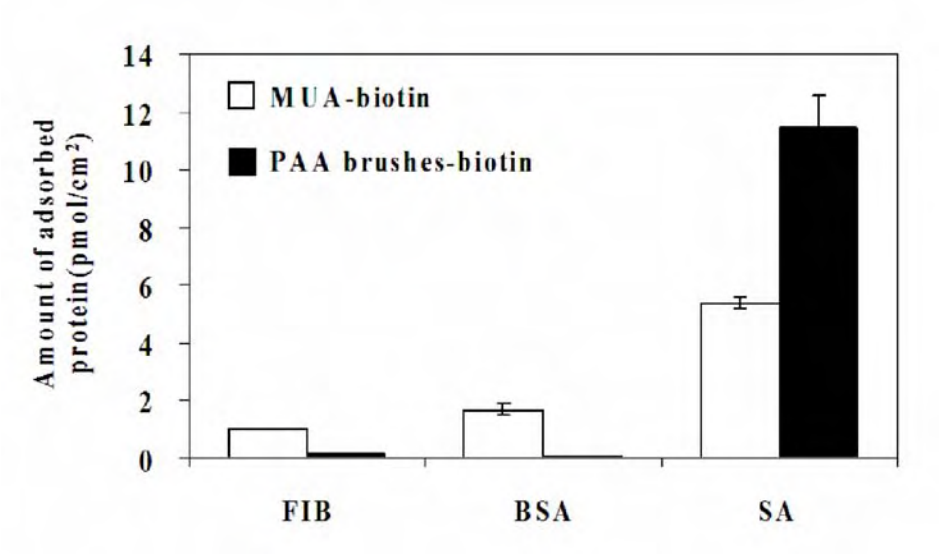

Figure 4.13 Adsorption of proteins in PBS (10 mM, pH 7.4) on the MUA-biotin and PAA brushes-biotin based sensing platforms. Data are shown as the mean ± SD and are derived from 3 repeats.

There are two important issues here. Firstly, it is certainly not necessary to have such a high probe density in the 3D sensing platform of PAA brushes in order to achieve a superior detection signal to that of the 2D SAM-based sensing platform. Secondly, it seems that the problem due to the diffusion barrier of the analyte still persists in the case of PAA brushes even though their thickness (3-10 nm) is some ten-fold lower than those of the commercial CM-dextran-based chips (30-100 nm). This may be caused by the densely packed characteristic of the polymer brushes generated by the SIP process, since the P*t*-BA brushes used to generate the PAA brushes in this research have a graft density in a range of 0.21 - 0.31 chains/nm^2 (calculated from AFM data). This polymer brush density falls well within an extended brush regime (graft density $>$ 0.08 chains/nm^2) [57], and should limit the accessibility of analytes, especially like SA that is of a relatively large size (MW = 60 kDa).

Yang and coworkers have reported that the large proteins, BSA and, especially, fibrinogen can penetrate into the layer of poly(D-gluconamidoethyl methacrylate (PGAMA), more difficultly than that of small protein, lysozyme, especially at high graft density of the polymer brushes [58]. When the grafting density is high, the space between polymer chains becomes much narrow and densely packed. It is thus more hindered for the protein to reach

inside the inner layer of the polymer. Yoshikawa and coworkers also reported the effect of grafting density of poly(2-hydroxyethyl methacrylate) (PHEMA) brushes on the diffusion of large protein into the inner layer of polymer brushes. The grafting density at 0.06 and 0.7 chain/cm^2 exhibited exclusion effect to BSA and IgG proteins [59]. As demonstrated by Gautrot and coworkers, the swelling of the polymer brushes facilitated the penetration of histidine-tagged proteins, and subsequently provided the high protein loading levels [60]. On the other hand, a low ability to swell should diminish protein infiltration into the inner polymer layer. Particularly in the case of the PAA brushes, after being immobilized by biomolecules, the polymer chains are no longer ionizable and not charged. Therefore, the biomolecule-functionalized PAA film in the aqueous environment was found to exhibit inferior swellability as compared to the unmodified one [61].

For this reason, the next step was to vary the graft density of the PAA brushes by controlling the graft density of the surface initiator. In addition, we also tried to determine whether the extent of the carboxyl group activation would have any impact on the swellability of the sensing layer based on PAA brushes after probe immobilization and analyte detectability in terms of selectivity/specificity as well as detection limits. These issues are likely to be equally important for the optimization and development of this 3D platform for biosensing applications.

4.3 Swelling behavior of the PAA brushes

In general, the conformation of PAA which is a weak polyelectrolyte should be pH sensitive. In other words, the grafted PAA chains can adopt extended or collapsed/coiled conformation depending on pH. This pH dependent conformational change should result in a variation of thickness which can be directly correlated with the degree of film swelling. In principle, the thickness change leads to the refractive index variation of the surface that the PAA brushes are grafted from. For this reason, SPR technique can readily be used for the determination of PAA brushes swelling behavior because the change of SPR angle depends upon the change of thickness and refractive index. Figure 4.14(a) shows SPR angle shift of the surface grafted PAA brushes having target DP of 100 upon pH switching between 6.5, 4.5, and 9.5. Considering that pK_a of PAA is ~4.5, the carboxyl groups (COOH) should be ionized into negatively charged carboxylate ion (COO-) upon pH elevation above pKa and converted back to neutral carboxyl group when pH becomes lower than pKa. At pH 6.5, the chains of PAA brushes should be quite extended due to the electrostatic repulsion between the negative

carboxylate ions along the PAA backbone. Upon decreasing the pH to 4.5, the chains should be somewhat collapsed and adopt more coil-like conformation because a certain percentage of COO- groups were converted to neutral COOH so there was much less charge-charge repulsion. The lowering of SPR angle shift due to pH switching from 6.5 to 4.5 is in good agreement with this explanation. When pH was raised to 9.5, the PAA chains became more extended again. The chain extension at this pH was apparently more pronounced than that happened at pH 6.5. This outcome suggested that there were many more ionized carboxyl groups at higher pH. It should be emphasized that this pH dependent conformational change is reversible. According to Figure 4.14(b), a similar trend can also be observed for the PAA brushes having target DP of 200 except that the magnitude of the angle shift upon pH switching are much greater implying the PAA brushes having longer chain length possess higher swellability than the lower one. The transitional change became lower in magnitude when biotin was immobilized. This helps explaining why it became more difficult for SA to access inside the layer of PAA brushes, especially when a large number of COOH were bound with biotin.

Here we proposed 2 strategies to enhance the swellability of the biotinylated PAA layer in order to overcome the limitation of SA accessability. One is to reduce the degree of activation in order not to convert all COOH groups into the activated form that was later bound with biotin. The preserved COOH groups should somewhat maintain the swellability of the biotinylated PAA layer and allows SA to penetrate inside more efficiently. Another approach is to decrease the PAA grafting density by incorporating and inactive hydroxyl-terminated thiol along with the bromoester-terminated thiol in the step of surface grafting of initiator.

As depicted in Figure 4.15, the amount of activated ester in the form of *N*-succimidyl groups has a significant impact on the biotin/SA binding ratio. Although the degree of activation of 0.43 ± 0.18 nmol/cm^2 gave rise to much lower quantity of immobilized biotin in comparison with that of 2.14 ± 0.21 nmol/cm^2 (~1/8), the former yielded relatively the same magnitude of SA binding as the latter. This result coincides with our speculation that too many bound biotin molecules deteriorated the SA binding efficiency due to the suppressed swellability. The optimized degree of activation that gave the highest SA binding quantity was at 1.09 ± 0.14 nmol/cm^2.

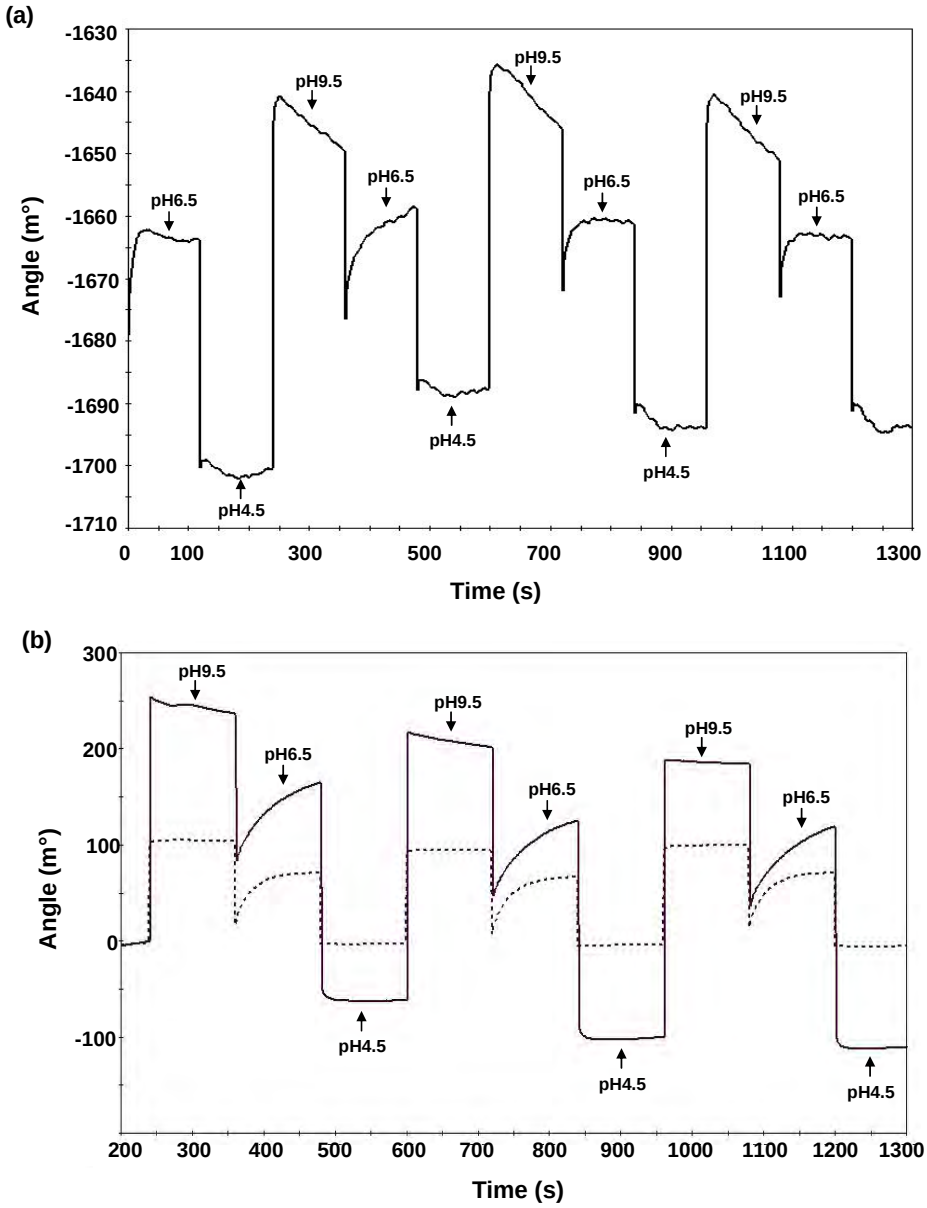

Figure 4.14 SPR angle shift of PAA brushes: (a) target DP = 100 and (b) target DP = 200 before (solid line) and after (dashed line) biotin immobilization.

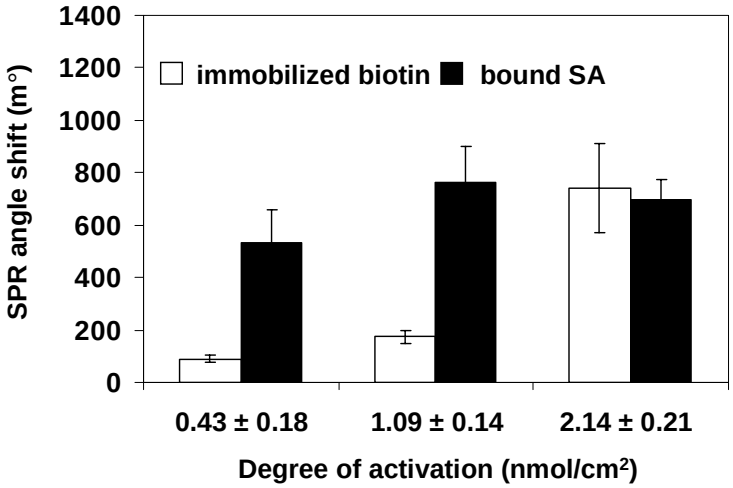

Figure 4.15 SPR angle shift of PAA brushes having target DP = 200 after biotin immobilization and SA binding as a function of degree of carboxyl group activation which is expressed in term of the amount of introduced *N*-succimidyl groups.

4.4 Effect of the PAA brushes graft density on the SA binding of the biotin-attached PAA brushes

A schematic illustration of the synthetic pathway for preparation of grafted PAA brushes having varied graft density onto SPR chip is shown in Figure 4.16. The growth of the PAA brushes on gold substrate was confirmed by water contact angle measurements. As the molar fraction of initiator increased from 10 to 100%, the advancing water contact angle (θ_A) increased from 41± 4.8° to 70 ±2.9° implying that the amount of the graft initiator corresponded quite well with the ratio thiol-modified intiator introduced to the mixed solution that the gold-coated SPR disk was exposed in the first step. The SPR chips were then allowed to react with *t*-BA monomer in the presence of an ATRP catalyst system at ambient temperature to grow polymer brushes. As a consequence of the P*t*-BA brushes formation, the θ_A markedly increased. After hydrolysis, the θ_A decreased drastically from the hydrophobic surface having P*t*-BA brushes to the hydrophilic surface having PAA brushes. All contact angle data well correlated with the amount of grafted polymer brushes both in the cases of P*t*-BA and PAA. It should be emphasized that $MeSO_3H$ in CH_2Cl_2 was used as hydrolyzing agent. This is mainly due to the fact that it is more effective in removing the *t*-butyl groups than TFA.

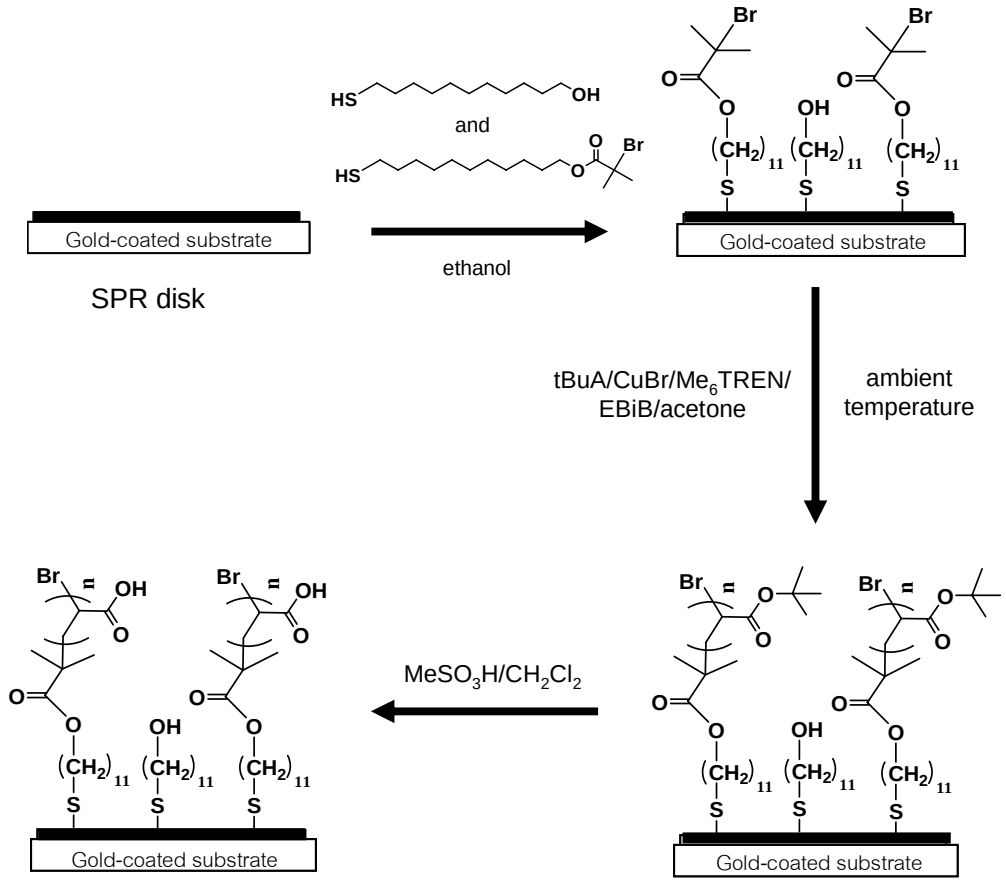

Figure 4.16 The synthetic pathway for preparation of grafted PAA brushes having varied graft density onto SPR chip.

Table 4.2 Advancing (θ_A) water contact angle of the functionalized gold-coated SPR substrates obtained with a targeted DP of 200. Data are shown as the mean ± SD and are derived from 5 repeats.

	Molar fraction of initiator (%)		
Sample	10	50	100
gold-coated of SPR chip	88 ± 2.1	90 ± 1.4	87 ± 2.2
surface-grafted initiator	41± 4.8	59 ± 6.0	70 ±2.9
P*t*-BA brushes	70 ± 1.7	87 ± 3.4	91 ± 4.0
PAA brushes	58 ± 0.8	28 ± 2.6	18 ± 1.4

The formation of PAA brushes on SPR chip can also be confirmed by atomic force microscopy (AFM). Figure 4.17 shows AFM images demonstrating the coverage of PAA brushes at different graft density on the gold-coated SPR surface. The surface of bare gold was apparently smooth with mean roughness (Ra) of 0.96 nm (Figure 4.17a). The surface roughness was elevated after being grafted with the PAA brushes. The maximum Ra was 2.1 nm. Moreover, it was found that the size of protrusions seem to be larger as the graft density increased implying the different quantity of PAA brushes were grafted on the surface.

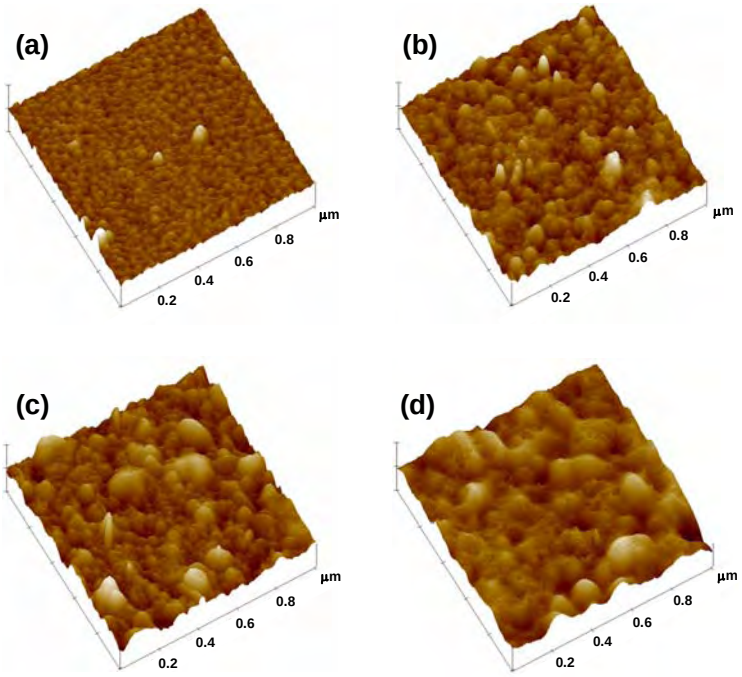

Figure 4.17 AFM images of (a) bare gold surface before and after being grafted with PAA brushes having (b) 10%, (c) 50%, and (d) 100% graft density.

As determined by toluidine blue O assay, the density of carboxyl groups of the PAA brushes increased as a function of graft density of the polymer brushes (shown in Figure 4.18). These results suggested that the carboxyl group density of the PAA brushes can be varied as a function of graft density of the polymer brushes.

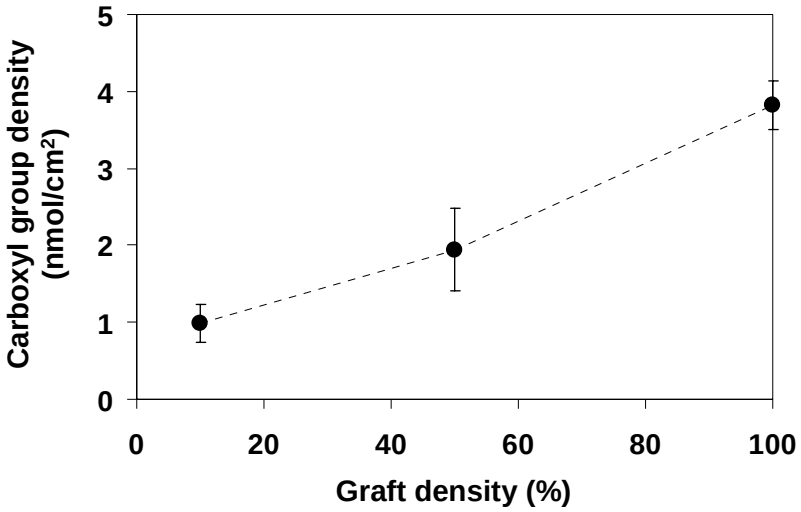

Figure 4.18 Carboxyl group density as a function of graft density of PAA polymer brushes.

Figure 4.19 demonstrates relation between amount of biotin immobilization and SA binding capacity as a function of graft density. As expected, when the grafting density of the polymer brushes or the amount of carboxyl groups increased, the biotin binding capacity of the PAA was also increased. However, the accessibility of SA (60 kD) which is a relatively large protein was limited at high graft density of polymer brushes even though more biotin molecules were immobilized onto the PAA brushes. The biotin/SA binding ratio of the PAA brushes having 50% graft density was closest to the theoretical values of 4 indicating its superior performance to the PAA brushes having 10 and 100% graft denstity.

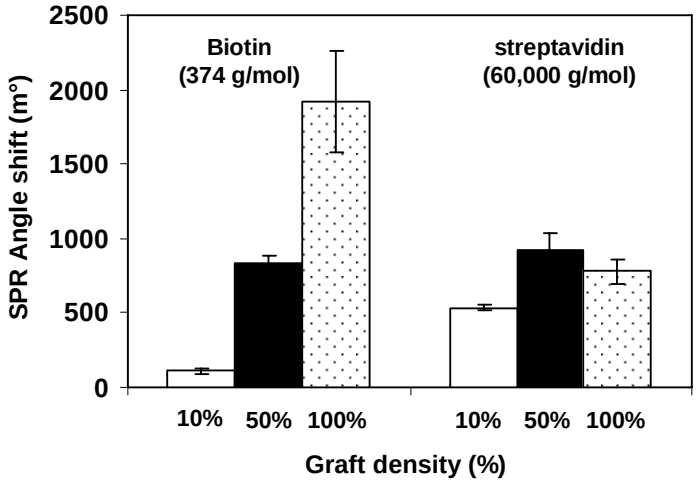

Figure 4.19 SPR angle shift of PAA brushes having target DP = 200 after biotin immobilization and SA binding as a function of graft density.

One of the major concern when dealing with biosensing applications is the undesirable non-specific adsorption. In this work, we investigated the protein adsorption of the PAA brushes in comparison with MUA. Figure 4.20 shows the amount of adsorbed protein after soaking with protein solution in PBS (pH 7.4). The adsorption of negatively charged protein: streptavidin (SA, 60 kD, pI = 5), bovine serum albumin (BSA, 69 kD, pI = 4.8), and fibrinogen (FIB, 340 kD, pI = 5.5) on the PAA brushes having 50 and 100% graft density was much lower than that of the MUA. Despite its greater SA binding efficiency, the PAA brushes with 10% graft density suffer a great extent of non-specific adsorption with all proteins tested. However, in the case of positive charge protein (lysozyme, 14 kD, pI = 12) highly adsorbed on PAA brushes especially at high graft density which may be caused by the negative charges of the PAA brushes (pKa = 6.5-6.6).

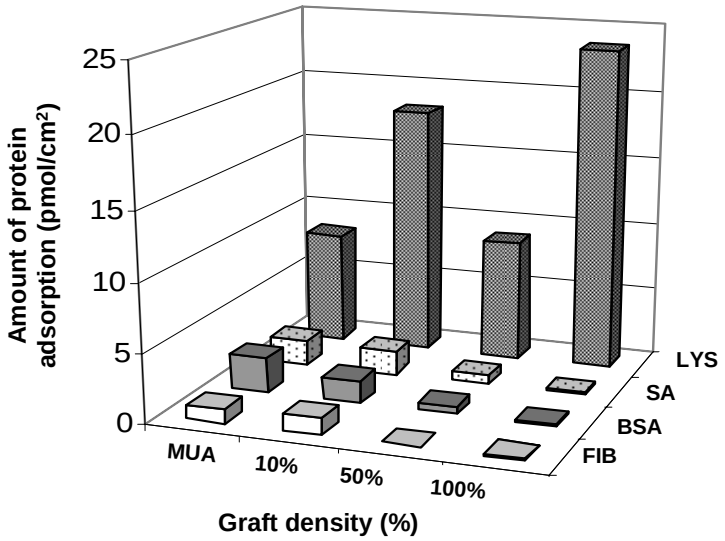

Figure 4.20 Adsorption of proteins at pH 7.4 on PAA brushes having target DP of 200 as a function of graft density in comparison with MUA.

Figure 4.21 indicates that the developed biotinylated surface not only has a good specific binding with SA but also resists nonspecific adsorption of other non-specific proteins. This is a desirable characteristic of the sensing platform. The best performance was found on the PAA brushes having 50% graft density, of which the amount of bound SA was the highest with essentially no non-specific adsorption of other proteins. These results also suggested that the 3D layer of PAA brushes possessed greater binding capacity towards streptavidin (SA) detection as compared with the 2D monolayer of MUA.

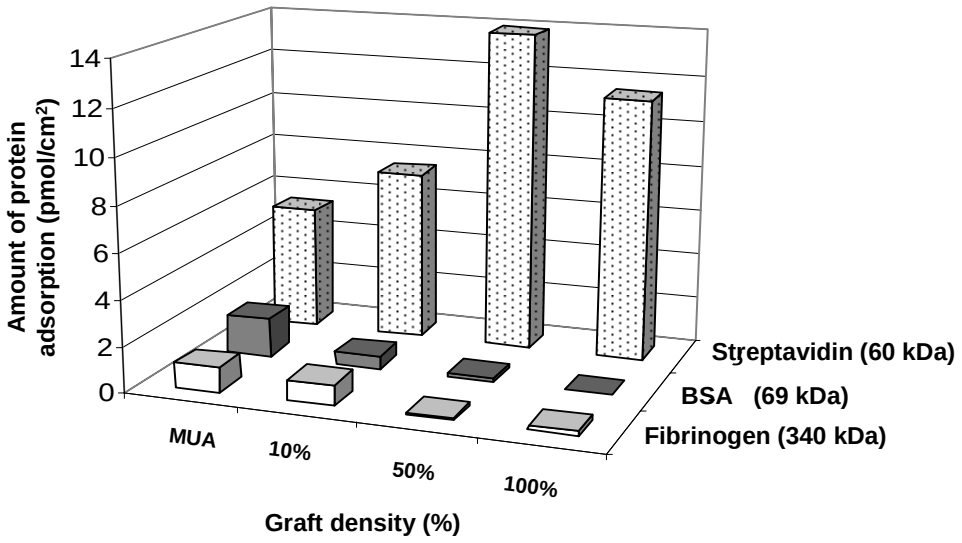

Figure 4.21 Adsorption of proteins at pH 7.4 on biotinylated PAA brushes having target DP of 200 as a function on graft density in comparison with biotinylated MUA.

4.5 Multilayer assembly on the surface-tethered PAA brushes

In this part of the studies, the surface-tethered PAA brushes were used as a substrate for multilayer assembly. Generated by SIP, the graft density of the PAA brushes should be high enough to induce chain stretching allowing a thicker individual layer to be formed. If that is the case, the thicknesses of individual layer and multilayer should be varied as a function of PAA brushes thickness. In order to test the concept, two multilayer systems which are chitosan/ poly(10,12-pentacosadiynoic acid) (PPCDA)) vesicles and chitosan/PAA were fabricated on the surface-tethered PAA brushes having two different molecular weights and thicknesses. Chitosan (CHI) was chosen as a cationic polyelectrolyte because it is natural polymer that possesses several interesting bioactivities that might be beneficial for the bio-related applications. The adsorption of CHI (pKa = 6.3-6.5) was done at pH 4 so CHI was entirely protonated. The adsorption of both PAA and PPCDA having COOH groups (pKa = 4.50-4.75) was conducted at pH 4 and 5.6, respectively. Thus, PAA was partly dissociated meaning that it exists in the form of carboxylate anion (COO-) as well as carboxyl group (COOH) which is uncharged. Unlike PAA, PPCDA is completely dissociated at pH 5.6. Therefore, the assembly of the CHI/PAA multilayer should be driven by both hydrogen bonding and electrostatic

attraction, whereas the assembly of CHI/PPCDA multilayer should mainly be driven by electrostatic attraction.

PPCDA vesicles were first selected as anionic species for multilayer assembly. The maximum absorption of UV-Vis light at the wavenumber of 640 nm of PPCDA vesicles allows the growth of CHI/PPCDA on glass-tethered PAA brushes to be conveniently monitored by UV-Vis spectroscopy. CHI as a cationic polyelectrolyte was deposited as the first layer followed by PPCDA. According to Figure 4.22, the absorbance at 640 nm increases linearly with the number of deposited layer indicating a stepwise growth of the multilayer between CHI and PPCDA. More importantly, it was observed that the absorbance of the multilayer grew from PAA brushes having $\overline{M}_n$ = 12,661 was greater than that of the multilayer grew from PAA brushes having $\overline{M}_n$ = 9125. These evidences implied that the amount of CHI as well as the PPCDA deposited depended upon the carboxyl group density of PAA brushes which can be varied as a function of the molecular weight of polymer brushes. Obviously, the absorbance increment for the PAA brushes having higher $\overline{M}_n$ was greater implying once again that the amount of CHI as well as the PPCDA depended upon the carboxyl group density of PAA brushes. This evidently suggests that the large quantity of the assembled film can be achieved without having to do a great number of deposition.

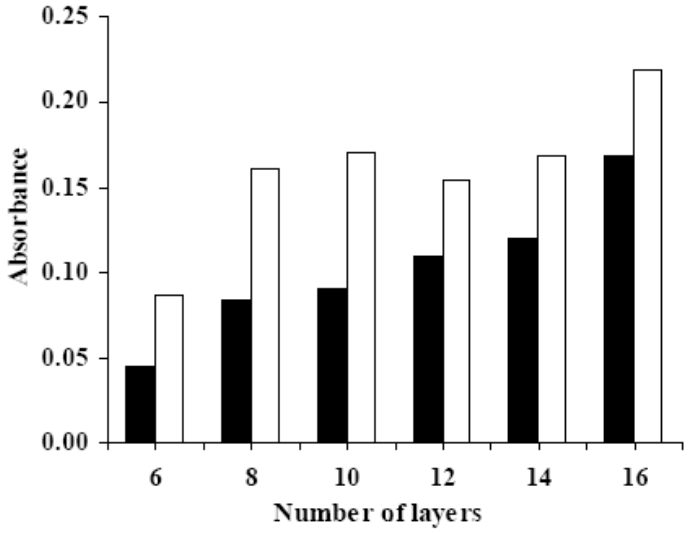

Figure 4.22 UV-Vis absorbance at 640 nm of CHI/ PPCDA vesicles multilayer ($\overline{M}_n$ of CHI =100,000 g/mole) on glass-tethered PAA brushes having $\overline{M}_n$ = 9,125 (■) and 12,661(□) as a function of number of layer.

To determine the effect of PAA brushes thickness on the thicknesses of individual layer and multilayer, the growth of CHI/PAA multilayer on the silicon tethered PAA brushes were characterized by ellipsometry. Chitosan as a cationic polyelectrolyte was deposited as the first layer followed by PAA. The PAA brushes having two different $\overline{M}_n$ and thickness were used for multilayer assembly. One has $\overline{M}_n$ of 13,835 and the thickness of 6.7 nm. The other has $\overline{M}_n$ of 24,797 and the thickness of 10.4 nm. The results shown in Figure 4.23 suggested that the thickness of the multilayer film proportionally increased as a function of the number of deposition on both substrates. Also, the thickness increment of each individual layer corresponded very well with the initial thickness of PAA brushes. One deposition step can elevate the thickness of as much as 5-10 nm. Thus, the thick multilayer film can easily be generated by using a thick PAA brushes as substrate. The thickness of the multilayer tended to level off after 8 depositon steps. It should be noted that the substrate with 9 layers appeared randomly opaque. It is thus assumed that there was some polymer aggregation taking place on the substrate causing the rough surface to be formed. Thus, the uniform coating of the layer cannot be achieved and the reliable thickness can no longer be measured by ellipsometry. This is the reason why we see the unchanged thickness beyond 8 layers. The results in this section implied that the graft density of PAA brushes was high enough to induce chain stretching and thereby allowed a thicker individual layer to be formed.

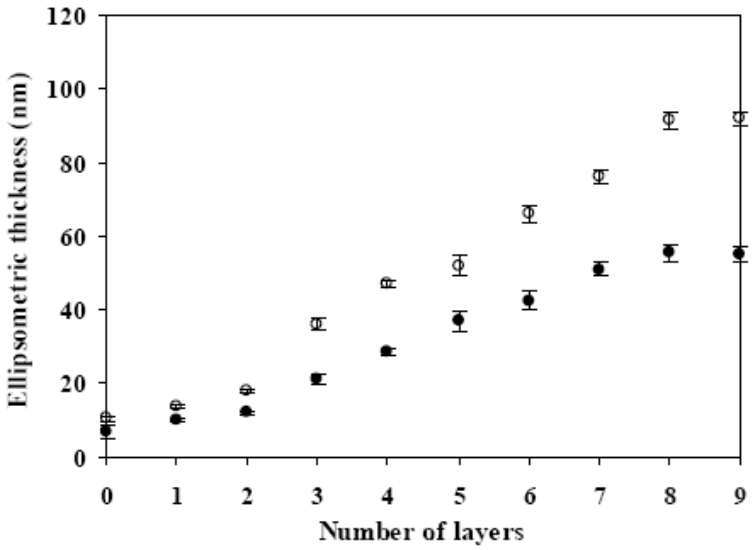

Figure 4.23 Ellipsometric thickness of CHI/PAA multilayer on silicon-tethered PAA brushes having $\overline{M}_n$ = 24,797 (○) and 13,835 (●) as a function of number of layer.

FT-IR technique was used to characterize the functional groups of the CHI/PAA multilayer film on PAA brushes tethered to silica particles. In addition to the carbonyl stretching at 1716 cm^{-1} of PAA, the signal at 1548 cm^{-1} assigned to the N-H bending (amide II) appeared in the spectrum of CHI/PAA bilayer on PAA brushes (Figure 4.24c) indicating the presence of CHI in the multilayer. Due to the masking of the signal from C-Si-O stretching of silica, the carbonyl stretching (amide I) of chitosan which should appear at 1650 cm^{-1} cannot be observed.

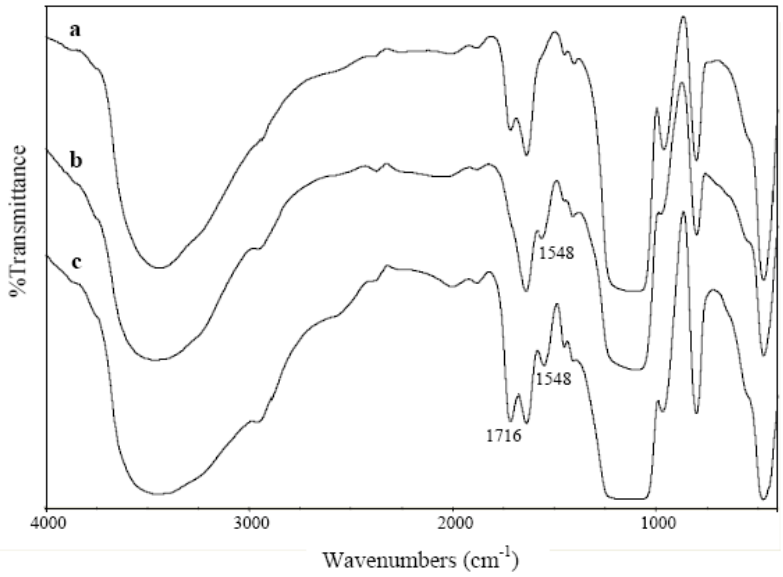

Figure 4.24 FT-IR spectra of silica particles having (a) PAA brushes, (b) 1 layer of CHI on PAA brushes, and (c) CHI/PAA bilayer on PAA brushes.

If the concept of alternative adsorption is valid, the surface property of the multilayer film should alternately change. In other words, the multilayer film should be stratified. Water contact angle data shown in Figure 4.25 confirmed that the assembled film was stratified. The number appearing on the horizontal scale represented the number of deposition. If the number of layer is odd, CHI is the top layer and the charge of the outermost layer is positive. If the number of layer is even, PAA is the top layer and the charge of the outermost layer is negative. In this case, each individual layer are definitely thicker than the sampling depth of contact angle measurement (a few Å) so that the wettability of the multilayer film was strongly dependent on the last layer deposited and the influence of the underlying layers was not observed. The assembled film having the odd number of deposited layer (positively-charged surface) was clearly more hydrophobic than the one having the even number of deposited layer (negatively-charged surface). The results from contact angle analysis also implied that other surface properties of the multilayer film such as surface topography, bioactivity should also be stratified.

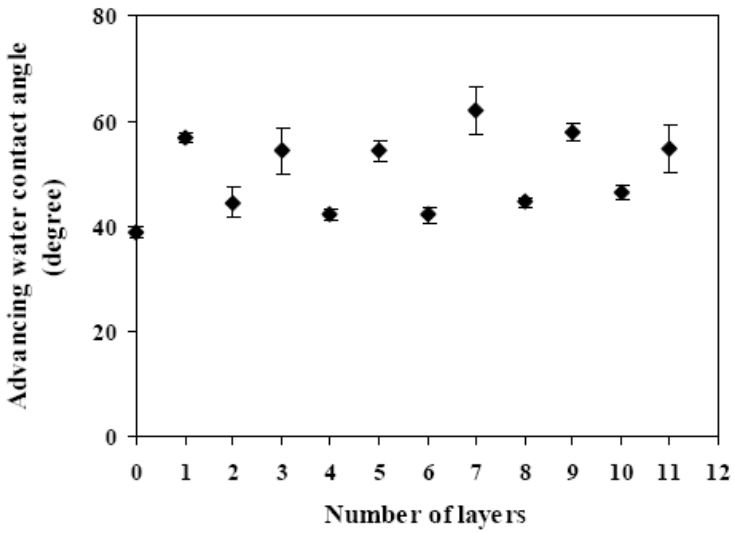

Figure 4.25 Water contact angle of CHI/PAA multilayer on surface-tethered PAA brushes.

Atomic force microscopy (AFM) was used as a tool to determine the surface topography and roughness of the PAA brushes as well as the deposited multilayer. Similar to the cleaned silicon surface, AFM images of the P*t*-BA brushes displayed in Figure 4.26 are almost featureless with relatively low surface roughness suggesting that the grafted P*t*-BA brushes of both molecular weights are relatively smooth and uniform.

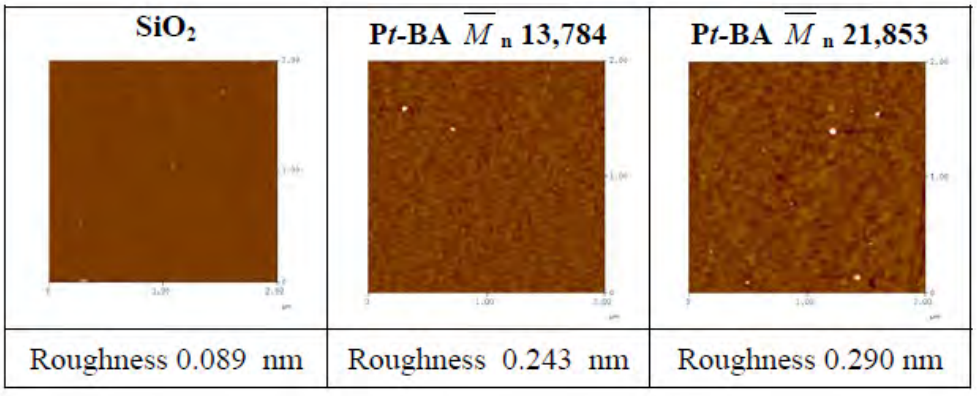

Figure 4.26 AFM images of surface-tethered P*t*-BA brushes in comparison with the virgin silicon surface.

AFM images shown in Figure 4.27 implied that the grafted PAA brushes of both molecular weights are relatively smooth and uniform similar to the grafted P*t*-BA brushes. Also, the multilayer films having PAA as the top layer are obviously smoother than those having CHI as the top layer. The additional roughness introduced by the deposition of CHI progressively increases as a function of the number of layer. The size of the ripple-like feature of the multilayer having CHI as the top layer became correspondingly larger as the number of deposition increased. Interestingly, the roughness of the multilayer significantly decreased after it was covered by PAA suggesting that the roughness of the multilayer is also stratified. Having the same number of the deposited layer, the multilayer assembled on the PAA brushes with higher molecular weight are apparently rougher. This can be explained by the fact that the thicknesses of both the individual layer and overall multilayer are larger in the case of high molecular weight PAA brushes.

Sample	$\overline{M}_n$ 13,784 g/mol	$\overline{M}_n$ 21,853 g/mol
PAA brushes	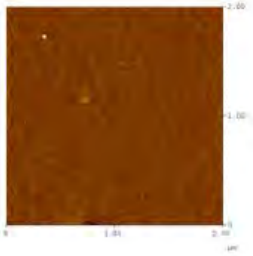	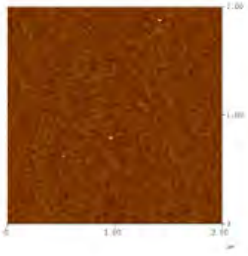
Roughness (nm)	0.193	0.238
CHI on PAA brushes (1 layer)	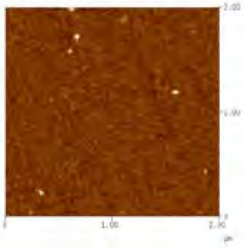	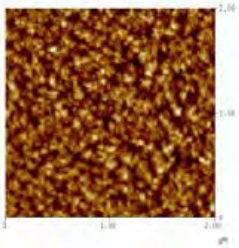
Roughness (nm)	0.361	2.186
$(CHI/PAA)_2CHI$ on PAA brushes (5 layers)	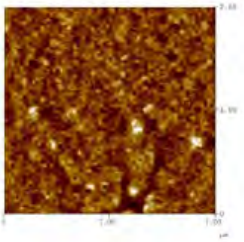	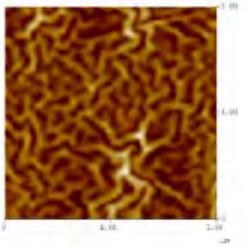
Roughness (nm)	0.747	5.461
$(Chitosan/PAA)_3$ on PAA brushes (6 layers)	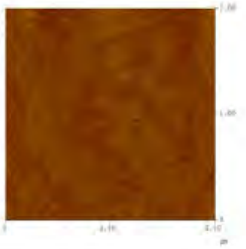	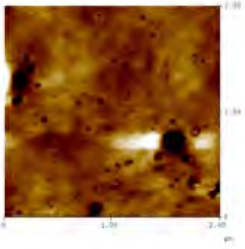
Roughness (nm)	0.018	0.575

Figure 4.27 AFM images of surface-tethered PAA brushes with CHI/PAA multilayer.

$(CHI/PAA)_3CHI$ on PAA brushes (7 layers)	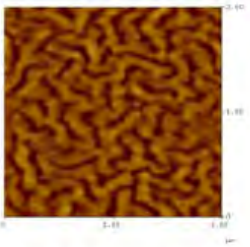	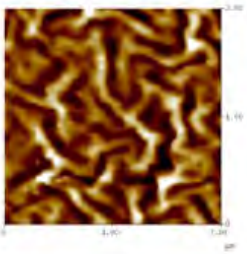
Roughness (nm)	5.143	10.615

Figure 4.27 AFM images of surface-tethered PAA brushes with CHI/PAA multilayer (continue)

4.6 Stability of CHI/PAA multilayer films on the surface-tethered PAA brushes

The stability of the multilayer system is often of concern, especially in the environment that causes the displacement of the first adsorbed layer of polyelectrolyte and the subsequent desorption of the whole multilayer assembly i.e. changing the sign of the surface charge of the substrate or by addition of competing low molecular weight electrolytes. In this particular study, it is believed that the problem of the stability can be overcome since the PAA brushes are attached to the substrate by covalent bonds. To test the stability of the multilayer, the CHI/PAA multilayer on PAA brushes was subjected to soaking in buffer solutions having different pH for 24 h before being characterized by water contact angle and FT-IR analytes. It can be demonstrated from Table 4.3 that the water contact angle of the multilayer became slightly higher after soaking in neutral and acidic buffer solution implying that the surface still hold the characteristic of CHI whose contact angle is higher than that of PAA (See Figure 4.25). In contrast, the water contact angle was a few degrees lower after soaking in basic buffer solution suggesting that the surface was somewhat more hydrophilic. This may be caused by the partial aggregation of CHI in the basic solution which made the underlying PAA more accessible to the contact angle measurement. According to the FT-IR spectra shown in Figure 4.28, it is obvious that the common features and the relative peak intensity remained unchanged after the soaking independent of the pH of the buffer. Results from both techniques suggest that the multilayers are quite stable. Nonetheless, these results have not indicated that there was no polymer desorbed after the soaking. Such information require a more quantitative measure that is sensitive to the change of mass such as quartz crystal microbalance (QCM).

Table 4.3 Advancing water contact angle of $(CHI/PAA)_2CHI$ on PAA brushes before and after soaking in buffer solutions

Condition	Advancing water contact angle (degree)
Before soaking	43.6 ± 1.0
After soaking in buffer solution	
pH 3.5	44.8 ± 2.6
pH 7.4	46.8 ± 4.6
pH 10.0	39.9 ± 1.9

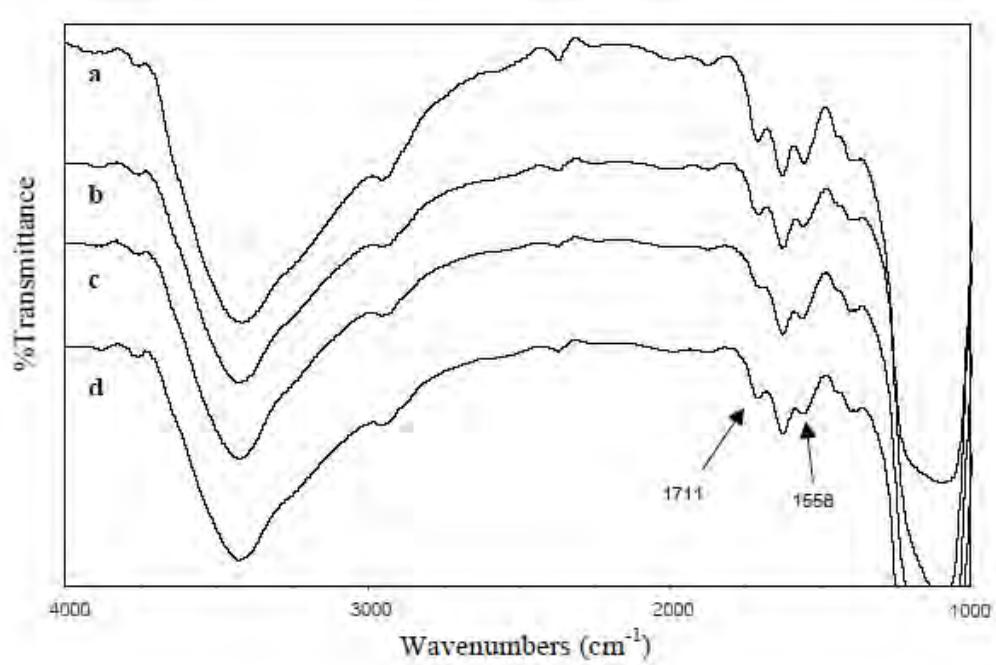

Figure 4.28 FT-IR spectra of silica particles having $(CHI/PAA)_2CHI$ on PAA brushes (a) before and after soaking in buffer solution at (b) pH 3.5, (c) pH 7.4, and (d) pH 10.0.

4.7 Protein adsorption of the multilayer film deposited on the surface-tethered PAA brushes

It is important to determine whether the multilayer film deposited on the surface-tethered PAA brushes can be of practical uses. In particular, this study is interested in the bio-related applications of the multilayer film. Biological response based on protein adsorption was the

tested. Albumin protein, a carboxylic acid-rich protein, was selected for protein adsorption study. Its carboxylic acid group is converted to a negatively charged carboxylate ion at pH 7.4. The amount of adsorbed protein was determined by BCA assay. As shown in Figure 4.29, the adsorbed amount of albumin on the multilayer having an odd number of layers (CHI as the top layer) and a positive charge was higher than those having an even number of layers (PAA as the top layer) and a negative charge. Such a trend can be explained by the fact that the adsorption was promoted by electrostatic attraction between the positively-charged surface of the outermost layer and albumin. On the other hand, the adsorption of the negatively charged albumin was suppressed on the negatively charged surface having PAA as the top layer due to the electrostatic repulsion. The alternate trend is realized for both surface-tethered PAA regardless of the molecular weight. The roughness which increases with the number of layer seems to influence the quantity of adsorbed protein. The rougher the surface is, the greater the quantity of adsorbed protein was found.

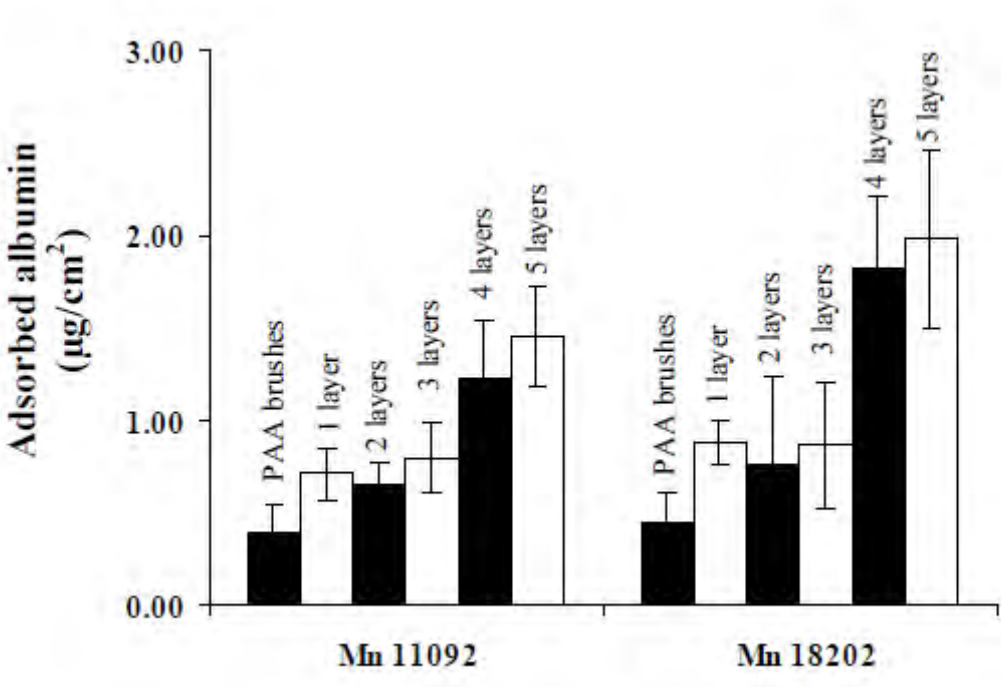

Figure 4.29 Amount of adsorbed albumin on CHI/PAA multilayer on PAA brushes. The number written above the bar graph is the number of layer.

We also attempt to alter the bioactivity of the CHI/PAA multilayer by depositing other charged bioactive polyelectrolyte (Figure 4.30) as the top layer. The amount of adsorbed

albumin on all multilayer films is outlined in Table 4.4. Apparently, the amount of adsorbed albumin decreased when the outermost layer was changed to HTACC and heparin indicating that the response to the protein was changed, especially in the case of heparin, a well-known protein-repelling polymer, whose charge characteristic is negative.

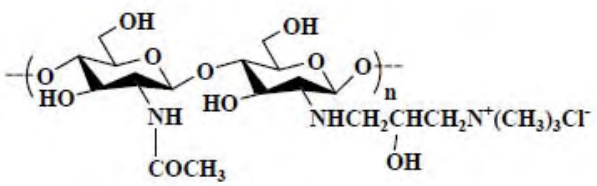

HTACC

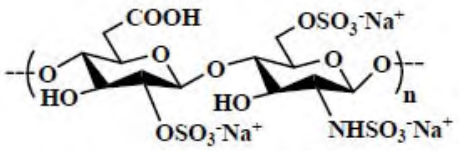

heparin sodium salt

Figure 4.30 Chemical structures of HTACC and heparin.

Table 4.4 Adsorbed albumin on CHI/PAA multilayer on PAA brushes.

Sample	Adsorbed albumin (μg/cm^2)
PAA brushes, $\overline{M}_n$ = 22,391	0.58 ± 0.13
(CHI-PAA)$_2$	0.67 ± 0.19
(CHI-PAA)$_2$CHI	1.10 ± 0.30
(CHI-PAA)$_2$HTACC	0.67 ± 0.11
(CHI-PAA)$_2$CHI-heparin	0.39 ± 0.11

CHAPTER V

EXECUTIVE SUMMARY

It has been demonstrated that poly(*tert*-butyl acrylate) (P*t*-BA) brushes can be prepared from the surfaces bearing α-bromoester groups by surface-initiated atom transfer radical polymerization (ATRP) of *tert*-butyl acrylate (*t*-BA) both on silicon and gold-coated surface plasmon resonance (SPR) substrates via atom transfer radical polymerization (ATRP). Poly(acrylic acid) (PAA) brushes were subsequently obtained after *tert*-butyl groups of the P*t*-BA brushes were removed by acid hydrolysis. The molecular weight and thickness of the polymer brushes can be controlled by reaction time and monomer to initiatior ratio in the solution (targeted degree of polymerization). The graft density of P*t*-BA brushes was approximately 0.25 and 0.32 chains/nm^2 for the targeted DP = 100 and 200, respectively. The formation of polymer brushes was also monitored by a number of characterization techniques, namely water contact angle measurements, FT-IR and AFM analyses.

As determined by toluidine blue O assay, the carboxyl group density of the PAA brushes was varied as a function of the chain length (MW) as well as graft density of the surface-grafted initiator. These active carboxyl groups are readily available for the attachment of the biotin-sensing probe, as verified by monitoring the water contact angle and FT-IR analysis. The immobilized biotin on PAA brushes can bind effectively with streptavidin (SA) as visualized by fluorescence microscopy and thoroughly determined by SPR analysis. It was found that the carboxyl group activation and subsequent biotin binding have a significant impact on swellability of the PAA brushes and detectability of SA. The limited accessibility of the SA to the immobilized biotin of the densely packed PAA brushes can be overcome by the reduction of packing density of the polymer brushes. Therefore, to achieve high performance of the surface-tethered PAA brushes as a sensing layer for biosensor, the effect of graft density and the swellability of the PAA brushes should be optimized. In our case, the best performance was found on the PAA brushes having 50% graft density, of which the amount of bound SA was the highest with essentially no non-specific adsorption of other negatively charged proteins, bovine serum albumin (BSA), fibrinogen (FIB). The layer of PAA brushes exhibited superior SA binding

as well as the ability to resist non-specific adsorption as compared with the conventional self-assembled monolayer (SAM) system. This strongly suggests the potential of PAA brushes as precursor layer for biosensor.

Also, it has been demonstrated that the carboxyl groups of PAA brushes are readily available as negatively charged moieties for layer-by-layer assembly of selected polyelectrolytes, chitosan (CHI), poly(acrylic acid) (PAA) and poly(10,12-pentacosadiynoic acid) (PPCDA) vesicles, all of which are weak polyelectrolytes. The formation of CHI/PPCDA multilayer system was monitored by UV-VIS spectroscopy whereas the CHI/PAA multilayer system was characterized by ellipsometry, water contact angle measurements, FT-IR, and AFM. In the case of CHI/PPCDA multilayer system, it was found that the quantity of PPCDA deposited not only depended upon the number of deposition step but also varied as a function of the molecular weight of the surface-tethered PAA brushes and deposition time. It is also clear that the thickness of each layer in the CHI/PAA multilayer assembly depends heavily on the thickness of the initial PAA brush layer. As high as 5-10 nm thick film can be deposited by one deposition step. The results in this section implied that the graft density of PAA brushes was high enough to induce chain stretching and thereby allowed a thicker individual layer to be formed. According to the contact angle and AFM analyses, the alternate surface properties were observed indicating that the multilayer formed was stratified. The presence of the multilayer film was also confirmed by FT-IR analysis. In addition, the bioactivity of the CHI/PAA multilayer film can be tailored by changing the last polyelectrolyte deposited. This was realized from the studies of albumin adsorption.

The stability of the multilayer film assembled on the surface-tethered PAA brushes is a subject of our future investigation. We aim to use more sensitive techniques such as SPR or QCM to monitor the stability of the multilayer film under different environment. The CHI/PPCDA system is of particular interest because its potential as a chromogenic sensing applications. The behavior of the CHI/PPCDA multilayer deposited on the surface-tethered PAA brushes will be compared with that deposited on the conventional substrate.

.

REFERENCES

1. Zhao, B.; Brittain, W. J. “Polymer Brushes: Surface-Immobilized macromolecules” *Prog. Polym. Sci.* **2000**, *25,* 677-710.
2. Soga, K. G.; Zuckermann, M. J.; Guo, H. “Binary polymer brush in a solvent” *Macromolecules* **1996**, *29,* 1998-2005.
3. Mansky, P.; Liu, Y.; Huang, E.; Russell T. P.; Hawker, C. “Controlling polymer-surface interactions with random copolymer brushes” *Science* **1997**, *275,* 1458-1460.
4. Zhao, B.; Brittain, W. J. “Synthesis of tethered polystyrene-*block*-poly(methyl methacrylate) monolayer on a silicate substrate by sequential carbocationic polymerization and atom transfer radical polymerization” *J. Am. Chem. Soc.* **1999**, *1219,* 3557-3558.
5. Nakayama, Y.; Matsuda, T. “Surface macromolecular architectural designs using photo-graft copolymerization based on photochemistry of benzyl *N,N*-diethyldithiocarbamate” *Macromolecules* **1996**, *29,* 8622-8630.
6. Ejaz, M.; Yamamoto, S.; Ohno, K.; Tsujii, Y.; Fukuda, T. “Controlled graft polymerization of methyl methacrylate on silicon substrate by the combined use of the Langmuir-Blodgett and atom transfer radical polymerization techniques” *Macromolecules* **1998**, *31,* 5934-5936.
7. Husseman, M.; Malmström, E. E.; McNamara, M.; Mate, M.; Mecerreyes, D.; Benoit, D. G.; Hedrick, Mansky, P.; Huang, E. ; Russell, T. P.; Hawker, C. J. “Controlled synthesis of polymer brushes by "living" free radical polymerization techniques” *Macromolecules* **1999**, *32,* 1424-1431.
8. Huang, X.; Wirth, M. J. “Surface initiation of living radical polymerization for growth of tethered chains of low polydispersity” *Macromolecules* **1999**, *32,* 1694-1696.
9. Sedjo, R. A.; Mirous, B. K.; Brittain, W. J. “Synthesis of polystyrene-*block*-poly(methyl methacrylate) brushes by reverse atom transfer radical polymerization” *Macromolecules* **2000**, *33,* 1492-1493.
10. de Boer, B.; Simon, H. K.; Werts, M. P. L.; van der Vegte, E. W.; Hadziioannou, G. “"Living" free radical photopolymerization initiated from surface-grafted iniferter monolayers” *Macromolecules* **2000**, *33*, 349-356.
11. Matyjaszewski, K.; Miller, P. J.; Shukla, N.; Immaraporn, B.; Gelman, A.; Luokala, B. B.; Siclovan, T. M.; Kickelbick, G.; Vallant, T.; Hoffmann, H.; Pakula, T. “Polymers at

Interfaces: Using Atom Transfer Radical Polymerization in the Controlled Growth of Homopolymers and Block Copolymers from Silicon Surfaces in the Absence of Untethered Sacrificial Initiator" *Macromolecules* **1999**, *32,* 8716-8724.

12. *von* Werene, T.; Patten, T. E. "Atom transfer radical polymerization from nanoparticles: A tool for the preparation of well-defined hybrid nanostructures and for understanding the chemistry of controlled/"living" radical polymerizations from surfaces" *J. Am. Chem. Soc.* **2001**, *123*, 7497-7505.
13. Moad, G.; Rizzardo, E.; Solomon D. H. "Selectivity of the reaction of free radicals with styrene" *Macromolecules* **1982**, *15,* 909-914.
14. Georges, M. K.; Veregin, R. P. N.; Kazmaier, P. M.; Hamer, G. K. "Narrow molecular weight resins by a free-radical polymerization process" *Macromolecules* **1993**, *26,* 2987-2988.
15. Kato, M.; Kamigaito, M.; Sawamoto, M.; Higashimura, T. "Polymerization of methyl methacrylate with the carbon tetrachloride/dichlorotris-(triphenylphosphine)ruthenium(II)/methylaluminum bis(2,6-di-*tert*-butylphenoxide) initiating system: Possibility of living radical polymerization" *Macromolecules* **1995**, *28,* 1721-1723.
16. Wang, J. S.; Matyjaszewski, K. "Controlled/"living" radical polymerization. Atom transfer radical polymerization in the presence of transition-metal complexes" *J. Am. Chem. Soc.* **1995**, *117,* 5614-5615.
17. Percec, V.; Barboiu, B. ""Living" radical polymerization of styrene initiated by arenesulfonyl chlorides and CuI(bpy)$_n$Cl" *Macromolecules* **1995**, *28,* 7970-7972.
18. Wayland, B. B.; Poszmik, G.; Mukerjee, S. L.; Fryd, M. "Living radical polymerization of acrylates by organocobalt porphyrin complexes" *J. Am. Chem. Soc.* **1994**, *116,* 7943-7944.
19. Granel, C.; DuBois, P.; Jerome, R.; Teyssie, P. "Controlled radical polymerization of methacrylic monomers in the presence of a bis(ortho-chelated) aryl nickel(II) complex and different activated alkyl halides" *Macromolecules* **1996**, *29,* 8576-8582.
20. Matyjaszewski, K. "Controlled radical polymerization" *ACS Symposium Series NO. 685 American Chemical Society:* Washington, DC, **1997.**
21. Matyjaszewski, K. "Mechanistic and synthetic aspects of atom transfer radical polymerization" *J. Macromol. Sci., Pure Appl. Chem.* **1997**, *A34,* 1785-1801.

22. Chambard, G.; Klumperman, B.; German, A. L. “Effect of Solvent on the Activation Rate Parameters for Polystyrene and Poly(butyl acrylate) Macroinitiators in Atom Transfer Radical Polymerization” *Macromolecules* **2000**, *33,* 4417-4421.
23. Matyjaszewski, K.; Xia, J. “Atom transfer radical polymerization” *Chem. Rev.* **2001**, 101, 2921-2990.
24. Davis, K.A.; Matyjaszewski, K. “Atom transfer radical polymerization of tert-butyl acrylate and preparation of block copolymers” *Macromolecules* **2000**, 33, 4039–4047.
25. Davis, K. A.; Charleux, B.; Matyjaszewski, K. “Preparation of block copolymers of polystyrene and poly(t-butyl acrylate) of various molecular weights and architectures by atom transfer radical polymerization” *J Polym Sci, Part A: Polym Chem* **2000**, 38, 2274–2283.
26. Lee, B. S.; Chi, Y. S.; Lee, K. –B.; Kim, Y. –G.; Choi, I. S. “Functionalization of poly(oligo(ethylene glycol) methacrylate) films on gold and Si/SiO_2 for immobilization of proteins and cells: SPR and QCM studies” *Biomacromolecules* **2007**, *8*, 3922–3929.
27. Dai, J.; Bao, Z.; Sun, L.; Hong, S. U.; Baker, G. L.; Bruening, M. L. “High-capacity binding of proteins by poly(acrylic acid) brushes and their derivatives” *Langmuir* **2006**, *22*, 4274-4281.
28. Cullen, S. P.; Liu, X.; Mandel, I. C.; Himpsel, F. J.; Gopalan, P. “Polymeric brushes as functional templates for immobilizing ribonuclease A: Study of binding kinetics and activity” *Langmuir* **2008**, *24*, 913-920.
29. Dong, R.; Krishnan, S.; Baird, B. A.; Lindau, M.; Ober, C. K. “Patterned biofunctional poly(acrylic acid) brushes on silicon surfaces” *Biomacromolecules* **2007**, *8*, 3082-3092.
30. Kurosawa, S.; Aizawa, H.; Talib, Z. A.; Atthoff, B.; Hilborn, J. “Synthesis of tethered-polymer brush by atom transfer radical polymerization from a plasma-polymerized-film-coated quartz crystal microbalance and its application for immunosensors” *Biosens. Bioelectron.* **2004**, *20*, 1165-1176.
31. Caruso, F.; Furlong, D. N.; Ariga, K.; Ichinose, I.; Kunitake, T. “Characterization of polyelectrolyte-protein multilayer films by atomic force microscopy, scanning electron microscopy, and fourier transform infrared reflection absorption spectroscopy” *Langmuir* **1998**, *14,* 4559-4565.

32. Krasemann, L.; Tieke. B.; “Composite membranes with ultrathin separation layer prepared by self-assembly of polyelectrolytes” *Mat. Sci. Eng.* **1999***, C8-9,* 513-518.
33. Wu, A.; Yoo, D.; Lee, J. K.; Rubner, M. F. “Solid-state light-emitting devices based on the tris-chelated ruthenium (II) complex: 3. high efficiency devices via a layer-by-layer molecular-level blending approach” *J. Am. Chem. Soc.* **1999**, *121*, 4883-4891.
34. Decher, G.; Hong, J. -D.; “Schmitt, J. Buildup of ultrathin multilayer films by a self-assembly process: III. Consecutively alternating adsorption of anionic and cationic polyelectrolytes on charged surfaces” *Thin Solid Films* **1992**, *210-211*, 831-835.
35. Schoeler, B.; Kumaraswamy, G.; Caruso, F. “Investigation of the influence of polyelectrolyte charge density on the growth of multilayer thin films prepared by the layer-by-layer technique” *Macromolecules* **2002**, *35,* 889-897.
36. Shiratori, S. S.; Rubner, M. F. “pH-Dependent thickness behavior of sequentially adsorbed layers of weak electrolytes” *Macromolecules* **2000,** *33,* 4213.
37. Lvov, Y.; Onda, M.; Ariga, K.; Kunitake, T. “Ultrathin flims of charged polysaccharides assembled alternately with linear polyions” *J. Biomater. Sci. Polymer Edn.* **1998,** *9,* 345-355.
38. Serizawa, T.; Yamaguchi, M.; Akashi, M. “Alternating bioactivity of polymeric layer-by-layer assemblies : anti-vs procoagulation of human blood on chitosan and dextran sulfate layers” *Biomacromolecules* **2002,** *3,* 724-731.
39. Harris, J. J.; Derose, P. M.; Bruening, M. L. “Synthesis of passivating, Nylon like coatings through cross-linking of ultrathin polyelectrolyte films” *J Am. Chem. Soc*. **1999**, *121,* 1978-1979.
40. Nagal, M.; Kim, B. Y.; Bruening, M. L. **“**Ultrathin, hyperbranched poly(acrylic acid) membranes on porous alumina supports” *J. Am. Chem. Soc*. **2000,** *122*, 11670-11678.
41. Ansell, M. A.; Cogan, E. B.; Page, C. “Coordinate covalent cobalt- diisocyanide multilayer thin films grown one molecular layer at a time**”** *Langmuir* **2000,** *16*, 1172-1179.
42. Serizawa, T.; Nanameki, K.; Yamamoto, K.; Akashi, M. “Thermoresponsive ultrathin hydrogels prepared by sequential chemical reactions” *Macromolecules* **2002,** *35,* 2184-2189.
43. Yang, S. U.; Lee, D.; Cohen, R. E.; Rubner, M. F. “Bioinert solution-cross-linked hydrogen-bonded multilayers on colloidal particles” *Langmuir* **2004,** *20,* 5978-5981.

44. Van der Steeg, H. G. M.; Cohen Stuart, M. A.; de Keizer, A. Bijsterbosch, B. H. “Polyelectrolyte adsorption: a subtle balance of forces” *Langmuir* **1992**, *8*, 2538-2546.
45. Cohen Stuart, M. A. “Polyelectrolyte adsorption” *J. Phys. (France)* **1988**, *49*, 1001-1008.
46. Decher, G.; Hong, J. D. “Buildup of ultrathin multilayer films by a self assembly process. 1. Consecutive adsorption of anionic and cationic bipolar amphiphiles on charged surfaces” *Makromol. Chem. Makomol. Symp.* **1991**, *46,* 321-327.
47. Zhang, H.; Rühe, J. “Interaction of strong polyelectrolytes with surface attacted polyelectrolyte brushes polymer brushes as substrates for the layer-by-layer deposition of polyelectrolyte” *Macromolecules* **2003,** *36,* 6593-6598.
48. Zhang, H.; Rühe, J. “Weak polyelectrolyte brushes as substrates for the formation of surface-attached polyelectrolyte-polyelectrolyte complexes and polyelectrolyte multilayers” *Macromolecules* **2005,** *38,* 10743-10749.
49. Queffelec, J.; Gaynor, S. G. ; Matyjaszewski, K. “Optimization of atom transfer radical polymerization using Cu(I)/Tris(2-(dimethylamino)ethyl)amine as a catalyst” *Macromolecules* **2000**, *33*, 8629-8639.
50. Jones, D. M.; Brown, A. A.; Huck, W. T. S. “Surface-initiated polymerizations in aqueous media: Effect of initiator density” *Langmuir* **2002**, *18*, 1265-1269.
51. Potisatityuenyong, A.; Tumcharern, G.; Dubas, S. T.; Sukwattanasinitt, M. “Layer-by-layer assembly of intact polydiacetylene vesicles with retained chromic properties” *J. Colloid Interface Sci.* **2006**, *304,* 45-51.
52. Seong, H. -S.; Whang, H. S.; Ko, S. -W. “Synthesis of a Quaternary Ammonium Derivative of Chitooligosaccharide as Antimicrobial Agent for Cellulosic Fibers” *J. Appl. Polym. Sci.* **2000**, *76,* 2009-2015.
53. Ying, L.; Yin, C.; Zhuo, R. X.; Leong, K. W.; Mao, H. Q.; Kang, E. T.; Neoh, K. G. “Immobilization of galactose ligands on acrylic acid graft-copolymerized poly(ethylene terephthalate) film and its application to hepatocyte culture” *Biomacromolecules* **2003**, *4* 157-165.
54. Su, X.; Wu, Y. –J.; Knoll, W. “Comparison of surface plasmon resonance spectroscopy and quartz crystal microbalance techniques for studying DNA assembly and hybridization” *Biosens. Bioelectron.* **2005**, *21*, 719-726.

55. Marutani, E.; Yamamoto, S.; Ninjbadgar, T.; Tsujii, Y.; Fukuda, T.; Takano, M. “Surface-initiated atom transfer radical polymerization of methyl methacrylate on magnetite nanoparticles” *Polymer* **2004**, *45*, 2231-2235.

56. Rastogi, A.; Nad, S.; Tanaka, M.; Da Mota, N.; Tague, M.; Baird, B. A.; Abruna, H. D.; Ober, C.K. “Preventing nonspecific adsorption on polymer brush covered gold electrodes using a modified ATRP initiator” *Biomacromolecules* **2009**, *10*, 2750-2758.

57. Wu, T.; Gong, P.; Szleifer, I.; Vlcek, P.; Subr, V.; Genzer, J. “Behavior of surface-anchored poly(acrylic acid) brushes with grafting density gradients on solid substrates: 1. Experiment” *Macromolecules* **2007**, *40*, 8756-8764.

58. Yang, Q.; Kaul, C.; Ulbricht, M. “Anti-nonspecific protein adsorption properties of biomimetic glycocalyx-like glycopolymer layers: Effects of glycopolymer chain density and protein size” *Langmuir* **2010**, *26*, 5746–5752.

59. Yoshikawa, C.; Goto, A.; Tsujii, Y.; Fukuda, T.; Kimura, T.; Yamamoto, K.; Kishida, A. “Protein repellency of well-defined, concentrated poly(2-hydroxylethyl methacrylate) brushes by the size-exclusion effect” *Macromolecules* **2006**, *39*, 2284-2290.

60. Gautrot, J. E.; Huck, W. T. S.; Welch, M.; Ramstedt, M. “Protein-resistant NTA-functionalized polymer brushes for selective and stable immobilization of histidine-tagged proteins” *ACS Appl. Mater. Interfaces* **2010**, *2*, 193-202.

61. Chu, L. –Q.; Tan, W. –J.; Mao, H. –Q.; Knoll, W. “Characterization of UV-induced graft polymerization of poly(acrylic acid) using optical waveguide spectroscopy” *Macromolecules* **2006**, *39*, 8742-8746.

OUTPUT

International Publication (Manuscripts are in Appendix)

1. Akkahat, P.; Hoven, V. P. “Introducing Surface-tethered Poly(acrylic acid) Brushes as 3D Functional Thin Film for Biosensing Application” *revision submitted to Colloids and Surface B: Biointerface*
2. Akkahat, P.; Mekboonsonglarp, W.; Kiatkamjornwong, S.; Hoven, V. P. “Using Carboxyl-containing Polymer Brushes as SPR-precursor Layer for Biosensing Applications” *In Preparation*

International Presentation

1. Hoven, V. P.; Akkahat, P.; Mekboonsonglarp, W. “Poly(acrylic acid) Brushes: A Versatile 3D Matrix for Biosensing Applications” *The 3rd IUPAC International Symposium on Macro- and Supramolecular Architectures and Materials: Synthesis, Properties and Applications,* September 7-11, **2008**, Düsseldorf, Germany, Poster
2. Akkahat, P.; Mekboonsonglarp, W.; Hoven, V. P. “Using Carboxyl-containing Polymer Brushes as SPR-precursor Layer for Detection of Antigen-antibody Binding” *Pure and Applied Chemistry International Conference 2009*, January 14-16, **2009**, Naresuan University, Phitsanulok, Thailand, Poster.
3. Hoven, V. P.; Akkahat, P., Srikaenjan, P.; Vilaivan, T. “Polymer Brushes for Biosensing Applications” *International Symposium in Science and Technology at Kansai University 2009,* August 23-25, **2009**, Osaka, Japan, Invited Presentation.
4. Akkahat, P.; Mekboonsonglarp, W.; Hoven, V. P. “Using Carboxyl-containing Polymer Brushes as SPR-precursor Layer for Biosensing Applications” *International Symposium in Science and Technology at Kansai University 2009,* August 23-25, **2009**, Osaka, Japan, Poster.
5. Akkahat, P.; Mekboonsonglarp, W.; Kiatkamjornwong, S.; Hoven, V. P. “Using Poly(acrylic acid) Brushes as SPR-precursor Layer for Biosensing Applications” *The Fifth Mathematics and Physical Science Graduate Congress*, December 7-9, **2009**, Thailand, Oral.
6. Akkahat, P.; Mekboonsonglarp, W.; Vilaivan, T.; Kiatkamjornwong, S.; Hoven, V. P. “Using Poly(acrylic acid) Brushes as SPR Precursor Layer for DNA Sensor” *The 59th SPSJ Symposium on Macromolecules*, September 15-17, **2010**, Sapporo, Japan, Poster.

7. Hoven, V. P.; Akkahat, P.; Srikaenjan, P.; Vilaivan, T.; Kiatkamjornwong, S. “The Power of Polymer Brushes in Biosensing Applications” *The 7th International Symposium on Advanced Materials in Asia-Pacific (7th ISAMAP) and JAIST International Symposium on NanoTechnology 2010 (NT2010)*, September 30 – October 1, **2010**, Ishikawa High Tech Center, Ishikawa, Japan, Invited presentation.

National Presentation

1. Akkahat, P.; Hoven V. P. “Surface-tethered Poly(acrylic acid) Brushes as Functional Thin Film for Biosensor Application” *The 5th National Conference on Biomedical Engineering : NCBME 2007*, July 8, **2007**, Bangkok, Thailand., Poster
2. Hoven, V. P. “Surface Design by Polymer Brushes for Applications in Nanotechnology and Biotechnology” *NSTDA Annual Conference (NAC 2008)*, March 24-26, **2008**, Bangkok, Thailand, Invited presentation
3. Akkahat, P.; Mekboonsonglarp, W.; Hoven, V. P. “Poly(acrylic acid) Brushes: A Versatile 3D Matrix for Biosensing Applications” *The 5thThailand Materials Science and Technology Conference*, September 18-19, **2008**, Bangkok, Thailand., Oral

Appendix

Revised manuscript was submitted to Colloids and Surface B: Biointerface for Consideration

Manuscript in Preparation

Using Carboxyl-containing Polymer Brushes as SPR-precursor Layer for Biosensing Applications

Piyaporn Akkahat[1,2], Wanwimon Mekboonsonglarp[3], Suda Kiatkamjornwong[4], Voravee P. Hoven[5]*

[1]Program in Petrochemistry, Faculty of Science,

[2]Center for Petroleum, Petrochemicals, and Advanced Materials,

[3]Scientific and Technological Research Equipment Center,

[4]Department of Imaging and Printing Technology, Faculty of Science,

[5]Organic Synthesis Research Unit, Department of Chemistry, Faculty of Science,

Chulalongkorn University, Bangkok, 10330, Thailand

Carboxyl groups along poly(acrylic acid) (PAA) brushes attached to the surface of gold-coated glass substrate can serve as precursor moieties for covalent immobilization of biotinyl-3,6,9-trioxaundecanediamine (NH_2-biotin) that acts as a sensing probe for streptavidin (SA) detection using surface plasmon resonance (SPR). Surface-modified PAA brushes were obtained by acid hydrolysis of poly(tert-butyl acrylate) (P*t*-BA) brushes, formerly prepared by surface-initiated atom transfer radical polymerization of tert-butyl acrylate (*t*-BA). The graft density of the polymer brushes ranged from 10% to100% controlled by varying the graft density of surface initiator. As demonstrated by surface plasmon resonance (SPR), the nons-pecific adsorption of bovine serum albumin (BSA) and fibrinogen (FIB) increased with decreasing graft density. The PAA brushes after immobilized biotin not only showed the specific binding with streptavidin (SA) but also maintained high resistance to non-specific protein adsorption. The effect of graft density and swellability of PAA brushes on the analyt detecability was study. The biotin binding capacity increased with increasing graft density or the amount of carboxyl group. However, the accessibility of SA was limited at high graft density of the PAA brushes. It was also found that the swellability of the PAA brushes had significant impact on both biotin immobilization and SA binding. In this study, the swelling of the PAA brushes was controlled by varying the degree of carboxyl group activation. The amount of immobilized biotin increased with increasing degree of activation whereas the access of SA to the immobilized biotin was also limited at high degree of activation. This investigation has demonstrated the potential of the PAA brushes as SPR-precursor layer for biosensing application

* Corresponding author

Tel: +66-2218-7626-7, Fax: +66-2218-7598, e-mail: vipavee.p@chula.ac.th,

Introduction

Selectivity of sensor or measurement platforms for target proteins plays an important role for successful biosensor development. In order to achieve specific recognition for target proteins, the covalent attachment of active biomolecules such as protein, antibody, enzyme, and DNA has been immobilized to sensor surface.[1-3] However, the resistance of non-specific adsorption of sensor surface is also important. Non-specific adsorption leads to undesirable features such as high background noise or "false positives".[4,5] Thus, excellent sensor platform should not only allow for covalent immobilization of bioactive species but also resist non-specific adsorption.

To date, there are many strategies to create functionalized layer onto sensor surface such as self-assembled monolayer (SAM) of end-functionalized alkanethiol,[1,6,7] and polymer brushes.[1,4,8] It has been demonstrated previously that polymer brushes could be used for enhancement of sensor response by increasing the number of bioactive site due to high concentration of functional groups at the brush interface in comparison with SAM.[9-12] For example, the frequency response, monitored by quartz crystal microbalance (QCM), between anti-C-reactive protein (CRP) antibodies attached to PAA brushes and CPR in solution was shown to be 10 times higher than that immobilized on SAM of cysteamine.[12] Most of strategies to establish functionalized polymer brushes onto surface have been achieved by either the grafting to or the grafting from method. Surface-initiate polymerization (SIP), or so-called grafting from has attracted much interest in recent years due to providing well control of polymer films, such as polymer chain length, grafting density, and thickness.[13-15] In other words, the number of binding sites for biomolecule could also be controlled. A number of polymer brushes generated by SIP, such as poly(oligo(ethylene glycol)methacrylate) (*p*OEGMA),[9] poly(2-methacryloyloxyethyl phosphorylcholine)-*b*-poly(glycidyl methacrylate),[16] poly(carboxybetaine methacrylate),[17] and poly(acrylic acid),[18] perform both functionalizability and non-specific binding property. As shown in Lee and coworkers work,[9] *p*OEGMA brushes, having hydroxyl groups in polymer chain, were grown form gold and Si/SiO_2 surface. The hydroxyl groups were utilized for the immobilization of biotin having biospecific binding with streptavidin, while ethylene glycol part presented a non-specific binding.

In our previous work,[18] we generated densely packed PAA brushes (0.21 - 0.32 chain/nm^2) on SPR chip. The biotin (NH_2-biotin), a model of sensing probe, was immobilized onto carboxyl group via 1-ethyl-3-(3-dimethylaminopropyl)-carbodiimide and *N*-hydroxysuccinimide (EDC/NHS) chemistry. The biotinylated PAA brushes showed a high specific binding with streptavidin (SA) and a low non-specific adsorption of non-target proteins (bovine serum albumin and fibrinogen) in comparison with a self-assembled monolayer (SAM) of carboxyl-terminated alkanethiol. However, densely packed PAA brushes still have some limitations in diffusion of SA molecule inside polymer layer resulting in inaccessible to sensing probe. As shown in Song and coworkers work,[19] the mixed layer of biotin and poly(N-isopropylacrylamide) (PNIPAAm) were grafted on polyamidoamine dendrimer layer. From their results showed that the biospecific interaction between biotinylated surface and anti-biotin antibody was remarkably decreased by steric hindrance of poly(N-isopropylacrylamide) (PNIPAAm) brushes caused by applying the temperature below LCST (18°C) to form extended polymer chain. Nevertheless, most of researches on the polymeric surface have been mainly focused on making surface having a high surface density of sensing probe in order to achieve a superior analyst detactability.

To the best of our knowledge, no report study about the effect of graft density of polymer brushes on the detection of analyst. Therefore, in this paper, we try to vary the graft density of the PAA brushes by controlling the graft density of the surface initiator in order to demonstrate the effect of polymer graft density on binding efficiency of sensing probe to analyte in solution. At the same time, the non-specific adsorption of proteins on PAA brushes having different graft density was also determined. Furthermore, we also try to determine whether the extent of the carboxyl group activation would have any impact on the swellability of the sensing layer based on PAA brushes after probe immobilization and analyte detectability in terms of selectivity/specificity. For the analysis, surface plasmon resonance (SPR) technique was used to investigate biospecific interaction on the sensor chip. SPR is a surface sensitive to change in refractive index or thickness caused by the interaction between a biomolecular recognition molecule immobilized on sensor surface and an analyte molecule from solution on gold surface and transforms then into the signal.

Experimental Section

Materials. Absolute ethanol (99.9%**,** Merck), acetone (99.99%**,** Merck), (+)-biotinyl-3,6,9-trioxaundecanediamine (biotin-NH_2, Bioactive), bovine serum albumin (BSA, Aldrich), CuBr (95%, Fluka), ethyl 2-bromoisobutyrate (EBiB, 98%, Fluka) dichloromethane (CH_2Cl_2, 99.9%**,** Merck), 1-(3-Dimethylaminopropyl)-3-ethylcarbodiimide hydrochloride (EDC, 98**%**, Fluka), hydrogen peroxide (H_2O_2, 30%, Univar), fibrinogen (FIB, Aldrich), *N*-hydroxysuccinimide (NHS, 98**%**, Fluka), Lysozyme (LYS, Aldrich), magnesium sulfate anhydrous (Unilab), 11-mercaptoundecanol (MUD, Aldrich), 11-mercaptoundecanoic acid (MUA, Aldrich), methanesulfonic acid ($MeSO_3H$, Aldrich), phosphate buffered silane (PBS, Aldrich), streptavidin (SA, Bioactive), tetrahydrofuran (THF, 99.9%, Carlo) and Toluidine Blue O (TBO, 98%, Fluka), were used as received. *t*-Butyl acrylate (*t*-BA, 98%, Aldrich) was extracted three times with 5% aqueous NaOH and then washed with distilled water. After drying over $MgSO_4$ and filtering off the drying agent, the monomer was distilled under vacuum (60°C/60mmHg). ω–mercaptoundecyl bromoisobutyrate ($BrC(CH_3)_2COO(CH_2)_{11}SH$)[14] and Tris(2-(dimethylamino)ethyl)amine (Me_6TREN)[20] were prepared accroding to the literature.

Preparation of SAMs of ATRP Initiator. The gold-coated SPR chip was clean in piranya solution (7:3 mixtures of H_2SO_4 and H_2O_2)**,** washed with water and ethanol, and dried in a stream of nitrogen. A freshly cleaned substrates were then immersed in 1 mM ethanolic mixed solutions of $BrC(CH_3)_2COO(CH_2)_{11}SH$ (ATRP initiator) and $HO(CH_2)_{11}SH$ (MUD) for 24 h at room temperature. The molar fraction of ATRP initiator and MUD ranged from 10% to 100% (v/v). After this treatment, the gold substrates were rinsed with ethanol and dried in a stream of nitrogen.[14]

Formation of PAA brushes on SPR chip (3D chip). The polymerization of *t*-BA monomer on SPR chip has been described previously by our research.[18] Briefly, CuBr, *t*-BA, Me_6TREN and acetone were added to Schlenk flask containing SPR chip having surface grafted ATRP initiators in the presence of EBiB. The polymerization was allowed for 24 h at ambient temperature. The substrates were removed from the solution, rinsed sequentially by acetone and constant agitation in THF for 24h, and dried in a stream of nitrogen. The

substrates bearing polymer brushes were then analyzed by contact angle measurement to monitor the growth of polymer brushes.

The mixture of methanesulfonic acid (0.1 mL) and dichloromethane (10 mL) was added to a Schlenk flask containing the substrates having P*t*-BA brushes. After stirring at ambient temperature for 15 min, the substrates were removed and rinsed thoroughly with dichloromethane and ethanol, and then dried in a stream of nitrogen.[21] The surface COOH concentrations were determined by using the toluidine blue O (TBO) method.[22] In brief, the COOH concentration is determined by the amount of cationic dye adsorbed on the polymer surface through complexation with the COOH groups at pH 10. The absorbance of the solution containing the desorbed complex was measured at 633 nm. The COOH content was obtained from a calibration plot of the optical density versus dye concentration

SPR measurement. SPR assays were conducted using a double channel, AutoLab ESPR (Eco Chemie, The Netherlands) at 25°C, with the plane face of the prism coupled to the gold coated glass via index matching fluid. An auto-sampler was used to inject the test solutions and the measurement of the SPR angle shift was done under non-flow liquid conditions. The shift of the SPR angle at the end-point of each step and after baseline subtraction ("angle shift") was used to calculate the amount of the molecules bound onto the surface or target density, using a sensitivity factor of 120 mDegrees equals 100 ng/cm^2 and its molecular weight, as previously reported. [23]

For comparison, a gold-coated SPR dish bearing a monolayer of carboxyl terminated thiol, 11-mercatoundecanoic acid (MUA), were prepared by immersing the cleaned disk in an ethanolic solution of MUA (1 mM) at ambient temperature for 24 h. The disk was then rinsed thoroughly with ethanol and dried in a stream of nitrogen.

The swelling behavior of PAA brushes. The pH response of PAA brushes in aqueous solution was measured by SPR. After SPR chip grafted PAA seated in the SPR cell, the cycle of buffer solutions under different pH values (sodium acetate pH 4.5 and 6.5, and sodium hydroxide pH 9.5) were flowed over the surface. The change of SPR angle was monitored in real time corresponding to the change in reflective index and thickness of polymer layer.

Protein adsorption of PAA brushes. The protein adsorption on PAA brushes was tasted with four proteins, streptavidin, BSA, fibrinogen, and lysozyme, in a PBS buffer (10mM,

pH 7.4). The protein solution of 0.2 mg/ml was flowed over the gold-coated SPR disks bearing PAA brushes and MUA for 15 min and then was washed with PBS buffer for 5 min. The amount of protein adsorption was quantified by the difference of base line between before and after soaking with each protein.

Specific and non-specific interaction of biotinylated PAA brushes. NH_2-biotin can immobilize on PAA brushes and MUA monolayer via an amide bond formation between the amine group of biotin and the carboxyl group of PAA brushes and MUA (Figure 2). The gold-coated SPR disks bearing PAA brushes and MUA was first seated in the SPR cell before being rinsed with a running solution of sodium acetate buffer (10 mM, pH 4.5). After a baseline SPR response was established, the activation by EDCI (0.05 M) and NHS (0.05 M), the attachment of NH_2-biotin (1 mg/mL), and the subsequent blocking by ethanolamine (1 M) were all carried out sequentially *in situ* in the sodium acetate buffer for 5, 15, and 5 min, respectively. At the end of each step, the substrate was washed with a running solution of sodium acetate buffer to remove unbound molecules. After a baseline SPR response was recorded, 50 μL of SA in PBS (0.1 mg/mL) was applied to the biotin-immobilized disk and left for 15 min. The unbound SA was removed by washing with PBS for 5 min. Non-specific interactions of the gold-coated SPR disks bearing PAA brushes-biotin (3D matrix) and MUA-biotin (2D matrix) were tested against BSA and FIB by passing the 0.2 mg/mL protein solution in PBS over the discs for 15 min. The angle shift was calculated by the difference of SPR angle at the baseline and after the washing procedure.

Results and Discussion

Formation of PAA brushes on SPR chip. A schematic illustration of the synthetic pathway for preparation of grafted PAA brushes onto SPR chip is shown in Figure 1. The growth of PAA brushes on gold substrate was confirmed by water contact angle measurements. The molar fraction of initiator increased from 10% to 100%, the water contact angle (θ_A) increased from 41± 4.8° to 70 ±2.9°, which agreed with the reported θ_A values for bromoester-terminated initiator (shown in Table 1).[14] The contact angle values imply that the amount of initiator in monolayer is similar to the ratio in mixed solution. The

SPR chips were then allowed to react with *t*-BA monomer in the presence of an ATRP catalyst system at ambient temperature to grow polymer brushes. As a consequence of the formation of P*t*-BA brushes, the θ_A markedly increased. After hydrolysis, the θ_A decreased drastically from the hydrophobic surface having P*t*-BA brushes to the hydrophilic surface having PAA brushes.

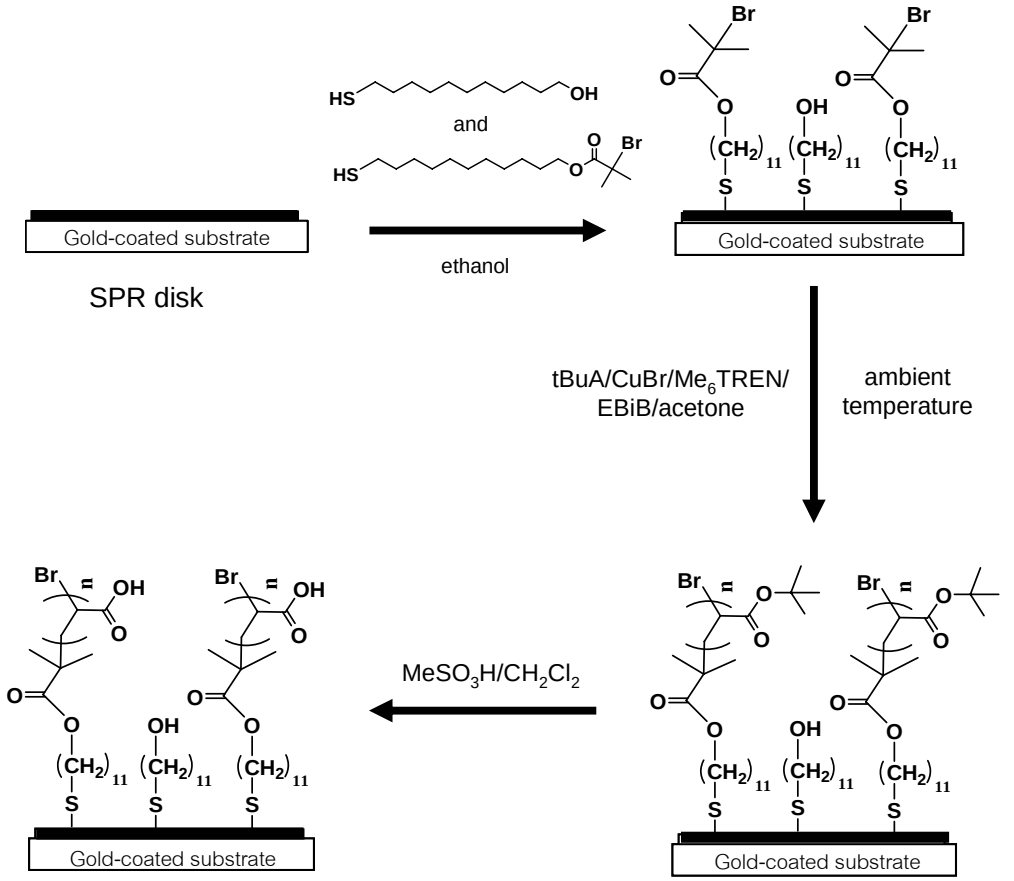

Figure 1. The synthetic pathway for preparation of grafted PAA brushes onto SPR chip.

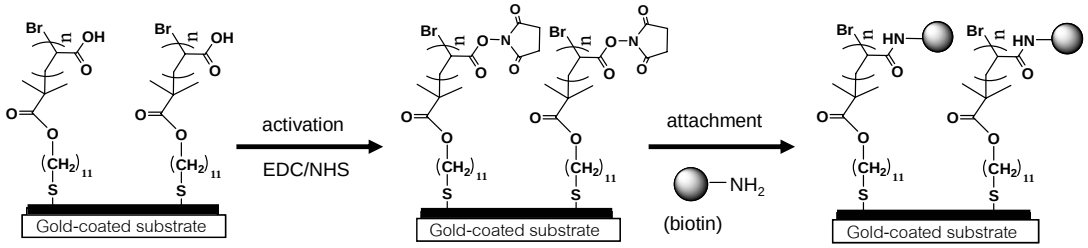

Figure 2. The formation of attachment amino biotin on PAA brushes.

Table 1. Advancing (θ_A) Water Contact Angle of Functionalized SPR chip

Molar fraction of initiator

Sample	10%	50%	100%
Gold surface of SPR chip	88 ± 2.1	90 ± 1.4	87 ± 2.2
Surface-Initiator	41± 4.8	59 ± 6.0	70 ±2.9
P*t*BA	70 ± 1.7	87 ± 3.4	91 ± 4.0
PAA (after hydrolysis)	58 ± 0.8	28 ± 2.6	18 ± 1.4

The formation of PAA brushes on SPR chip can be confirmed by atomic force microscopy (AFM). Figure 3 shows AFM images of PAA brushes coverage on surface at different graft density. The surface of bare gold was smooth with mean roughness (Ra) of 0.96 nm (Figure 3a). After grafted PAA brushes, surface roughness of all graft density increased compared with that of bare gold substrate (the maximum Ra: 2.1). Moreover, AFM image showed that the difference of surface morphology was observed at different graft density. Large protrusions are distributed on high graft density (100%, Figure 3d) of PAA brushes. On the other hand, at low graft density (10%, Figure 3b) showed small protrusions, while medium graft density (50%, Figure 3c) showed an intermediate. This data indicated that surface coverage of PAA brushes could be controlled by varied graft density of surface initiator.

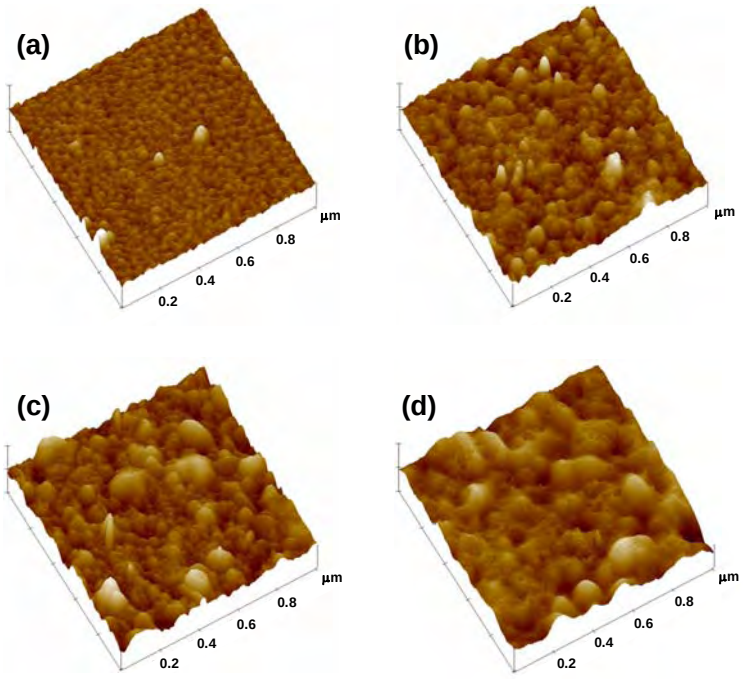

Figure 3. AFM images of (a) gold surface, (b) 10%, (c) 50%, and (d) 100% graft density of PAA brushes.

The toluidine blue O (TBO) staining method was employed to determine the amount of carboxyl groups on PAA brushes. As determined by toluidine blue O assay, the density of carboxyl groups of the PAA brushes increased as a function of graft density of the polymer brushes (shown in Figure 4). From this result showed that the carboxyl group density of PAA brushes can be varied as a function of graft density of polymer brushes.

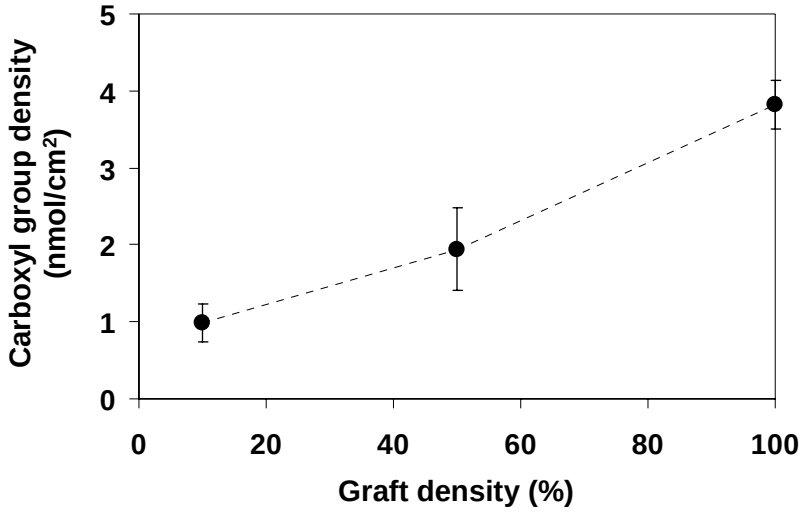

Figure 4. Carboxyl group density of PAA brushes as a function of graft density of polymer brushes

Swelling behavior of PAA brushes. PAA brushes which could have a stretched or coiled conformation are sensitive to pH of aqueous medium, resulting in the change of the thickness and refractive index of polymer layer.[24,25] In this study, the swelling of PAA brushes were determined using SPR measurement to monitor the change of SPR resonence angle depending on the change of thickness and refractive index. Figure 5 showed the pH response of PAA brushes under different pH values in real time. The reversibility of the angle change was observed. The alternating change in the angle continues as long as the pH alternation is continued. We found that the change of SPR response of MUA monolayer shows an angle change value which is a magnitude less than those observed here. Therefore, we can attribute the change of SPR angle for pH in to conformational changes of PAA layer caused by ionization of carboxyl groups. At high pH, all of COOH was deprotonated leading to the electrostatic repulsion in the polymer backbone, resulting in a thickness of polymer layer will be increased. On the other hand at low pH, not all of COOH was deprotonated leading to the

decrease of thickness. It is known that SPR resonance angle was changed by changing thickness and refractive index. Consequently, the increase in the thickness leads to an increase in the SPR angle.

In addition, we investigated the swelling of PAA brushes after probe (NH_2-biotin) immobilization (Figure 5, dashed line). It was found that the pH response of PAA brushes after biotin immobilization was lower than that of those before immobilization due to the replacement of COOH group by biotin. Therefore, the PAA chains are not ionizable and not charged, thus showing a low swelling in the aqueous environment. This result completely agree with the work reported by Chu and coworkers,[25] who found that the thickness of PAA layer immobilized with galactose ligand was lower than the original PAA layer in PBS buffer solution.

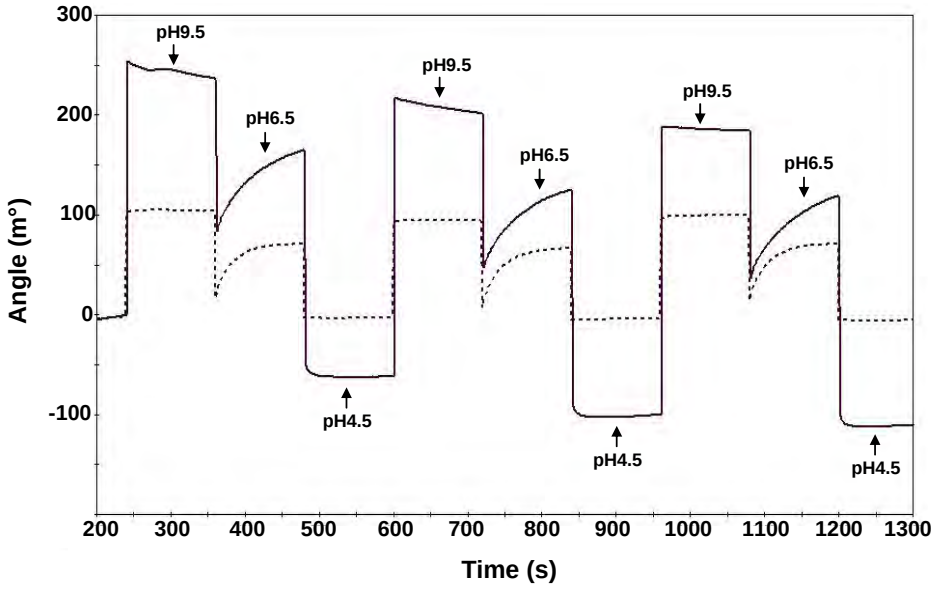

Figure 5. The effect of pH solution on PAA brushes before (solid line) and after (dashed line) immobilized biotin.

Protein adsorption of PAA brushes with different graft density. In this work, we investigated the protein adsorption onto PAA brushes varied graft density compared with MUA. Figure 6 show the amount of adsorbed four proteins on PAA brushes and MUA after soaking with protein solution in PBS (pH 7.4) measured by SPR. At low graft density (10%) adsorbed all of negative charge proteins: streptavidin (SA, 60 kD, pI = 5), bovine serum

albumin (BSA, 69 kD, pI = 4.8), and fibrinogen (FIB, 340 kD, pI = 5.5). While middle (50%) and high (100%) graft density, the adsorption of these proteins was decreased and was much lower than that of MUA. These results are in agreement with AFM result (Figure 3). At low graft density had lower overall surface coverage of PAA brushes on gold surface than that of medium and high graft density. Thus, proteins could penetrate and adsorb on non-coverage gold surface resulting in high-level of non-specific adsorption at low graft density. As shown in a recent study by Yoshikawa and co-workers, who showed that surface adsorption of protein can be greatly suppressed by densely graft of poly(2-hydroxyethyl methacrylate) brushes.[26] However, in the case of positive charge protein (lysozyme, 14 kD, pI = 12) highly adsorbed on PAA brushes especially at high graft density which may be caused by many negative charges of PAA brushes (pKa = 6.5-6.6).[27] These data showed that PAA grafted on surface could only reduce protein adsorption of negative charge protein.

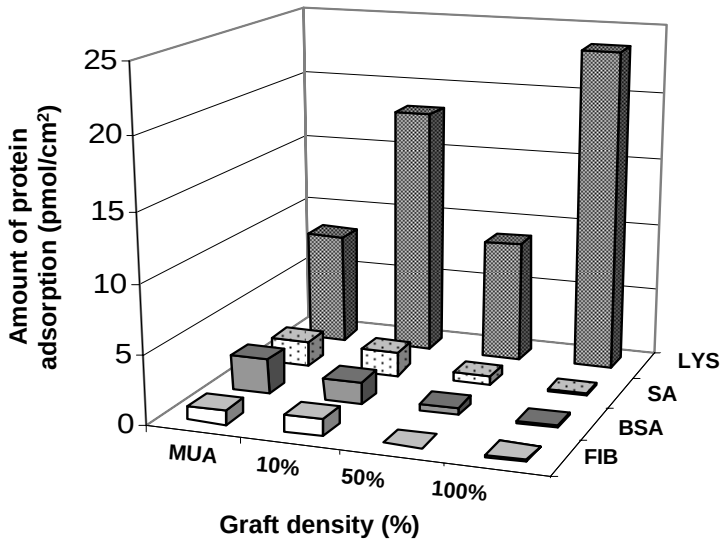

Figure 6. Adsorption of four proteins solution in PBS (10 mM, pH 7.4) on PAA brushes compared with MUA**.**

Specific and non-specific interaction of biotinylated PAA brushes. We used SPR spectroscopy to determine binding specificity of biotinylated surface with target protein (streptavidin). The changes of SPR angle is proportional to the quantity of streptavidin bound with biotin immobilized on PAA brushes and MUA (Figure7). Apparently, the amount of streptavidin bound to the substrates bearing PAA brushes was higher than that of the

substrate bearing the monolayer of MUA. The result thereby suggested that the layer of PAA brushes possessed greater biotin densities and greater binding capacity towards streptavidin (SA) detection as compared with the monolayer of MUA. Nevertheless, the highest value was at 50% graft density. This may be caused by steric hindrance effect of SA to some of immobilized biotin in polymer film at high graft density, whereas in the case of low graft density provided low SA binding owing to small amount of biotin probe.

The non-specific binding of the biotinylated surface was tested against model protein (BSA and fibrinogen). From data in Figure 7 indicated that the PAA brushes are still nonfouling after biotin immobilization. Furthermore, we found that the nonspecific binding of PAA brushes was lower than that of MUA. In other words, the introduction of PAA brushes film simultaneously increased the biospecific biotin-streptavidin interaction and decreased the non-specific adsorption of the model protein. This is a desirable characteristic of the sensing platform.

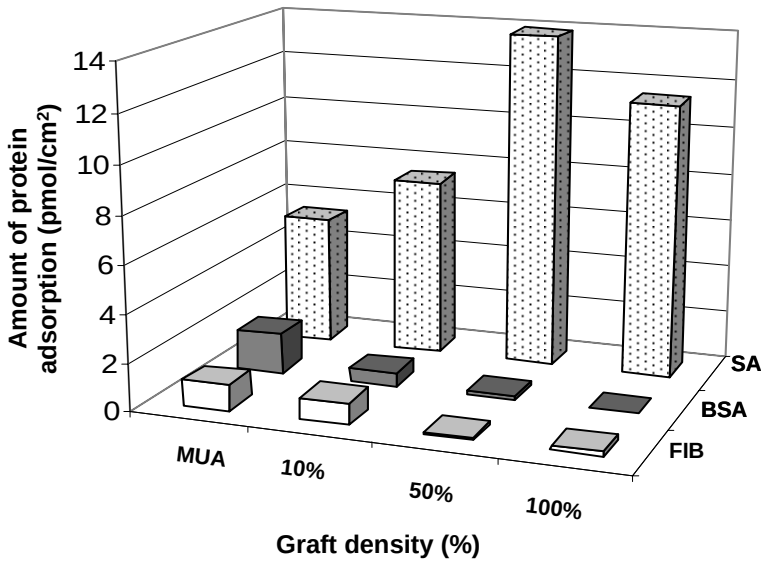

Figure 7. Specific and non-specific binding of proteins on to biotinylated surface of PAA brushes compared with MUA

From our previous work (paper1), we found that the densly packed PAA brushes had the limited accessibility of the SA to the immobilized biotin inside the inner layer of the polymer brushes. In order to demonstrate the effect of graft density, we investigated the relation between amount of biotin immobilization and SA binding capacity as a function of graft

density. As expected, with the increase in grafting density or the amount of carboxyl group, the binding capacity of PAA for biotin also increased (Figure 8). However, the accessibility of SA (60 kD) which is large protein was limited at high graft density of polymer brushes. When the correlation between amount of immobilized biotin and SA binding was considered, it was obvious that biotin immobilized on the high graft density of PAA brushes showed the lowest reactivity with SA even though more biotin molecules were immobilized into PAA brushes. This result implied that most of the immobilized biotin was not bound to SA. One reason could be explained by steric hindrance effect of large molecule in densely packed polymer brushes.

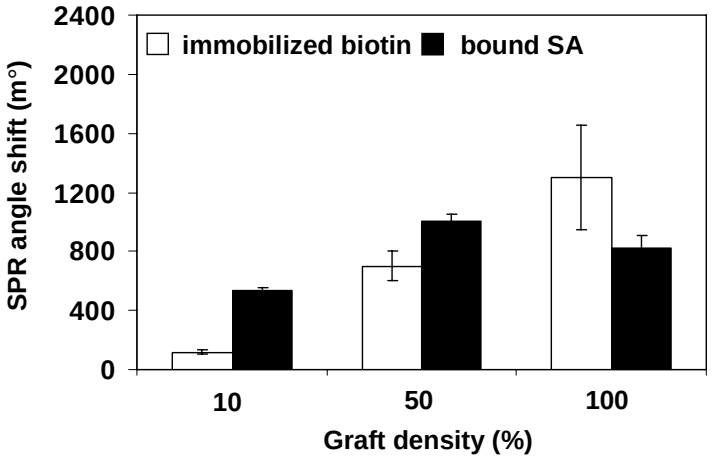

Figure 8. SPR angle shifts after the step of biotinimmobilization and SA binding on PAA brushes as a function of graft density

The effect of degree of activation. The swelling of polymer brushes has significant effect on probe immobilization and target molecule binding. As showed in previous result (Figure 5), the swelling of PAA brushes could be reduced by immobilization of biotin. Thus we are interested in the effect of swelling on SA binding efficiency. In order to study the effect of the swelling of sensing layer on analyte detectability, the swelling of PAA brushes were controlled by varying the degree of carboxyl group activation depending on the molar ratio between EDC and NHS, and the reaction time. From Figure 9, the amount of immobilized biotin increased with the increase of degree of activation. On the contrary, the access of SA to some of biotin was affected at high degree of activation which is low swelling. This result

indicated that the swelling of PAA brushes has influence to the accessibility of large protein into the polymer film.

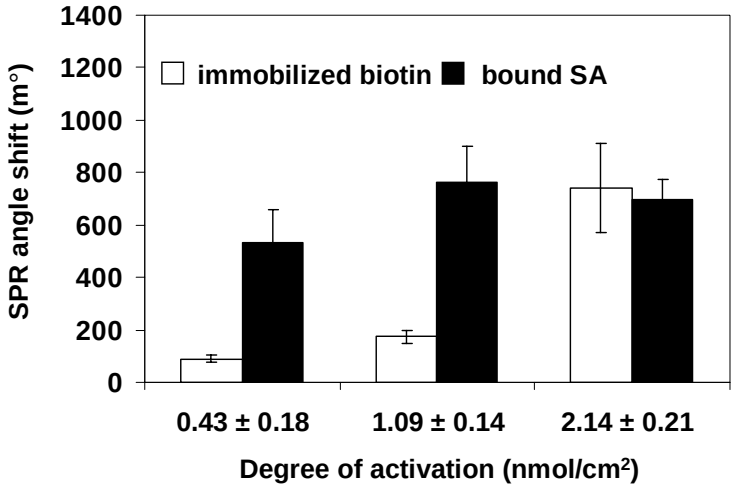

Figure 9. SPR angle shifts after the step of biotinimmobilization and SA binding on 100% graft density of PAA brushes as a function of degree of activation

Conclusions

It has been demonstrated that graft density of surface-tethered PAA brushes synthesized by SIP-ATRP on SPR chip can be controlled by controlling the graft density of the surface initiator. As determined by TBO assay, the carboxyl group density can be varied as a function of the graft density of PAA brushes. The carboxyl groups of PAA brushes are readily available for the covalent attachment of biotin-NH_2. The face that the introduction of PAA brushes film simultaneously increased the biospecific biotin-streptavidin interaction and decreased the nons-pecific adsorption of BSA and FIB. However, the lowest graft density of PAA brushes showed poor resistance of non-specific adsorption. The limited accessibility of the SA to the immobilized biotin of the densely packed PAA brushes can be greatly suppressed by reducing packing density of polymer chain. Moreover, the amount of carboxyl group activation has impact on swellability of sensing layer based on PAA brushes and detectability of analyte. Therefore, to achieve high performance of the surface-tethered PAA brushes as a sensing layer for biosensor, the effect of graft density and the swellability of PAA brushes should be optimized.

Acknowledgment. This research was financially supported by The Thailand Research Fund (RMU5080072), and Ph.D. scholarship to PA from Strategic Scholarships Fellowships Frontier Research Networks. The authors are grateful to the Scientific and Technological Research Equipment Center, Chulalongkorn University, for providing the SPR facility.

References

1. Rusmini, F.; Zhong, Z.; Feijen, J. *Biomacromolecules* **2007**, *8*, 1775-1789.
2. Senaratne, W.; Andruzzi, L.; Ober, C. K. *Biomacromolecules* **2005**, *6*, 2427-2448.
3. Xu, F. J.; Neoh, K. G.; Kang, E. T. *Prog. Polym. Sci*. **2009**, *34*, 719-761.
4. Masson, J. –F.; Battaglia, T. M.; Kim, Y. –C.; Prakash, A.; Beaudoin, S.; Booksh, K. S. *Talanta* **2004**, *64*, 716-725.
5. Masson, J. –F.; Battaglia, T. M.; Davidson, M. J.; Kim, Y. –C.; Prakash, A. M. C.; Beaudoin, S.; Booksh, K. S. *Talanta* **2005**, *67*, 918-925.
6. Nakamura, F.; Ito, E.; Hayashi, T.; Hara, M. *Colloids Surf., A* **2006**, *284-285*, 495-498.
7. Subramanian, A.; Irudayaraj, J.; Ryan, T. *Sensor. Actuat., B* **2006**, *114*, 192-198.
8. Dong, R. ; Krishnan, B. ; Baird, B. A.; Lindau, M.; Ober, C. K. *Biomacromolecules* **2007**, 8, 3082-3092.
9. Lee, B. S. ; Chi, Y. S. ; Lee, K. –B.; Kim, Y. –G.; Choi, I. S. *Biomacromolecules* **2007**, 8, 3922-3929.
10. Yang, N. ; Su, X. ; Tjong, V. ; Knoll, W. *Biosens. Bioelectron*. **2007**, *22*. 2700-2706.
11. Feng, C. L.; Zhang, Z.; Förch, R.; Knoll, W.; Vancso, G. J.; Schönherr, H. *Biomacromolecules* **2005**, 6, 3243-3251.
12. Kurosawa, S.; Aizawa, H.; Talib, Z. A.; Atthoff, B.; Hilborn, J. *Biosens. Bioelectron*. **2004**, *20*. 1165-1176.
13. Husseman, M.; Malmström, E. E.; McNamara, M.; Mate, M.; Mecerreyes, D.; Benoit, D. G.; Hedrick, J. L.; Mansky, P.; Huang, E.; Russell, T. P.; Hawker, C. J. *Macromolecules* **1999**, 32, 1424-1431.
14. Jones, D. M.; Brown, A. A.; Huck, W. T. S. *Langmuir* **2002**, 18, 1265-1269.
15. Edmondson, S.; Osborne, V. L.; Huck, W. T. S. *Chem. Soc. Rev*. **2004**, *33*, 14-22.
16. Iwata, R.; Satoh, R.; Iwasaki, Y.; Akiyoshi. *Colloids Surf., B* **2008**, *62*, 288-298.

17. Zhang, Z.; Chen, S.; Jiang, S. *Biomacromolecules* **2006**, 7, 3311-3315.
18. Paper 1
19. Song, S. Y.; Choi, H. G.; Hong, J. W.; Kim, B. W.; Sim, S. J.; Yoon, H. C. *Colloids Surf., A* **2008**, *313-314*, 504-508.
20. Queffelec, J.; Gaynor, S. G.; Matyjaszewski, K. *Macromolecules* **2000**, 33, 8629-8639.
21. Dai, J.; Bao, Z.; Sun, L.; Hong, S. U.; Baker, G. L.; Bruening, M. L. *Langmuir* **2006**, 22, 4274-4281.
22. Ying, L.; Yin, C.; Zhuo, R. X. Leong, K. W.; Mao, H. Q.; Kang, E. T.; Neoh, K. G. *Biomacromolecules* **2003**, 4, 157-165.
23. Su, X.; Wu, Y. –J.; Knoll, W. *Biosens. Bioelectron*. **2005**, *21*. 719-726.
24. Sarkar, D.; Somasundaran, P. *Langmuir* **2004**, 20, 4657-4664.
25. Chu, L. –Q.; Tan, W. –J. ; Mao, H. –Q. ; Knoll, W. *Macromolecules* **2006**, 39, 8742-8746.
26. Yoshikawa, C.; Goto, A.; Tsujii, Y.; Fukuda, T.; Kimura, T.; Yamamoto, K.; Kishida, A. *Macromolecules* **2006**, 39, 2284-2290.
27. Dong, R.; Lindau, M.; Ober, C. K. *Langmuir* **2009**, 25, 4774-4779.

Elsevier Editorial System(tm) for Colloids and Surfaces B: Biointerfaces
Manuscript Draft

Manuscript Number: COLSUB-D-10-00868R1

Title: Introducing surface-tethered poly(acrylic acid) brushes as 3D functional thin film for biosensing applications

Article Type: Full Length Article

Keywords: polymer brushes; poly(acrylic acid); surface-initiated polymerization; atom transfer radical polymerization; biotin; streptavidin

Corresponding Author: Dr. Voravee Hoven, Ph.D.

Corresponding Author's Institution: Chulalongkorn University

First Author: Piyaporn Akkahat, MS

Order of Authors: Piyaporn Akkahat, MS; Voravee Hoven, Ph.D.

Abstract: Carboxyl groups of surface-tethered poly(acrylic acid) (PAA) brushes should be able to serve as versatile moieties for a wide range of chemical modifications, including an attachment of bioactive species that can act as sensing probes for biosensors. In this research, poly(tert-butyl acrylate) (Pt-BA) brushes were prepared by surface-initiated atom transfer radical polymerization of tert-butyl acrylate. PAA brushes were then obtained after removal of the tert-butyl groups from the Pt-BA brushes by acid hydrolysis. The carboxyl group density of the PAA brushes can be varied as a function of chain length or molecular weight. The reactivity of the carboxyl groups of PAA brushes towards the immobilization of biotin, a frequently used model bioactive probe in biosensing applications, was evaluated. Qualitative determination of streptavidin (SA) binding to the biotin-attached PAA brushes was verified by fluorescence microscopy. The efficiency of the PAA brushes to act as a three dimensional (3D) precursor layer for biosensing applications was further demonstrated using surface plasmon resonance (SPR), where the biotin-attached PAA brushes showed an enhanced signal for the biospecific binding of SA in comparison with a self-assembled monolayer (SAM) of a carboxyl-terminated alkanethiol, used as a model two-dimensional (2D) conventional precursor layer. The PAA brushes showed very low non-specific interactions with two other tested proteins of a similar pI but different sizes. This desirable feature should be highly beneficial for the development of biosensors.

March 6, 2011

RE: Submission of revised manuscript # COLSUB-D-10-00868

Dear Editor:

Thank you for your consideration of our manuscript entitled: **"*Introducing surface-tethered poly(acrylic acid) brushes as 3D functional thin film for biosensing applications*"**. The manuscript has been reviewed and you had invited us to submit a revised manuscript to you. We have provided a detailed listing of our response to the reviewers and the changes made in the manuscript that appear in red.

We believe that we have addressed all reviewers' comments. We hope that you will be able to accept the revised manuscript expeditiously. Should there be any further information which may be required or if any problems arise, please contact me at the address shown below.

Sincerely yours,

Vp. Hoven

Voravee P. Hoven, Ph.D.

Organic Synthesis Research Unit, Department of Chemistry, Faculty of Science, Chulalongkorn University
Phayathai Road, Patumwan, Bangkok 10330, THAILAND
Telephone +(662) 218-7626-7 ext 102, Facsimile +(662) 218-7598
e-mail: vipavee.p@chula.ac.th

Responses to Reviewers
Ms. No.: COLSUB-D-10-00868
Title: Introducing surface-tethered poly(acrylic acid) brushes as 3D functional thin film for biosensing applications
Corresponding Author: Associate Professor Voravee P. Hoven
Authors: Piyaporn Akkahat, Voravee P. Hoven

Author Response to REVIEWER 1:

Reviewer Comment or Question 1

The molar mass of the polymer formed in solution may not represent the molar mass of the brushes. Despite this ambiguity, the authors should have proven that indeed brushes were formed. The layers are extremely thin. What is the grafting density?

Author Response

Although some studies have previously demonstrated that the molecular weight of the polymers form in solution of polymer in solution closely resembled that of the grafted polymer brushes cleaved from the surface, the reviewer's comment on the statement "the molar mass of the polymer formed in solution may not represent the molar mass of the brushes" is absolutely true in our particular case since it is not practically possible to do so since the amount of the removed polymer brushes should be too low to be characterized by GPC. Nonetheless, we have already given a number of experimental data that can be used as evidences of polymer brushes formation. First, the change in refractive index of the silicon substrate as a function of polymerization time suggested that poly(*t*-butyl acrylate) (P*t*-BA) brushes has been formed. The linear relationship of the polymer thickness with respect to the polymerization time is shown in Fig.2. Second, the appearance of C=O characteristic peaks in FT-IR spectra of both P*t*-BA brushes and PAA brushes grafted on silicon particles shown in Fig. 3 can also be used as another evidence of polymer brushes formation. Here in the revised manuscript, we have also provided an additional data based on AFM analysis. Due to the limited space available for figures and schemes, the AFM micrographs are displayed as Supplementary Material. According to the AFM micrographs shown in Fig.S1, the topography of the gold-coated SPR substrate has been changed with larger groove dimension upon the coating of the P*t*-BA brushes. The root mean square roughness (rms) was also increased from 1.2 to 1.9 nm. The presence of the polymer brushes layer can be clearly seen from the AFM micrograph in Fig.S2 demonstrating the section analysis of the gold-coated SPR substrate of which the P*t*-BA brushes layer was intentionally scraped off. The average thickness (9.5±0.6 nm) obtained from this particular image was later used for the calculation of graft density

At the targeted DP of 200, the graft density of the P*t*-BA brushes coated on the silicon substrate calculated from ellipsometric thickness and the free P*t*-BA formed in solution is 0.32 chain/nm^2 while the one coated on the gold-coated SPR substrate calculated from the thickness obtained from AFM analysis and the free P*t*-BA formed in solution is 0.31 chain/nm^2. The similarity of these two values suggested that the method for the preparation is potentially reliable although they were determined on different substrates by different techniques. In response to this particular comment, an additional explanation is included in the section of **Results and Discussion** on page 12 of the manuscript.

Reviewer Comment or Question 2

In view of the 3D nature of the films claimed in the context of biosensing, the film thicknesses achieved are basically a factor 2 off the size of a larger protein, thus not 3D.

Author Response

We absolutely agree with the comment of the reviewer about the fact that the thickness of the film (up to 10 nm) is basically a factor of 2 in comparison with large proteins (approximately 4-6 nm). However, the 3D nature of the film is defined based on the strategy that the active functional groups which are carboxylic acid distribute along the chains of the PAA brushes, inside the interior of the film, not only situate at the chain end of the polymer brushes that appear at the top of the film surface. This is defined in comparison with the carboxyl-terminated SAM-based system of which the carboxyl groups only appear on the top of the film surface so thus defined as the 2D film. This definition does not take into consideration the dimension of the binding proteins or even the target protein analytes. Whether or not the proteins can get inside the interior of the film should be considered as a separated issue.

Reviewer Comment or Question 3

The central criticism, however, is that I cannot figure out an element of novelty.

The authors should analyze the literature more carefully to be able to place their results in the appropriate context. PAA brushes are well established, see e.g.

(1) Poly(acrylic acid) with disulfide bond for the elaboration of pH-responsive brush surfaces
Author(s): Van Camp W, Du Prez FE, Alem H, et al.
Source: EUROPEAN POLYMER JOURNAL Volume: 46 Issue: 2 Pages: 195-201 Published: FEB 2010

(2) Preventing Nonspecific Adsorption on Polymer Brush Covered Gold Electrodes Using a Modified ATRP Initiator
Author(s): Rastogi A, Nad S, Tanaka M, et al.
Source: BIOMACROMOLECULES Volume: 10 Issue: 10 Pages: 2750-2758 Published: OCT 2009

(3) Covalent immobilization of quantum dots on macroscopic surfaces using poly(acrylic acid) brushes
Author(s): Gupta S, Uhlmann P, Agrawal M, et al.
Source: JOURNAL OF MATERIALS CHEMISTRY Volume: 18 Issue: 2 Pages: 214-220 Published: 2008

Bioconjugation with the (strept)avidin - biotin strategy is also established. While Navarro et al report e.g. on poly(methacrylic acid) brushes, the Ober group reported on patterned PAA brushes on silicon. Both approaches utilize similar bioconjugation chemistry ([strept]avidin - biotin).

(4) Navarro M et al. LANGMUIR Volume: 24 Issue: 19 Pages: 10996-11002 Published: OCT 7 2008

(5) Dong R et al. BIOMACROMOLECULES Volume: 8 Issue: 10 Pages: 3082-3092 Published: OCT 2007

Author Response

We do realize that the chemistry and the strategy for preparing PAA brushes on solid substrates as well as bioconjugation chemistry based on biotin-(strept)avidin interactions are not entirely new and have been well developed by other researchers as mentioned by the reviewer and those we have already included in the manuscript (Ref.#12-14). Eventhough there have been a number of research work reported that the surface-grafted PAA brushes exhibit high protein binding capacities. To the best of our knowledge, none of them have determined the influence of carboxyl group density which is directly related to molecular weight or film thickness of the polymer on analyte detectability. Therefore, the aim of this research is not trying to develop a new chemistry or new strategy to be used for preparing PAA brushes on substrate, but rather trying to demonstrate that the same successful chemistry can be applied for SPR biosensing applications, the situation that has not been reported before. To demonstrate that point, we focus on the investigation of biotin immobilization as a model probe to the PAA brushes (3D) and biospecific binding of SA to the immobilized biotin in comparison with a two-dimensional (2D) conventional precursor layer. We have also investigated further on the effect of carboxyl group density on the binding capacity of biotin and SA.

Considering the literature #1 and 3 as recommended by the reviewer in detail, we have found that both of them prepared PAA brushes using grafting-to strategy that yields a relatively low graft density of the PAA brushes so it is not reasonable to compare our results with theirs. In particular, the literature #3 investigated the immobilization on the quantum dots so it is hardly relevant to our work. As a result, we choose not to cite the literature #1 and 3. In the case of literature #4, the system was based on poly(methacrylic acid) brushes, not the PAA brushes and their work concentrated on the interactions between cells and the RGD-immobilized polymer brushes. This is absolutely not in the scope of our work so the literature #4 is not cited.

On the other hand, the literature #2 and 5 are quite relevant. We have put literature #2 as Ref#23 on page 16 of the revised manuscript where the ability to prevent non-specific adsorption of the PAA brushes. The work reported in the literature #5 is mostly relevant to our research work considering that the authors prepared the PAA brushes in the form of pattern using surface-initiated ATRP of sodium acrylate on silicon surface and test the ability of the PAA brushes as a platform for binding with a number of proteins including BSA, avidin, biotin, and streptavidin. The work concentrated on the development of a new strategy to indirectly immobilize small biological molecules using specific interactions between avidin that was attached to the PAA brushes and biotin-tagged proteins or between the biotin-tagged BSA that was bound to the PAA brushes and streptavidin which can later be used to bind with other biotinylated molecules. They have demonstrated the protein binding qualitatively mostly by fluorescence microscopy in order to test their new concepts. Quantitative determination on the effect of carboxyl group density which is directly related to molecular weight or film thickness of the PAA brushes on analyte detectability was definitely in the scope of their investigation. Nonetheless, we have cited the literature #5 as Ref#15 in the **Introduction section** on page 5 where we have discussed the potential application of polymer brushes in the biotechnology-related fields.

Author Response to REVIEWER 2:

Reviewer General Comment

The manuscript describes formation of poly(acrylic acid) brushes via atom transfer radical polymerization of tert-butyl acrylate and subsequent hydrolysis of the ester groups. Similar strategies have been carried out previously, so the main novelty of the work lies in the investigation of biotin attachment to these brushes and protein binding to the immobilized biotin. The conclusion is that the brushes allow for 11-fold more immobilization of biotin on the surface, but only 2-fold more binding of streptavidin to the immobilized biotin. The authors suggest that better control over chain density on the surface may help to alleviate this problem. This manuscript is probably worthy of publication.

Authors: We addressed all specific points commented by the reviewer as follows:

Reviewer Comment or Question 1

But I would suggest that the authors make more comparisons with the literature**.** Ulbricht and coworkers have looked at the effects of chain density on binding in membranes. Huck and coworkers recently showed how swelling may greatly increase binding capacity without leading to increased non-specific adsorption, and Bruening and coworkers directly prepared relatively thick polyacid brushes and examined protein binding to these materials on surfaces and in membranes. Bergbreiter and Crooks studied protein immobilization in hyperbranched poly(acrylic acid) films a number of years ago. There may be other relevant comparisons.

Author Response

As advised by the reviewer, we have provided an additional paragraph giving comparative detail of some relevant literatures on page 17 in the **Results and Discussion** section. Unfortunately, we cannot access all the literatures recommended by the reviewer. However, we have found substituted papers that are also relevant.

Reviewer Comment or Question 2

The caption to Figure 2 talks about standard deviation, but I did not see any error bars in the figure.

Author Response

We have put SD on all data in Figure 2 as recommended by the reviewer.

Reviewer Comment or Question 3

In Figure 3, it would be nice to have a spectrum of initiator-coated or bare silica particles for comparison. What is the band around 1650 cm-1? Does this appear due to the silica?

Author Response

As suggested by the reviewer, the spectrum of bare silica particles has been put in Figure 3 in the revised manuscript. The peak around 1600-1700 cm^{-1} is the absorption attributed to the OH bending of Si-OH group in silica. We assume that there may be a small amount of initiator coated on silica particles. As a result, no characteristic signals from initiator were found on the FT-IR spectrum of the initiator-coated silica particles. For this reason, the spectrum was not shown in Figure 3.

Reviewer Comment or Question 4

The caption to Figure 4 is a little confusing, as it suggests there should only be two data points, one for a targeted DP of 100 and one for a targeted DP of 200. I presume the data points represent different polymerization times, but this should be clarified. Similarly, what was the polymerization time for Figure 5?

Author Response

As suggested by the reviewer, the caption of Figure 4 has been changed to "the density of carboxyl groups of the PAA brushes on the silicon oxide surface as a function of M_n when derived from a targeted DP of 100 (○) or 200 (●) at different polymerization time". Data are shown as the mean + SD and are derived from 3 repeats" in the revised manuscript. The polymerization time of 24 h is specified in the caption of Figure 5 in the revised manuscript

Reviewer Comment or Question 5

At the bottom of page 13, the manuscript talks about "PAA (30 kDa)". Is this the Mn value for PAA or PTBA? None of the earlier figures show a molecular weight this high. How was this achieved?

Author Response

PAA (30 kDa) means PAA brushes which was prepared from P*t*-BA having Mn of 30 kDa. This specification is now put on page 14. It should be emphasized that, in the case of the gold-coated SPR substrate the more active ligand, Me_6TREN was used instead of PMDETA that was previously used in the case of the silicon substrate so that the polymerization could be performed at ambient temperature without thermal treatment. This was done in order to avoid the gold detachment from the substrate upon elevating the temperature. The more active ligand allows higher $\overline{M}_n$ of the polymer to be formed than the less active one considering that the same polymerization time was used.

Reviewer Comment or Question6

Figure 6 should state which line refers to PAA and which refers to MUA.

Author Response

As advised by the reviewer, Figure 6 was edited accordingly in the revised manuscript.

Reviewer Comment or Question 7

The sensitivity of SPR to streptavidin binding may depend on the distance of the protein binding from the surface. Was this taken into account in these studies and does it need to be? I would appreciate some comment on this issue.

Author Response

The reviewer is absolutely right about the fact that the distance between the surface of SPR sensor and the protein analyte, streptavidin in this case, should affect the sensitivity, detection limit as well as signal-to-noise ratio of the biosensor. This issue has definitely been taken into account in our studies. To the best of our knowledge, the effective decay length or probing depth of SPR is about 100-200 nm. Therefore, the analysis of the analyte can still be accurately determined considering that the greatest thickness of the polymer brushes obtained in this case is approximately 10 nm.

*Graphical Abstract

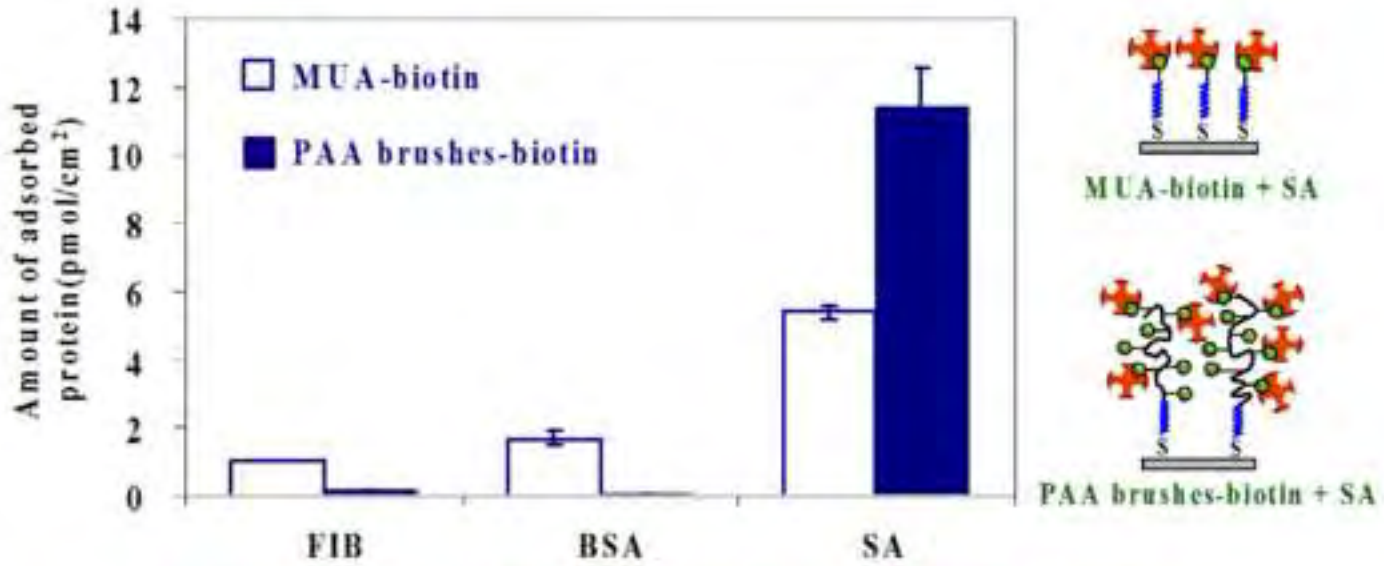

FIB = Fibrinogen, BSA = Bovine serum albumin, SA = Streptavidin

Research highlights

- A correlation between carboxyl group density and the chain length or molecular weight of the poly(acrylic acid) brushes was evaluated.
- The layer of poly(acrylic acid) brushes exhibited higher biotin density as compared with the self-assembled monolayer of a carboxyl-terminated alkanethiol, and revealed both a specific binding with streptavidin and also prevented adsorption of other non-specific proteins.

Introducing surface-tethered poly(acrylic acid) brushes as 3D functional thin film for biosensing applications

Piyaporn Akkahat[a,b], Voravee P. Hoven[c,*]

[a]*Program in Petrochemistry and Polymer Science, Faculty of Science, Chulalongkorn University, Bangkok 10330, Thailand*

[b]*Center for Petroleum, Petrochemicals, and Advanced Materials, Chulalongkorn University, Phayathai Road, Pathumwan, Bangkok, 10330, Thailand*

[c]*Organic Synthesis Research Unit, Department of Chemistry, Faculty of Science, Chulalongkorn University, Bangkok, 10330, Thailand*

* Corresponding author. Tel.: +66-2218-7626-7 ext 102; Fax.: +66-2218-7598

E-mail address: vipavee.p@chula.ac.th

Abstract

Carboxyl groups of surface-tethered poly(acrylic acid) (PAA) brushes should be able to serve as versatile moieties for a wide range of chemical modifications, including an attachment of bioactive species that can act as sensing probes for biosensors. In this research, poly(*tert*-butyl acrylate) (P*t*-BA) brushes were prepared by surface-initiated atom transfer radical polymerization of *tert*-butyl acrylate. PAA brushes were then obtained after removal of the *tert*-butyl groups from the P*t*-BA brushes by acid hydrolysis. The carboxyl group density of the PAA brushes can be varied as a function of chain length or molecular weight. The reactivity of the carboxyl groups of PAA brushes towards the immobilization of biotin, a frequently used model bioactive probe in biosensing applications, was evaluated. Qualitative determination of streptavidin (SA) binding to the biotin-attached PAA brushes was verified by fluorescence microscopy. The efficiency of the PAA brushes to act as a three dimensional (3D) precursor layer for biosensing applications was further demonstrated using surface plasmon resonance (SPR), where the biotin-attached PAA brushes showed an enhanced signal for the biospecific binding of SA in comparison with a self-assembled monolayer (SAM) of a carboxyl-terminated alkanethiol, used as a model two-dimensional (2D) conventional precursor layer. The PAA brushes showed very low non-specific interactions with two other tested proteins of a similar pI but different sizes. This desirable feature should be highly beneficial for the development of biosensors.

Keywords: polymer brushes; poly(acrylic acid); surface-initiated polymerization; atom transfer radical polymerization; biotin; streptavidin

1. Introduction

The development of biosensors largely relies on the immobilization of bioactive species to a sensor or measurement platform. The density of the immobilized bioactive species, as well as the distance between the surface of sensor and the bioactive species, should, in principle, affect the sensitivity, detection limit and signal-to-noise ratio of the biosensor. The precursor layer onto which the bioactive molecules (probes) are immobilized is conventionally based on a self-assembled monolayer (SAM) of end-functionalized alkanethiol, especially for gold-coated substrates, but the density of this cannot be greatly enhanced [1-3]. Variation of the alkyl chain length, which is generally used for controlling the distance between the measurement platform and the sensing probes, is also limited due to the fact that long alkyl chains tend to induce non-specific adsorption of the bioactive molecules during the immobilization [4]. This often causes an adverse effect on the biosensor efficiency.

Polymeric thin film has recently been recognized as an alternative precursor layer for the covalent attachment of biomolecules, such as proteins, antibodies, enzymes and DNA [1,5-7]. In principle, its three-dimensional (3D) characteristic should allow for a higher functional group density or binding capacity (mole of bioactive species per unit area), a less confined reactivity, and provides a greater design flexibility than the two dimensional (2D) SAM-based system. Carboxymethylated dextran (CM-dextran) is currently the most popular 3D matrix system. It is commercially available as 3D chips with different thicknesses and modifiers that can readily be used for biosensing applications. By using surface plasmon resonance (SPR), Yang and coworkers have reported that when a streptavidin (SA) layer was immobilized on the 3D matrix of the CM-dextran, it provided twice the amount of immobilized biotinylated DNA in comparison with the SA layer that was built on the 2D carboxyl-terminated SAM [8]. The greater DNA probe density of the 3D matrix, however,

yielded an inferior DNA hybridization efficiency than that of the 2D matrix. The authors explained this unsatisfactory performance as the result of limited accessibility of the DNA analyte to the immobilized DNA probes embedded inside the 3D matrix of the 50 nm thick polymeric film. If so, it should become even more problematic for larger sized biomolecules with a much more diversified structural variation in comparison to DNA.

Surface-initiated polymerization (SIP) has been introduced as a potential tool to generate a thin film of surface-tethered polymer brushes that can act as a modifying layer for the material's surface and so should be useful for biotechnology- and nanotechnology-related applications. The SIP, or so-called "grafting from", method holds advantages over the "grafting to" method of which the process suffers from the entropic barrier due to the crowding of the initial grafting polymer chains that prevent further insertion of the polymer onto the surface and so leads to a relatively low graft density. The "grafting from" method, on the other hand, involves a stepwise growth of the polymer chain from the surface by insertion of monomer, which allows a better control over the polymer chain length, graft density and thickness. SIP coupled with "living radical polymerization" has proven to be the most popular method for creating surface-tethered polymer brushes [9-11].

The ability to fine tune the thickness of polymer brushes, even as thin as a few nanometers, by controlling the polymerization conditions has led to the suggestion that SIP can be employed as an alternative method to overcome the above-mentioned obstacles imposed by the diffusion barrier of analytes into the relatively thick polymeric coating, especially in the case of the CM-dextran. In fact, the success of utilizing polymer brushes in the fields of biotechnology has been continuously demonstrated. As monitored by SPR, the enhanced binding specificity/capacity of biotin-SA can be achieved through the use of poly(oligo(ethylene glycol) methacrylate) brushes as linkers with a 10-fold higher signal-to-noise ratio compared to that obtained with the SAM-based system [12]. Poly(acrylic acid)

(PAA) brushes, on the other hand, were employed as matrices for binding a number of proteins, namely bovine serum albumin (BSA), myoglobin, anti-IgG antibodies [13] and ribonuclease A [14]. Their high-protein binding capacity has made the surface-tethered PAA brushes a potential candidate for the development of affinity-based chromatography media for protein purification and protein microarrays. A new strategy to indirectly immobilize small biological molecules has been recently reported on the patterned surface-grafted PAA brushes using specific interactions between avidin that was attached to the PAA brushes and biotin-tagged proteins or between the biotin-tagged BSA that was bound to the PAA brushes and streptavidin which can later be used to bind with other biotinylated molecules [15]. The immunoreaction between anti-C-reactive protein (CRP) antibodies attached to PAA brushes and CRP in solution has also been described but with the detection being based upon quartz crystal microbalance analysis [16]. However, it should be noted that,in this particular case, the PAA brushes were grown via atom transfer radical polymerization (ATRP) from a plasma-polymerized allyl alcohol film that was functionalized with a bromoester inititator.

Here, in this research, we are interested in developing 3D matrices for biosensing applications from surface-tethered PAA brushes. Unlike the previously reported work [16], the PAA brushes used here were generated via a less complicated process by SIP of the monomer directly from the substrate having a SAM of bromoester-terminated alkanethiol. For this reason, the thickness of polymer brushes can then be correctly monitored as a function of polymerization time. The correlation between the carboxyl group density and the chain length or molecular weight of the polymer brushes was then evaluated. Biospecific recognition between the biotin-attached PAA brushes and SA was investigated using SPR in comparison with the 2D matrix of the SAM carboxyl-terminated alkanethiol. In addition, the ability to resist non-specific interactions with two non-target proteins of a similar pI but

different sizes and structures was also evaluated to determine the applicability of the developed 3D platform for biosensing applications.

2. Materials and methods

2.1. Materials

t-Butyl acrylate (*t*-BA, 98%, Aldrich) was extracted three times with 5% (w/v) aqueous NaOH and then washed with distilled water. After drying over anhydrous $MgSO_4$ and filtering off the drying agent, the *t*-BA was distilled under reduced pressure (60 °C/60 mmHg). Tris(2-(dimethylamino)ethyl)amine (Me_6TREN), 2-bromo-2-methylpropionic acid 3-(ethoxydimethylsilanyl)propyl ester ($BrC(CH_3)_2COO(CH_2)_3(CH_3)_2Si(OC_2H_5)$) and ω–mercaptoundecyl bromoisobutyrate ($BrC(CH_3)_2COO(CH_2)_{11}SH$) were prepared following the methods described in the literature [17-19]. CuBr (95%, Fluka), ethyl 2-bromoisobutyrate (EBiB, 98%, Fluka), Toluidine Blue O (TBO, 98%, Fluka), 1-(3-dimethylaminopropyl)-3-ethylcarbodiimide hydrochloride (EDCI, 98%, Fluka), *N*-hydroxysuccinimide (NHS, 98%, Fluka), *N*,*N*,*N*′,*N*″,*N*‴-pentamethyldiethylenetriamine (PMDETA, 99%, Aldrich), (+)-biotinyl-3,6,9-trioxaundecanediamine (NH_2-biotin, Bioactive), fluorescein-conjugated streptavidin (FITC-SA, Bioactive), bovine serum albumin (BSA, Aldrich), 11-mercaptoundecanoic acid (MUA, Aldrich), fibrinogen (FIB, Aldrich), streptavidin (SA, Bioactive), phosphate buffered saline (PBS, Aldrich) and trifluoroacetic acid (TFA, Fluka) were used as received. Ultrapure distilled deionized water was obtained after purification using a Millipore Milli-Q system (USA) that involves reverse osmosis, ion exchange and a filtration step. Anhydrous toluene was prepared by distillation over calcium hydride under a nitrogen atmosphere.

2.2. Preparation of the surface grafted α-bromoester initiator

Silicon substrates (wafers or particles) were submerged in a freshly prepared piranha solution (7:3 (v/v) mixture of concentrated H_2SO_4 and 30% (v/v) H_2O_2) at ambient temperature for 2 h, rinsed with 5 - 7 aliquots of deionized water and dried in a clean oven at 120 °C for 2 h. Anhydrous toluene (30 mL) containing 4 mmol (33 μL) of $BrC(CH_3)_2COO(CH_2)_3(CH_3)_2Si(OC_2H_5)$ was added via a syringe to a dried Schlenk flask containing freshly cleaned silicon substrates. Reactions were carried out under a nitrogen atmosphere at ambient temperature for 18 h. The substrates were sequentially rinsed with (all 10 mL) toluene, 2-propanol (twice), ethanol (twice), 1:1 (v/v) ethanol-water, water, ethanol and finally water before being dried *in vacuo*.

In the case of the gold-coated SPR disks, the disks were cleaned in a freshly prepared piranha solution at ambient temperature for 15 min, rinsed with 5 - 7 aliquots of deionized water and dried by a gentle stream of nitrogen gas. Freshly cleaned disks were then immersed in a 1 mM ethanolic solution of $BrC(CH_3)_2COO(CH_2)_{11}SH$ for 24 h at ambient temperature. After this treatment, the disks were rinsed with ethanol and dried by a gentle stream of nitrogen gas.

2.3. Formation of PAA brushes

The synthetic route for the formation of PAA brushes is schematically shown in Fig.1. The substrates having surface grafted initiators, $BrC(CH_3)_2COO(CH_2)_3(CH_3)_2SiO\text{-}SiO_2$ **(1)** or $BrC(CH_3)_2COO(CH_2)_{11}S\text{-}Au$ **(2)** (obtained from section *2.2)*, were placed in a Schlenk flask and sealed with a rubber septum. The flask was evacuated and back-filled with nitrogen three times and then left under a nitrogen atmosphere. CuBr (49.3 mg, 0.34 mmol), *t*-BA (10 mL, 68 mmol) and acetone (15 mL) were added to a separate Schlenk flask with a magnetic bar, sealed with a rubber septum, and degassed by purging with nitrogen for 1 h. PMDETA (71.8 μL, 0.34 mmol) was added to the mixture via a syringe, and the solution was stirred at 60 °C

until it became homogeneous. For the gold-coated substrates, the more active ligand, Me_6TREN (88 μL, 0.34 mmol) was used instead of PMDETA so that the polymerization could be performed at ambient temperature without thermal treatment. This was done in order to avoid the gold detachment from the substrate upon elevating the temperature. The solution was then transferred to the flask containing the substrates, **(1)** or **(2)**, via a cannula, followed by the addition of the sacrificial initiator, EBiB (54.6 μL, 0.34 mmol). The polymerization was allowed to proceed for a set reaction time (0 - 24 h) at 60 °C for the silicon substrates and at ambient temperature for the gold-coated substrates. The substrates were removed from the solution, rinsed by acetone and THF, and soxhlet extracted with THF before being dried *in vacuo*. The substrates bearing P*t*-BA brushes were then analyzed by surface characterization techniques. Free polymer from the polymerization solution was isolated by first evaporating the residual monomer and solvent under reduced pressure, dissolving in THF, and then passing the polymer solution in THF through a short column of silica to remove any residual catalyst and analyzed by gel permeation chromatography (GPC).

The substrates containing the tethered P*t*-BA brushes were placed in a Schlenk flask. A solution of 2.5 M TFA in dichloromethane was added and stirred at ambient temperature for 6 h. The substrates were removed and rinsed thoroughly with dichloromethane, and then dried *in vacuo*. This step was carried out in order to remove the *t*-butyl groups from the P*t*-BA brushes. The resulting surface-tethered linear and branched PAA brushes were then subjected to characterization and biotin binding.

2.4. Characterization of surface-tethered polymer brushes

The dynamic advancing and receding water contact angles were measured using a contact angle goniometer, model 100-00, equipped with a Gilmont syringe and a 24-gauge flat-tipped needle (Ramé-Hart, Inc., USA). The FT-IR spectra of surface-modified silica

particles prepared as KBr pellets were recorded with a FT-IR spectrometer (Perkin Elmer), model system 2000, with 32 scans at a resolution of 4 cm^{-1} using a TGS detector. The molecular weight and the molecular weight distribution of the P*t*-BA homopolymer were determined by a Water GPC system (USA) with a Water E600 column connected to a RI detector. The column was eluted with THF at a flow rate of 1 mL/min. Narrow PS standards were used for generating a calibration curve. ^{1}H NMR spectra were recorded in $CDCl_3$ using a Varian NMR spectrophotometer (model Mercury-400; USA) operating at 400 MHz. The thickness of samples was analyzed by an L115C Wafer^{TM} Ellipsometer operating with a 70° of incidence angle at 632.8 nm. The calculation was based on refractive indices of 1.443, 1.460 and 1.462 for $N_{initiator}$, $N_{t\text{-}BA}$ and $N_{hydroxyl}$, respectively, and a silicon substrate refractive index ($N_{substrate}$) of 3.858. AFM images were recorded with Scanning Probe Microscope model NanoScope®IV, Veeco, USA. Measurements were performed in air using tapping mode. Silicon nitride tip with a resonance frequency of 267-295 KHz and a spring constant 20-80 N/m were used.

The TBO staining method was employed to determine the amount of carboxyl groups on the PAA brushes. A 0.5 mM TBO aqueous solution was prepared at pH 10 and the substrate bearing PAA brushes were immersed in the dye solution for 6 h at 30 °C. The substrates were then removed and thoroughly rinsed with a 0.4 mM NaOH (aq) (pH 9) for 2 h to remove any non-complexed dye adhering to the substrate. The dye complexed with the carboxyl groups was then desorbed from the surface by soaking the substrates in a 50% (v/v) acetic acid solution for 16 h, and the desorbed dye content was obtained by measuring the optical density of the solution at 633 nm with an UV-vis spectrophotometer (Model Techne Specgene, UK). The PAA content was determined from a predetermined calibration curve (0.001-0.05 mM) of the optical density versus dye concentration assuming one carboxyl group reacted with one dye molecule [20].

2.5. Determination of SA binding to biotin-attached PAA brushes by fluorescence microscopy

The carboxyl groups of the PAA brushes on the silica particles were activated by suspending the substrates bearing PAA brushes in an aqueous solution of 0.05 M EDCI / 0.1 M NHS for 30 min. The substrates were rinsed with deionized water before suspended in a solution of NH_2-biotin (1 mg/mL) in PBS (pH 7.4) for 2 h at ambient temperature and washed thoroughly with PBS solution. A schematic representation of the carboxyl group activation and biotin attachment step is outlined in Fig.1. The silica particles bearing biotin-attached PAA brushes were suspended in a solution of PBS containing 0.1% (w/v) BSA for 60 min and then rinsed thoroughly with PBS. The particles were then incubated in a solution of FITC-SA (0.1 mg/mL) in PBS at ambient temperature. After 14 h, the particles were rinsed thoroughly with PBS followed by distilled water and then spread on a glass slide and covered with a thin cover slip. A fluorescence microscope equipped with a digital camera was used to examine the SA bound on the particles.

2.6. Determination of SA binding to biotin-attached PAA brushes by SPR

SPR measurements were conducted using a double channel, AutoLab ESPR (Eco Chemie, The Netherlands) at 25 ^{o}C, with the plane face of the prism coupled to the gold-coated glass via index matching fluid. An auto-sampler was used to inject the test solutions and the measurement of the SPR angle shift was done under non-flow liquid conditions. The shift of the SPR angle at the end-point of each step and after baseline subtraction ("angle shift") was used to calculate the amount of the molecules bound onto the surface or target density, using a sensitivity factor of 120 mDegrees equals 100 ng/cm^2 and its molecular weight, as previously reported [21].

For comparison, a gold-coated SPR disk bearing a monolayer of the carboxyl-terminated thiol, MUA, as a so-called 2D substrate, was prepared by immersing the cleaned disk in an ethanolic solution of MUA (1 mM) at ambient temperature for 24 h. The disk was then rinsed thoroughly with ethanol and dried *in vacuo*. The gold-coated SPR disk bearing PAA brushes (3D) or MUA (2D) was first seated in the SPR cell before being rinsed with a running solution of sodium acetate buffer (10 mM, pH 4.5). After a baseline SPR response was established, the activation by EDCI (0.05 M) and NHS (0.1 M), the attachment of NH_2-biotin (1 mg/mL), and the subsequent blocking by ethanolamine (1 M) were all carried out sequentially *in situ* in the sodium acetate buffer for 15, 30, and 15 min, respectively. The disk was rinsed with a running solution of sodium acetate buffer for 3 - 5 min after each step. The binding of SA was performed in PBS. After a baseline SPR response was recorded, 50 μL of SA in PBS (0.1 mg/mL) was applied to the biotin-immobilized disk and left for 15 min. The unbound SA was removed by washing with PBS for 5 min. Non-specific interactions of the gold-coated SPR disks bearing PAA brushes-biotin (3D matrix) and MUA-biotin (2D matrix) were tested against BSA and FIB by passing the 0.2 mg/mL protein solution in PBS over the discs for 15 min.

3. Results and discussion

3.1. Formation of surface-tethered PAA brushes

The molecular weight and thickness of the PAA brushes can be controlled by the reaction time as well as the monomer to initiator ratio (the targeted DP) in the solution, (Fig. 2). The molecular weight of the P*t*-BA brushes on surface was determined by measuring the molecular weight of a free polymer simultaneously formed in the solution from the "sacrificial" or "added" initiator. It has previously been demonstrated that the molecular weight of this free polymer closely resembled that of the grafted polymer brushes cleaved

from the surface [22]. Thus, it can be used to monitor the SIP process. Fig. 2 clearly shows that the change in the molecular weight ($\overline{M}_n$) of the free P*t*-BA and the thickness of the P*t*-BA brushes on the silicon substrate both increased as the polymerization time increased (over the tested range of 0 – 24 h) for the P*t*-BA brushes made from both targeted DPs of 100 and 200. The fact that the molecular weight distribution is close to 1 and that the thickness of P*t*-BA brushes increased linearly as a function of the polymerization time suggests that the polymerization is living and can be well controlled. For the targeted DP of 200, the graft density of the P*t*-BA brushes coated on the silicon substrate calculated from ellipsometric thickness and the free P*t*-BA formed in solution is 0.32 chain/nm^2.

Another evidence of the P*t*-BA brushes formation, especially on the gold-coated SPR substrate is based on AFM analysis. According to the AFM micrographs shown in Fig.S1 (Supplementary Material), the topography of the gold-coated SPR substrate has been changed with larger groove dimension upon the coating of the P*t*-BA brushes. The root mean square roughness (rms) was also increased from 1.2 to 1.9 nm. The presence of the polymer layer can be clearly seen from the AFM micrograph in Fig.S2 (Supplementary Material) demonstrating the section analysis of the gold-coated SPR substrate of which the P*t*-BA layer was intentionally scraped off. Using the average thickness (9.5±0.6 nm) obtained from this particular image together with the free P*t*-BA formed in solution at the target DP of 200, the graft density of 0.31 chain/nm^2 can be calculated. The fact that the graft density calculated from the AFM data is essentially the same as that obtained from the ellipsometric analysis at the same targeted DP suggested that the method for the preparation is potentially reliable although the values were determined on different substrates by different techniques.

The growth of the P*t*-BA brushes and their hydrolyzed counterparts, PAA brushes, on the silica or gold substrates was also confirmed by water contact angle measurements and FT-IR analysis. As a consequence of the formation of P*t*-BA brushes, the advancing (θ_A) and

receding (θ_A) water contact angles of the substrate having surface-grafted initiator markedly increased (Table 1). After hydrolysis, the water contact angles decreased significantly as the hydrophobic P*t*-BA brushes were hydrolyzed to hydrophilic PAA brushes. To achieve the covalent attachment of biotin to the carboxyl group of the PAA brushes, a method to introduce the reactive intermediate NHS ester was used. The carboxyl group of the PAA brushes was first activated by the water-soluble carbodiimide EDCI and NHS to form the NHS group, and this was then coupled with NH_2-biotin, leading to amide bond formation. The increasing θ_A/θ_R observed after the activation (Table 1) suggests that the hydrophilic carboxyl groups of PAA brushes were converted to the hydrophobic *N*-succinimidyl groups. The water contact angles did not significantly change after biotin attachment.

The FT-IR spectra of the surface-functionalized silica particles revealed the presence of signals corresponding to the desired functionalities of the polymer brushes (Fig. 3). Evidently, the carbonyl stretching peak at 1727 cm^{-1} shifted slightly to 1713 cm^{-1} after the P*t*-BA brushes were transformed to PAA brushes. Also, the intensity of the O-H stretching peak (2400 - 3800 cm^{-1}) was enhanced after hydrolysis of the P*t*-BA brushes to PAA brushes due to H-bonded carboxyl groups of the PAA brushes. The shoulder peaks that appear at 1734 and 1778 cm^{-1} were assigned to the carbonyl stretching of the succinimidyl ester after activation of the PAA brushes and so indicate that the carboxyl group was transformed to a NHS group after activation by the EDCI / NHS treatment. The binding of NH_2-biotin can be verified by the appearance of the amide II band at 1558 cm^{-1} (N-H bending) and the disappearance of the signals belonging to succinimidyl ester at 1734 and 1778 cm^{-1}. It should be emphasized that the data shown in Table 1 and Fig. 3 were obtained from the polymer brushes having a targeted DP of 200. As determined by the TBO assay, the density of the carboxyl groups of the PAA brushes on the silicon oxide surface increased as a function of $\overline{M}_{n,}$ or chain length of the polymer brushes obtained with both a targeted DP of 100 and 200

(Fig. 4). The carboxyl group density increased some three-fold from 1.67 ± 0.19 to 5.04 ± 0.87 nmol/cm^2 as the $\overline{M}_n$ increased from 3.8 to 14 kDa.

3.2. Determination of SA binding to the biotin-attached PAA brushes

The attachment of the biotin was qualitatively confirmed by fluorescence microscopic analysis. The optical and fluorescence images of the PAA brushes-biotin grafted on silica particles after incubation in the solution of FITC-SA are shown in Fig. 5. The dark area of the optical images in the top row is the area that was covered by the silica particles while the bright area is the empty space on the glass slide. Upon exposure to fluorescent irradiation (λ = 488 nm), the dark area appeared green while the bright area turned dark and the control sample (blank silica particles) appeared totally dark indicating there was no FITC-SA adsorbed. This result strongly suggests that NH_2-biotin can covalently attach to the carboxyl groups of the PAA brushes, and that the attached biotin can effectively act as an active binding site for FITC-SA.

SPR is a surface-sensitive technique based on the detection of change in the refractive index (RI) that is known to provide quantitative information and can be used for the detection of the desired analyte with a high specificity and sensitivity. The changes in the SPR angle (angle shift, expressed as Δθ), can be determined from the difference in the SPR angle at the baseline and after the washing, and is proportional to the quantity of molecules on the gold-coated SPR disks. The Δθ values of the substrates bearing PAA brushes (derived from P*t*-BA having $\overline{M}_n$ of 30 kDa) after biotin attachment is 851 m° (Fig. 6(a)), which is equivalent to a biotin density of 709.2 ng/cm^2 or 1,896 pmol/cm^2 (based on a sensitivity factor of 120 m°/100 ng/cm^2 [21] and a MW of 374 g/mol for biotin). The calculated immobilized biotin density was 171 pmol/cm^2 (Δθ = 77 m°) for the MUA. The results, therefore, suggest that the layer of PAA brushes possessed an 11-fold higher biotin density compared to the MUA system.

Moreover, the Δθ following SA binding is proportional to the quantity of the immobilized biotin (Fig. 6(b)). Using a MW of 60,000 g/mol for SA, the 3D PAA brushes-biotin exhibited just over a two-fold higher SA binding density compared to the 2D MUA-biotin (12.2 and 5.9 pmol/cm^2), as calculated from a Δθ of 881 (734.2 ng/cm^2) and 428 m° (356.7 ng/cm^2), respectively. This is in good agreement with the work reported by Lee and coworkers [12], who found that the binding capacity of SA to the biotinylated layer prepared on poly(oligo(ethylene glycol) methacrylate) brushes was some 2.5-fold higher than that on the carboxylic acid terminated SAM (648.5 ng/cm^2 and 255.6 ng/cm^2, respectively).

Taking advantage of the ability to fine tune the carboxyl group density as a function of the molecular weight of the polymer brushes ($\overline{M}_n$), the effect of varying the carboxyl group density as a function of the $\overline{M}_n$ on the binding capacity of biotin and SA was evaluated (Fig. 7). As anticipated, the amount of attached biotin increased with increasing $\overline{M}_n$. It should be noted that the $\overline{M}_n$ of 8, 19 and 30 kDa yielded carboxyl group densities of 3.8, 7.0 and 10.6 nmol/cm^2, respectively. Considering the carboxyl group density, it was found that approximately 6 - 17% of the carboxyl groups were immobilized with biotin implying that there were still a significant proportion of free carboxyl groups along the chains of the PAA brushes. The SA binding density was increased less than 1.1-fold, from 12.7 to 13.6 pmol/cm^3, when the immobilized biotin density was increased over 2.9-fold from 600 to 1,760 pmol/cm^2. In principle, the binding ratio between biotin and SA should be four if all of biotin molecules were bound to SA. However, it was found that the biotin/SA binding ratios (the number written above each set of bar graphs in Fig.7) were significantly greater than the theoretical value indicating that most of the immobilized biotin was not bound to the SA. The biotin/SA binding was found to increase with increasing $\overline{M}_n$. This may be explained as a result of the limited accessibility of the SA to the immobilized biotin that was embedded inside the inner layer of the polymer brushes.

The success of a sensing platform cannot be judged only from the biospecific detection of the expected analyte, but it also depends upon the ability to resist adsorption of non-specific components. Here, the two model proteins, BSA and FIB, that have a similar isoelectric point (pI) to that of the target analyte, SA, were evaluated for non-specific binding. The pI of SA, BSA and FIB is 5.0, 4.8 and 5.5, respectively, and so these three proteins should be negatively charged in PBS at pH 7.4. The results (Fig. 8) indicated that the biotinylated PAA brushes not only have good specific binding with SA but also prevent adsorption of other non-specific proteins. Apparently, the non-specific adsorption of BSA and FIB was much more suppressed on the PAA brushes-biotin (3D-matrix) than that on the MUA-biotin (2D-matrix). This may stem from the hydrophilic nature of the PAA brushes as opposed to the hydrophobic hydrocarbon linker of the MUA. This is a desirable characteristic of the sensing platform. The ability to prevent non-specific adsorption is comparable with the PAA brushes prepared by ATRP of different monomer, sodium acrylate, as recently reported by Rastogi and co-workers [23].

There are two important issues here. Firstly, it is certainly not necessary to have such a high probe density in the 3D sensing platform of PAA brushes in order to achieve a superior detection signal to that of the 2D SAM-based sensing platform. Secondly, it seems that the problem due to the diffusion barrier of the analyte still persists in the case of PAA brushes even though their thickness (3-10 nm) is some ten-fold lower than those of the commercial CM-dextran-based chips (30-100 nm). This may be caused by the densely packed characteristic of the polymer brushes generated by the SIP process, since the P*t*-BA brushes used to generate the PAA brushes in this research have a graft density in a range of 0.21 - 0.31 chains/nm^2 (calculated from AFM data). This polymer brush density falls well within an extended brush regime (graft density $>$ 0.08 chains/nm^2) [24], and should limit the accessibility of analytes, especially like SA that is of a relatively large size (MW = 60 kDa).

Yang and coworkers have reported that the large proteins, BSA and, especially, fibrinogen can penetrate into the layer of poly(D-gluconamidoethyl methacrylate (PGAMA), more difficultly than that of small protein, lysozyme, especially at high graft density of the polymer brushes [25]. When the grafting density is high, the space between polymer chains becomes much narrow and densely packed. It is thus more hindered for the protein to reach inside the inner layer of the polymer. Yoshikawa and coworkers also reported the effect of grafting density of poly(2-hydroxyethyl methacrylate) (PHEMA) brushes on the diffusion of large protein into the inner layer of polymer brushes. The grafting density at 0.06 and 0.7 chain/cm^2 exhibited exclusion effect to BSA and IgG proteins [26]. As demonstrated by Gautrot and coworkers, the swelling of the polymer brushes facilitated the penetration of histidine-tagged proteins, and subsequently provided the high protein loading levels [27]. On the other hand, a low ability to swell should diminish protein infiltration into the inner polymer layer. Particularly in the case of the PAA brushes, after being immobilized by biomolecules, the polymer chains are no longer ionizable and not charged. Therefore, the biomolecule-functionalized PAA film in the aqueous environment was found to exhibit inferior swellability as compared to the unmodified one [28].

Therefore, future research should try to vary the graft density of the PAA brushes by controlling the graft density of the surface initiator. In addition, we are also trying to determine whether the extent of the carboxyl group activation would have any impact on the swellability of the sensing layer based on PAA brushes after probe immobilization and analyte detectability in terms of selectivity/specificity as well as detection limits. These issues are likely to be equally important for the optimization and development of this 3D platform for biosensing applications.

4. Conclusions

It has been demonstrated that the surface-tethered PAA brushes synthesized by surface-initiated ATRP can be used as a 3D sensing platform for the specific detection of biomolecules. As determined by TBO assay, the carboxyl group density can be varied three-fold as a function of the polymer molecular weight. These active carboxyl groups are readily available for the attachment of the biotin-sensing probe, as verified by monitoring the water contact angle and FT-IR analysis. The layer of PAA brushes with a molecular weight of 30 kDa exhibited an 11-fold higher biotin density compared with the MUA system, and revealed both a specific binding with SA and also prevented adsorption of two other non-specific proteins. Although the 3D sensing platform based on PAA brushes possessed a superior detection signal of the analyte to that of the 2D SAM-based system, the diffusion of the analyte was still limited due to the densely packed PAA brushes. It is, therefore, important to lower the packing density and enhance the swellability of the PAA brushes, the two parameters that should help improve the performance of the surface-tethered PAA brushes as a 3D platform for biosensors.

Acknowledgements

This research was financially supported by The Thailand Research Fund (RMU5080072), and a graduate research grant (Master Student) to PA from the Ratchadapisek Sompoj Endowment Fund, Chulalongkorn University. The authors are grateful to the Capability Building Unit for Nanoscience and Nanotechnology, Mahidol University, for providing the Ellipsometry facility. Appreciation is also extended to Assistant Professor Thanapat Palaka of Department of Microbiology, Faculty of Science, Chulalongkorn University, and to the National Material and Metal Technology Center (MTEC), for providing access to a fluorescence microscope and contact angle goniometer facilities, respectively. The authors appreciated a language editing service provided by Dr.

Robert Butcher, the Publication Counselling Unit (PCU), Faculty of Science, Chulalongkorn University.

References

1. W. Senaratne, L. Andruzzi, C. K. Ober, Self-assembled monolayers and polymer brushes in biotechnology: Current applications and future perspectives, Biomacromolecules 6 (2005) 2427-2448.
2. X. –L. Su, Y. Li, A self-assembled monolayer-based piezoelectric immunosensor for rapid detection of *Escherichia coli* O157:H7, Biosens. Bioelectron. 19 (2004) 563-574.
3. F. Nakamura, E. Ito, T. Hayashi, M. Hara, Fabrication of COOH-terminated self-assembled monolayers for DNA sensors, Colloids Surf. A. 284–285 (2006) 495–498.
4. S. Choi, J. Chae, Methods of reducing non-specific adsorption in microfluidic biosensors, J. Micromech. Microeng. 20 (2010) 075015.
5. B. S. Lee, J. K. Lee, W. –J. Kim, Y. H. Jung, S. J. Sim, J. Lee, I. S. Choi, Surface-initiated, atom transfer radical polymerization of oligo(ethylene glycol) methyl ether methacrylate and subsequent click chemistry for bioconjugation, Biomacromolecules 8 (2007) 744-749.
6. C. L. Feng, Z. Zhang, R. Förch, W. Knoll, G. J. Vancso, H. Schönherr, Reactive thin polymer films as platforms for the immobilization of biomolecules, Biomacromolecules 6 (2005) 3243-3251.
7. J. –F. Masson, T. M. Battaglia, Y. –C. Kim, A. Prakash, S. Beaudoin, K. S. Booksh, Preparation of analyte-sensitive polymeric supports for biochemical sensors, Talanta 64 (2004) 716-725.
8. N. Yang, X. Su, V. Tjong, W. Knoll, Evaluation of two- and three-dimensional streptavidin binding platforms for surface plasmon resonance spectroscopy studies of DNA hybridization and protein-DNA binding, Biosens. Bioelectron. 22 (2007) 2700-2706.

9. M. Husseman, E. E. Malmström, M. McNamara, M. Mate, D. Mecerreyes, D. G. Benoit, J. L. Hedrick, P. Mansky, E. Huang, T. P. Russell, C. J. Hawker, Controlled synthesis of polymer brushes by "living" free radical polymerization techniques, Macromolecules 32 (1999) 1424-1431.
10. R. A. Sedjo, B. K. Mirous, W. J. Brittain, Synthesis of polystyrene-*block*-poly(methyl methacrylate) brushes by reverse atom transfer radical polymerization, Macromolecules, 33 (2000) 1492-1493.
11. S. Edmondson, V. L. Osborne, W. T. S. Huck, Polymer brushes *via* surface-initiated polymerizations, Chem. Soc. Rev. 33 (2004) 14-22.
12. B. S. Lee, Y. S. Chi, K. –B. Lee, Y. –G. Kim, I. S. Choi, Functionalization of poly(oligo(ethylene glycol) methacrylate) films on gold and Si/SiO_2 for immobilization of proteins and cells: SPR and QCM studies, Biomacromolecules 8 (2007) 3922–3929.
13. J. Dai, Z. Bao, L. Sun, S. U. Hong, G. L. Baker, M. L. Bruening, High-capacity binding of proteins by poly(acrylic acid) brushes and their derivatives, Langmuir 22 (2006) 4274-4281.
14. S. P. Cullen, X. Liu, I. C. Mandel, F. J. Himpsel, P. Gopalan, Polymeric brushes as functional templates for immobilizing ribonuclease A: Study of binding kinetics and activity, Langmuir 24 (2008) 913-920.
15. R. Dong, S. Krishnan, B. A. Baird, M. Lindau, C. K. Ober, Patterned biofunctional poly(acrylic acid) brushes on silicon surfaces, Biomacromolecules 8 (2007) 3082-3092.,
16. S. Kurosawa, H. Aizawa, Z. A. Talib, B. Atthoff, J. Hilborn, Synthesis of tethered-polymer brush by atom transfer radical polymerization from a plasma-polymerized-film-coated quartz crystal microbalance and its application for immunosensors, Biosens. Bioelectron. 20 (2004) 1165-1176.

17. J. Queffelec, S. G. Gaynor, K. Matyjaszewski, Optimization of atom transfer radical polymerization using Cu(I)/Tris(2-(dimethylamino)ethyl)amine as a catalyst, Macromolecules 33 (2000) 8629-8639.
18. K. Matyjaszewski, P. J. Miller, N. Shukla, B. Immaraporn, A. Gelman, B. B. Luokala, T. M. Siclovan, G. Kickelbick, T. Vallant, H. Hoffmann, T. Pakula, Polymers at interfaces: using atom transfer radical polymerization in the controlled growth of homopolymers and block copolymers from silicon surfaces in the absence of untethered sacrificial initiator, Macromolecules 32 (1999) 8716-8724.
19. D. M. Jones, A. A. Brown, W. T. S. Huck, Surface-initiated polymerizations in aqueous media: Effect of initiator density, Langmuir 18 (2002) 1265-1269.
20. L. Ying, C. Yin, R. X. Zhuo, K. W. Leong, H. Q. Mao, E. T. Kang, K. G. Neoh, Immobilization of galactose ligands on acrylic acid graft-copolymerized poly(ethylene terephthalate) film and its application to hepatocyte culture, Biomacromolecules 4 (2003) 157-165.
21. X. Su, Y. –J. Wu, W. Knoll, Comparison of surface plasmon resonance spectroscopy and quartz crystal microbalance techniques for studying DNA assembly and hybridization, Biosens. Bioelectron. 21 (2005) 719-726.
22. E. Marutani, S. Yamamoto, T. Ninjbadgar, Y. Tsujii, T. Fukuda, M. Takano, Surface-initiated atom transfer radical polymerization of methyl methacrylate on magnetite nanoparticles, Polymer 45 (2004) 2231-2235.
23. A. Rastogi, S. Nad, M. Tanaka, N. Da Mota, M. Tague, B. A. Baird, H. D. Abruna, C.K. Ober, Preventing nonspecific adsorption on polymer brush covered gold electrodes using a modified ATRP initiator, Biomacromolecules 10 (2009) 2750-2758.

24. T. Wu, P. Gong, I. Szleifer, P. Vlcek, V. Subr, J. Genzer, Behavior of surface-anchored poly(acrylic acid) brushes with grafting density gradients on solid substrates: 1. Experiment, Macromolecules 40 (2007) 8756-8764.
25. Q. Yang, C. Kaul, M. Ulbricht, Anti-nonspecific protein adsorption properties of biomimetic glycocalyx-like glycopolymer layers: Effects of glycopolymer chain density and protein size, Langmuir 26 (2010) 5746–5752.
26. C. Yoshikawa, A. Goto, Y. Tsujii, T. Fukuda, T. Kimura, K. Yamamoto, A. Kishida, Protein repellency of well-defined, concentrated poly(2-hydroxylethyl mathacrylate) brushes by the size-exclusion effect, Macromolecules 39 (2006) 2284-2290.
27. J. E. Gautrot, W. T. S. Huck, M. Welch, M. Ramstedt, Protein-resistant NTA-functionalized polymer brushes for selective and stable immobilization of histidine-tagged proteins, ACS Appl. Mater. Interfaces 2 (2010) 193-202.
28. Li. –Q. Chu, W. –J. Tan, H. –Q. Mao, W. Knoll, Characterization of UV-induced graft polymerization of poly(acrylic acid) using optical waveguide spectroscopy, Macromolecules 39 (2006) 8742-8746.

Figure Captions

Fig. 1. Schematic diagram showing the formation of P*t*-BA and PAA brushes followed by carboxyl group activation and biotin immobilization**.**

Fig. 2. The molecular weight ($\overline{M}_n$) (●, ■) of the P*t*-BA in solution and thickness (○, □) of the P*t*-BA brushes as a function of the polymerization time and formed from a targeted DP of 100 (●,○) or 200 (■, □). Data are shown as the mean ± SD and are derived from 3 repeats.

Fig. 3. FT-IR spectra of (a) bare silica particles and the silica particles surface-functionalized with (b) P*t*-BA brushes, (c) PAA brushes, (d) activated PAA brushes, and (e) PAA brushes-biotin, obtained from a targeted DP of 200.

Fig. **4.** The density of carboxyl groups of the PAA brushes on the silicon oxide surface as a function of $\overline{M}_n$ when derived from a targeted DP of 100 (○) or 200 (●) at different polymerization time. Data are shown as the mean ± SD and are derived from 3 repeats.

Fig. 5. Optical (top) and fluorescence (bottom) images of silica particles grafted with biotin-attached PAA brushes after binding with FITC-SA, showing the (a) control and (b) PAA brushes-biotin obtained from a targeted DP of 200 using a polymerization time of 24 h. Images shown are representative of at least 3 such fields of view per sample and 3 independent samples.

Fig. 6. Representative SPR sensorgrams of the gold-coated SPR substrate bearing PAA brushes (3D-matrix) and MUA (2D-matrix) before and after (a) biotin immobilization and (b) SA binding. Sensorgrams shown are representative of 3 independent samples.

Fig. 7. SPR angle shifts after the step of biotin immobilization and SA binding on the PAA brushes as a function of their $\overline{M}_n$, as determined by SPR analysis. Numbers above each pair of bar graphs are the binding ratio between biotin and SA. Data are shown as the mean $\pm$ SD and are derived from 3 repeats.

Fig. 8. Adsorption of proteins in PBS (10 mM, pH 7.4) on the MUA-biotin and PAA brushes-biotin based sensing platforms. Data are shown as the mean $\pm$ SD and are derived from 3 repeats.

Figure 1

Click here to download high resolution image

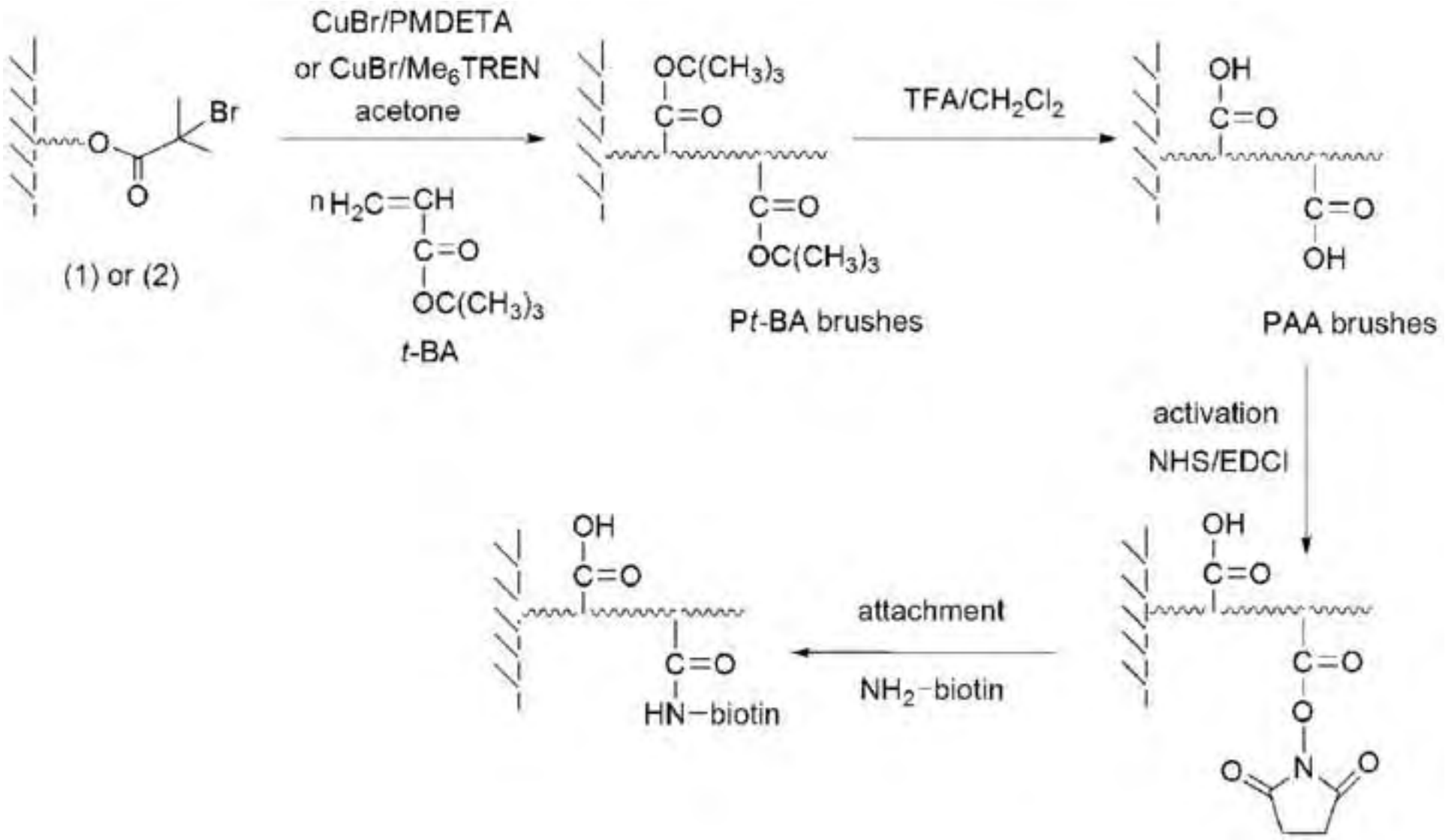

Figure 2

Click here to download high resolution image

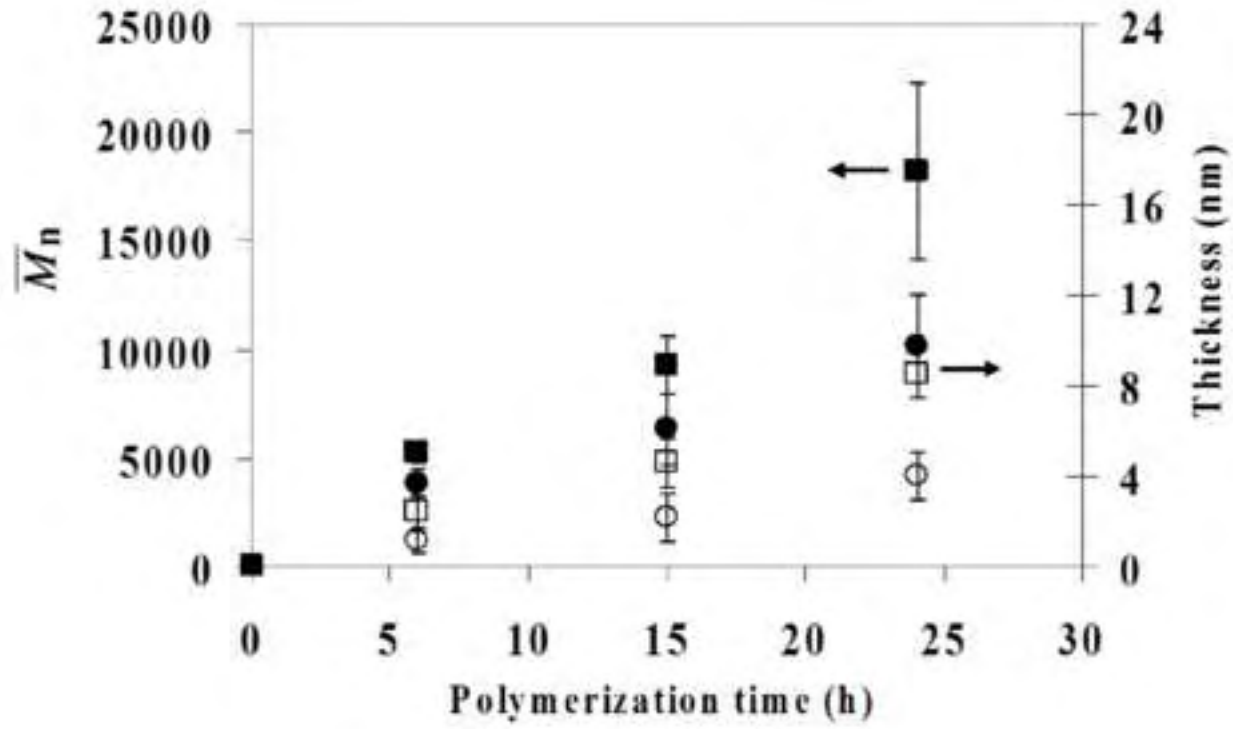

Figure 3

Click here to download high resolution image

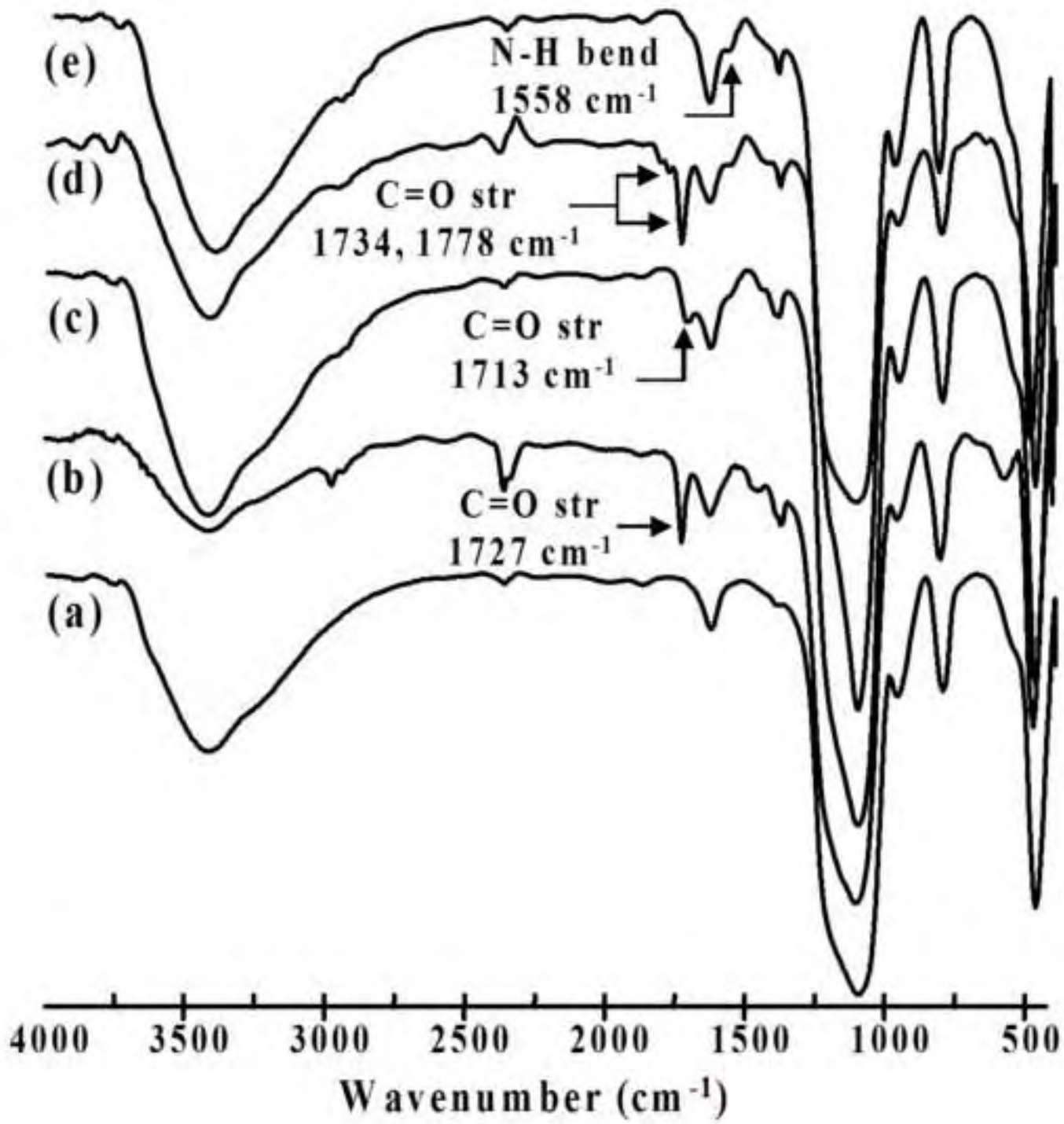

Figure 4

Click here to download high resolution image

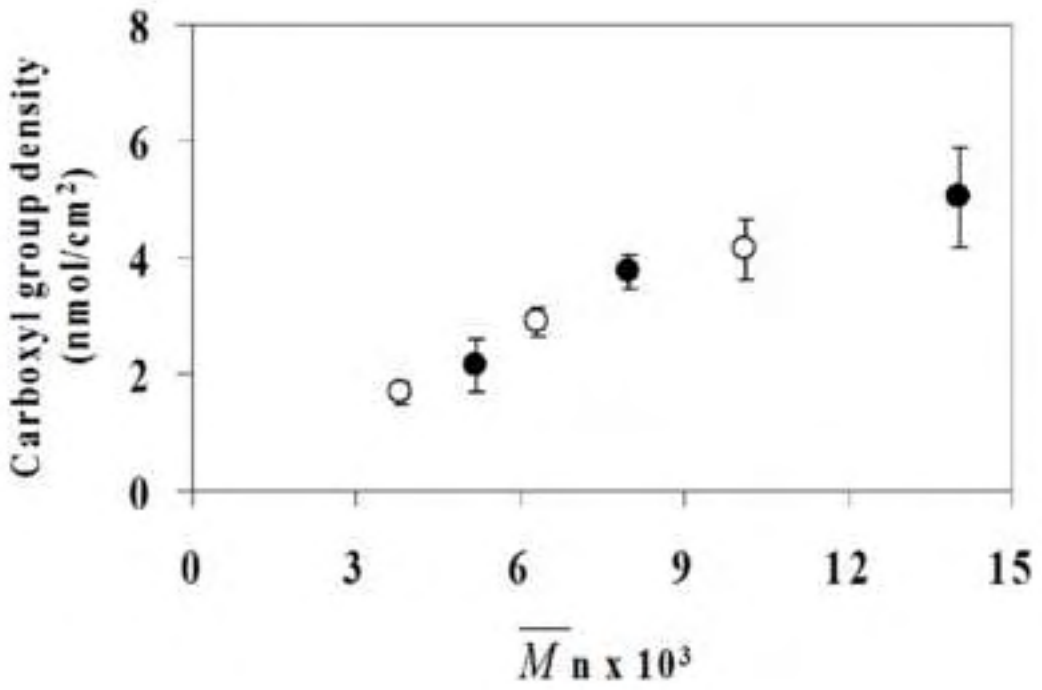

Figure 5

Click here to download high resolution image

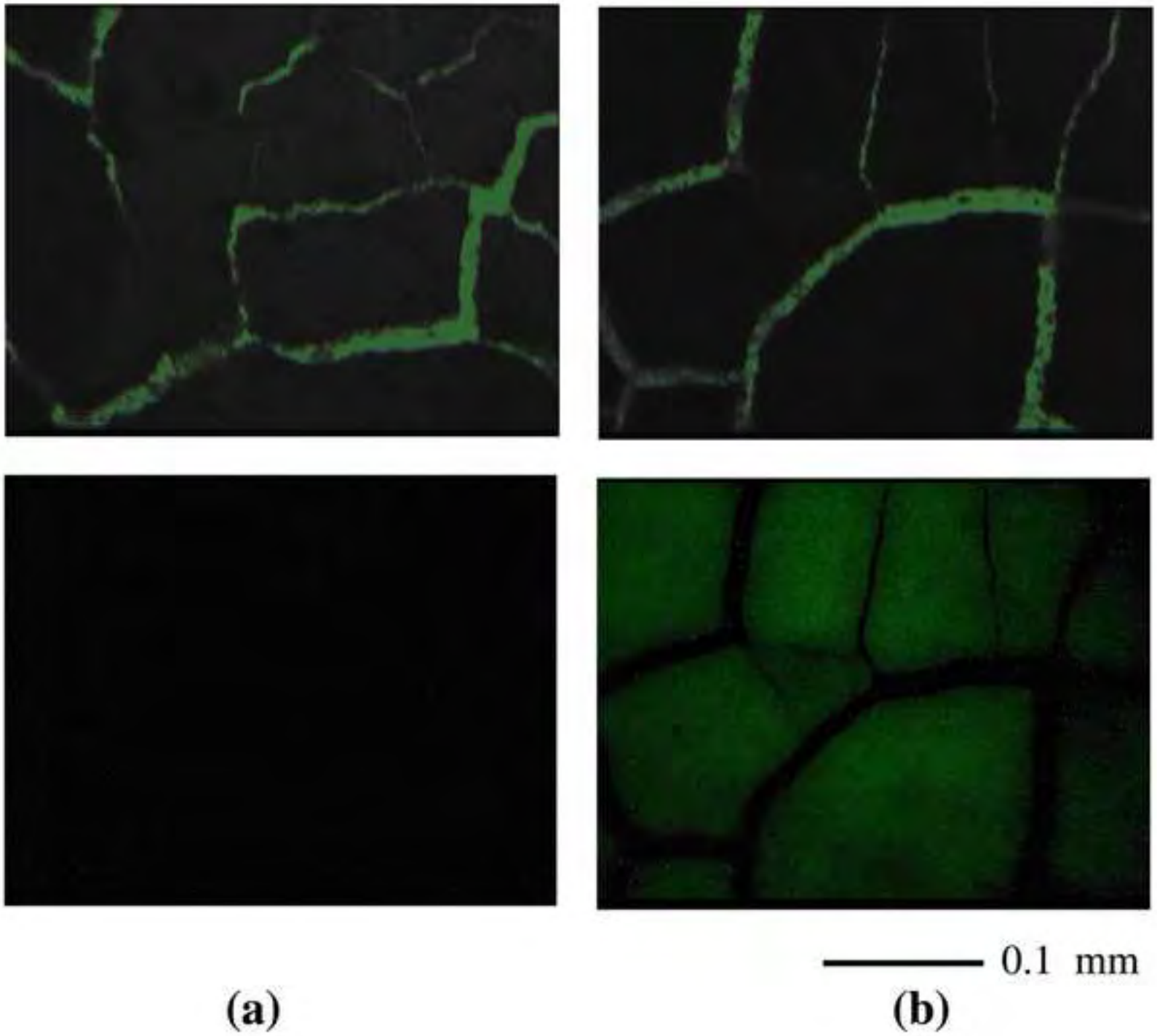

Figure 6

Click here to download high resolution image

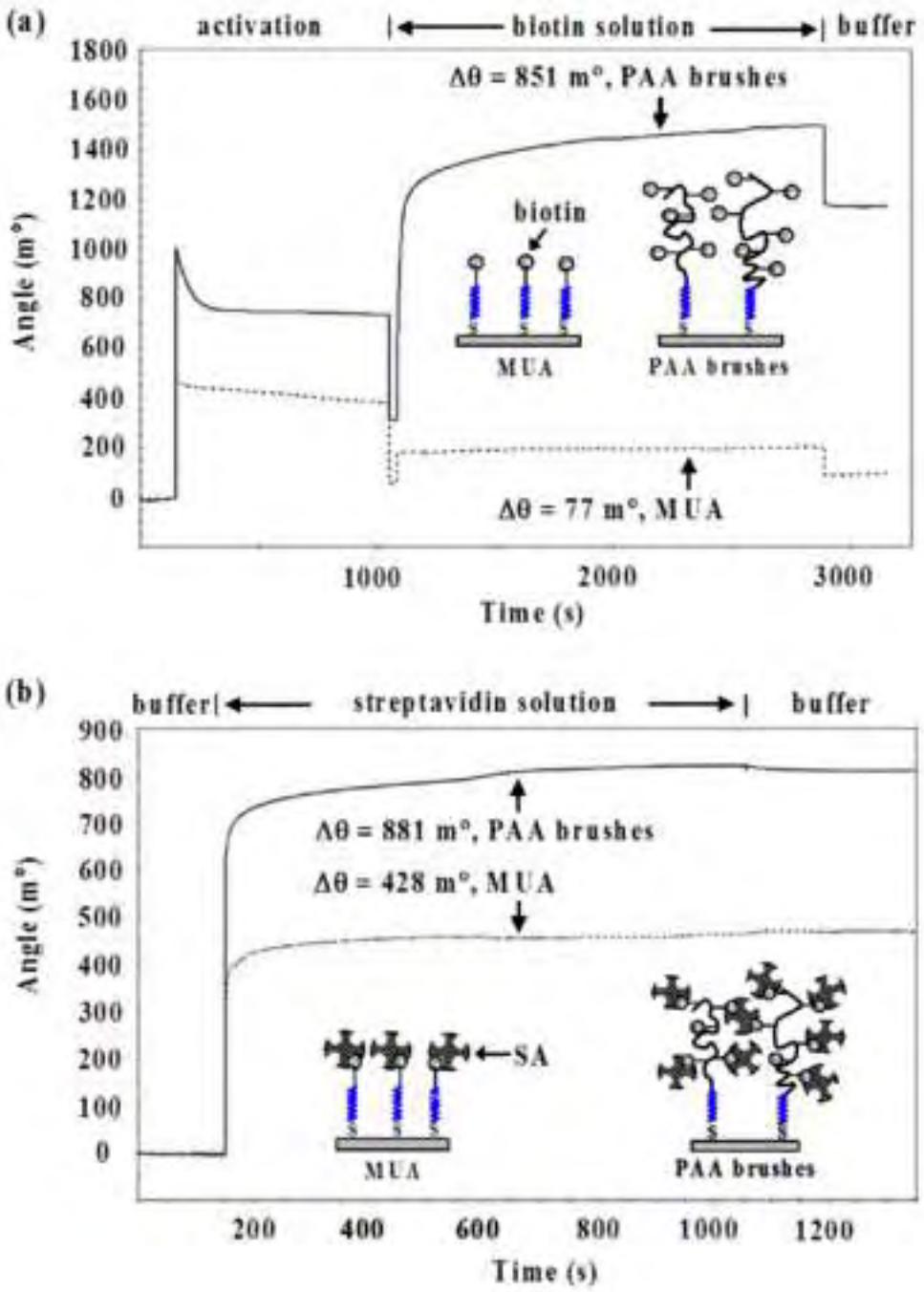

Figure 7

Click here to download high resolution image

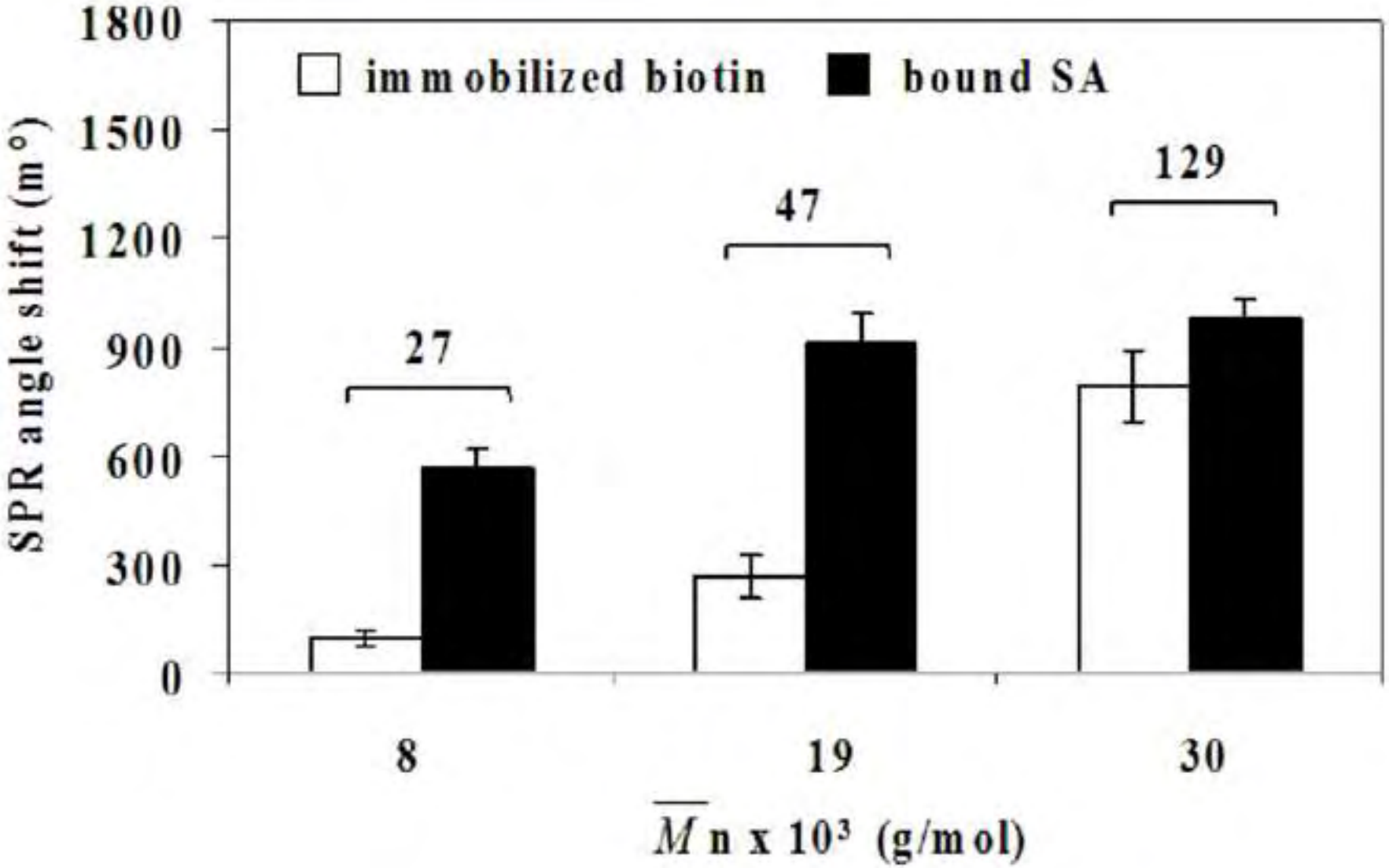

Figure 8

Click here to download high resolution image

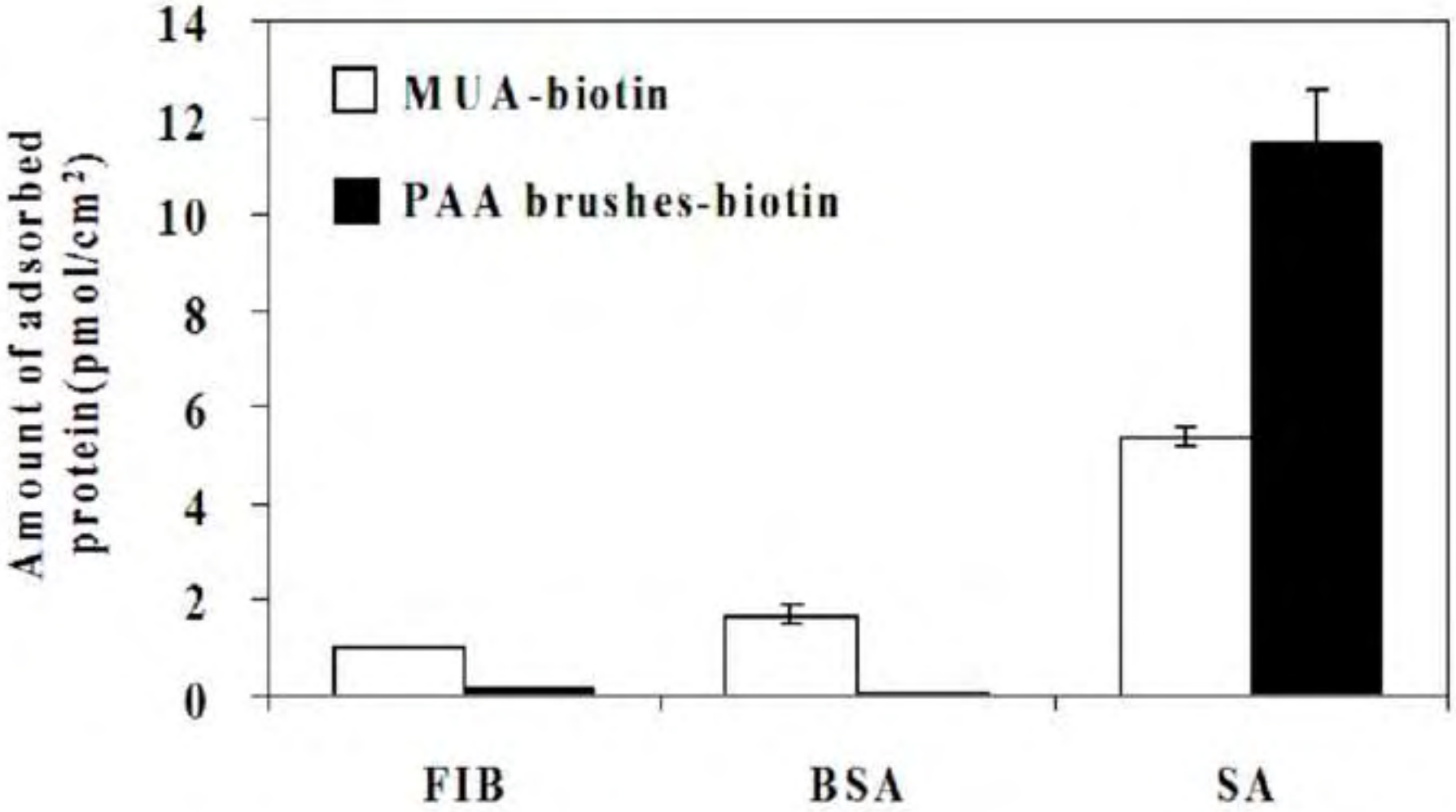

Table 1. Advancing (θ_A) and receding (θ_R) water contact angles of functionalized silicon substrates obtained with a targeted DP of 200. Data are shown as the mean $\pm$ SD and are derived from 5 repeats.

Sample	Water contact angle (degree)	
	Advancing (θ_A)	Receding (θ_R)
surface-grafted initiator	72 ± 1.8	68 ± 1.2
P*t*-BA brushes	95 ± 1.7	76 ± 4.0
PAA brushes	60 ± 1.7	43 ± 0.8
Activated PAA brushes	80 ± 0.8	47 ± 1.4
PAA brushes-biotin	79 ± 0.6	51 ± 1.7

Supplementary Material

Click here to download Supplementary Material: Supplementary Material_Akkahat_CSB.doc